약학석사학위논문

Chemical Constituents of the Leaves of *Cleistocalyx operculatus* and their PTP1B Inhibitory Activity

Cleistocalyx operculatus 잎의 화학 성분

2018 년 2 월

서울대학교 대학원

약학과 생약학 전공

이 주 용

Chemical Constituents of the Leaves of *Cleistocalyx operculatus* and their PTP1B Inhibitory Activity

Cleistocalyx operculatus 잎의 화학 성분

지도교수 오 원 근

이 논문을 약학석사 학위논문으로 제출함

2017 년 12 월

서울대학교 대학원

약학과 생약학 전공

이 주 용

이주용의 약학석사학위논문을 인준함

2018 년 1 월

위 원 장 김 진 웅 (인)

부위원장 성 상 현 (인)

위 원 오 원 근 (인)

Abstract

Protein tyrosine phosphatase 1B (PTP1B) inhibitor has been suggested that it plays a main function in the negative regulation of insulin and leptin signaling, thereby making it for a treatment of diabetes mellitus type 2 and obesity. Moreover, previously conducted research in breast cancer showed that overexpression of PTP1B is detected when selective PTP1B inhibition occurs. As part of our ongoing studies for new PTP1B inhibitor agents from medicinal plants, relative mass defect (RMD) analysis was applied to select the extensive range of triterpenoids in complex plant extracts. The rapid identification and specific metabolite classes of novel plant metabolites could be achieved by calculating RMDs from molecular and fragment ions. Therefore, three new triterpenoids (**1** - **3**) and seventeen previously reported triterpenoids (**4** – **20**) were isolated from a 50% EtOH extract of *Cleistocalyx operculatus* (Roxb.) Merr. et L.M. Perry. Their structures were determined on the basis of extensive spectroscopic analysis as well as comparison with previous data. All isolates were evaluated for their inhibitory effects on PTP1B. Compound **6** showed strong inhibitory effects while compounds **3**, **7**, **9**, **10**, **19** and **20** showed moderate inhibitory effects of on PTP1B enzyme.

Keywords: *Cleistocalyx operculatus*, Myrtaceae, triterpenoid, relative mass defects (RMDs), protein tyrosine phosphatase 1B (PTP1B)

Student Number : 2016-21854

Table of contents

List of Abbreviations

$[\alpha]_D^{20}$: specific rotation at 20 celsius degrees

br s : broad singlet

n-BuOH : *n*-butanol

CC : column chromatography

$CDCl_3$: chloroform-*d* (NMR solvent)

COSY : correlation spectroscopy

d : doublet

dd : double of doublet

dt : doublet of triplet

DTT : dithiothreitol

DMSO : dimethyl sulfoxide

DMSO-d_6 : dimethyl sulfoxide-d_6 (NMR solvent)

EDTA : ethylene diamine tetra acetic acid

ESI-MS : electrospray ionization mass spectroscopy

EtOAc : ethyl acetate

EtOH : ethanol

fr. : fraction

hrs : hours

HMBC : heteronuclear multiple bond correlation

HPLC : high performance liquid chromatography

HRESIMS : high resolution electrospray ionization mass spectroscopy

HSQC : heteronuclear single quantum coherence

Hz : hertz

IC_{50} : the concentration that inhibits 50% of enzymatic activity

IR : infrared absorption

m : multiplet

MC : dichloromethane

MeOH : methanol

MeCN : acetonitrile

m/z : mass to charge ratio

MS : mass spectrometry

NMR : nuclear magnetic resonance

NP : normal phase

NOESY : nuclear overhauser enhancement spectroscopy

ODS : octadecyl silane

p-NPP : *p*-nitrophenyl phosphate

q : quartet

qTOF : quadrupole time of flight

RMD : relative mass defect

RP : reversed phase

rt : room temperature.

s : singlet

t : triplet

td : triplet of doublet

TLC : thin layer chromatography

t_R : retention time

UV : ultraviolet absorption spectroscopy

w/w : weight to weight ratio

List of Figures

List of Tables

List of Schemes

I. Introduction

1. Obesity and type 2 diabetes

Obesity and type 2 diabetes have been emerged as one of the major pandemics to human health in the 21st centrury (Zimmet et al., 2001; Morris et al., 2015). The population in worldwide with diabetes has risen to 422 million in 2014, and it was estimated the prevalence of the global diabetes to reach over 366 million in 2030. According to the data from the Emerging Risk Factors Collaboration, around 1.6 million deaths were directly brought about by diabetes in 2015 (Mather et al., 2006). Some experts called "diabesity" as dual epidemic, the growth in the disseminate of the diabetes parallels that of obesity, and those are crucial causes of blindness, kidney failure, heart attacks, stroke, and high blood glucose (WHO, 2017). The world direct annual cost of diabetes is more than 825 million by cost estimates from a recent systematic review (NCD RisC., 2016). Although anti-diabetes candidates has continued to develop for the clinic, it is hard for many people to attain HbA1C target levels. Developing that new anti-diabetes agent is necessary with these insufficient opportunities to get therapy.

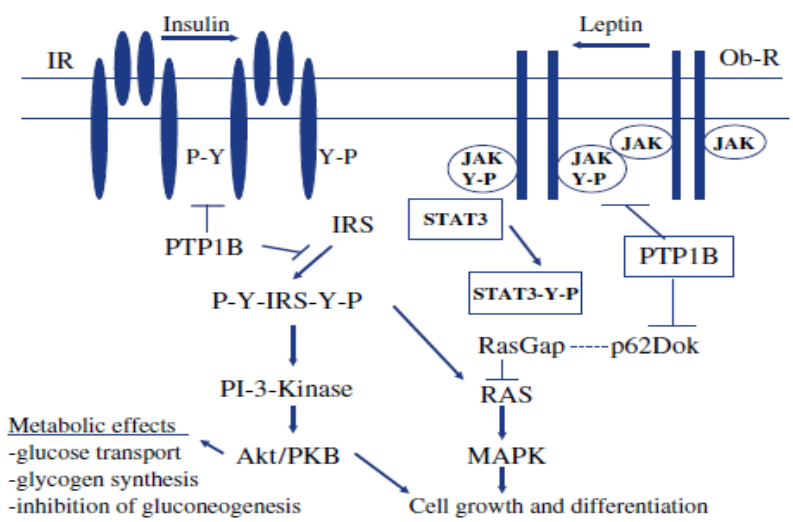

Figure 1. Illustration of PTP1B Pathway

2. Protein tyrosine phosphatases 1B (PTP1B) and its purpose of study

Protein tyrosine phosphatases 1B (PTP1B) of PTPs plays a significant role in the intracellular signaling by dephosphorylating tyrosine residues, and it exhibited increased sensitivity to insulin and resistance to diabetes and obesity (Na et al., 2007). PTP1B, a negative regulators of insulin signaling, has critical roles in the insulin pathway among the many PTPs such as PTP-a, SH2-domain-containing phosphotyrosine phosphatase (SHP2), and leukocyte antigen-related tyrosine phosphatase (LAR) (Nguyen et al., 2013). While PTP1B knockout mice show enhanced the level of insulin sensitivity and glucose homeostasis, PTP1B overexpression was observed to negatively regulates the IR signaling cascade and increased in insulin-resistant states (Uddin et al., 2014). Thus, PTP1B inhibitors could be useful for treating both type 2 diabetes and obesity.

3. Relative mass defect (RMD) analysis and its application

Relative mass defect, called RMD, is one of the mass defect filtering methods, which is usually refers to the deviation of a specific constituent's exacted mass from its nominal mass. The absolute mass defect reflects the ion's elemental composition that the reason is why each element has an appropriate mass defect, and it denotes the sum of the mass defects for all atoms in the molecule. Thus, mass measurement accuracy is frequently insufficient to provide well-defined formula assignments among higher molecular weight compounds with large error (Ekanayaka et al., 2015). However, the RMD reveals the fractional hydrogen content of a specific compound in naturally occurring metabolites that leads to classify ions in a mass spectrum by their relative mass defect (Sleno L., 2012). Each compound class usually has a set trend of mass defect with increasing mass. Although most elements have negative mass defects because of increasing nuclear binding energy with atomic number, hydrogen has the remarkable source for increasing the values of mass defect, +7.825 mDa, and it has a main contribution to the mass defect. RMD is calculated by

dividing mass defect by the monoisotopic mass multiplied by 10^6 because of ppm expression (Ekanayaka et al., 2015), so specific RMD ranges recognize as different compound classes. Therefore, it is convenient for the rapid identification of novel plant and assignments of newly discovered substances to natural product classes.

4. *Cleistocalyx operculatus* (Roxb.) Merr. et L.M. Perry. (Mytaceae)

The genus *Cleistocalyx* (Mytaceae) includes approximately 37 species, and was distributed in all around world. The most popular species, *Clesitocalyx operculatus* (Roxb. Merr. et L.M. Perry, commonly named "Voi" in Vietnamese and "Shui Rong (水榕)" in Chinese, is a famous evergreen plant that is spread throughout various Asia regions such as China, Vietnam and even northern territory of Australia (Dung et al., 2009). The plant has a long history of uses of beverage at the Vietnam and China as a traditional herbal tea and a medicine for the treatment of cold, fever, dysentery, vomiting, indigestion, gastrointestinal disorder, and inflammation (Ha et al., 2016). The chemical constituents, including chalcone, flavanones, flavones, and oleanane- and ursane- type triterpenoids, have been discovered in this plant's buds with variety of biological activities such as cancer cell growth inhibition and cholinesterase inhibition as well as anti-oxidation, anti-hyperglycemia, anti-influenza, and anti-inflammation (Ha et al., 2016). However, there are still few studies on its leaves. Taraxastane-type triterpene, acetophenone, flavanone, and pentacyclic triterpenoids were discovered from the leaves of this plant (Wang et al., 2016). The present study was to provide better understanding about the phytochemical profile of *C. operculatus* leaves. Its biologically active compounds were introduced from the natural sources as ethno-medicines. In addition, its application of RMD was showed to isolate the compounds.

II. Materials and Methods

1. Plant materials

The leaves of *C. Operculatus* were purchased from a market in My Duc district, Hanoi, Vietnam in February 2017 and were identified botanically by Prof. Won Keun Oh, College of Pharmacy, Seoul National University, Seoul, Korea. A voucher specimen (SNU2017-02) was deposited at the Laboratory of Pharmacognosy, College of Pharmacy, Seoul National University, Republic of Korea.

2. Chemicals, reagents and chromatography

2-1. Chemical reagents

- All solvents used for extraction and isolation (*n*-hexane, EtOAc, *n*-BuOH, acetone, MeOH, EtOH, and MeCN) were of analytical grade and HCl and H_2SO_4 for extraction, fractionation, and isolation from Daejung Chemical & Metals (Korea).
- Formic acid was purchased from Sigma Aldrich (USA).
- NMR solvents (chloroform-*d*, methanol-d_4, DMSO-d_6, and pyridine-d_5) were purchased from Cambridge Isotope Laboratories (USA).
- NP silica gel (40-63 μm and 63-200 μm) from ZEOchem AG (Switzerland).
- RP silica gel Cosmosil 75C_{18}-PREP was purchased from Nacalai Tesque (Japan).
- Sephadex LH-20 (18-111 μm) was purchased from GE Healthcare (USA).
- Solvents used for HPLC chromatography (MeCN and MeOH) were purchased from Daejung chemical & Metals (Korea).
- TLC Silica gel 60 F_{254} (20 x 20 cm plate) and TLC Silica gel 60 RP-18 F_{254S} (20 x 20 cm plate) were used from Merck Millipore (USA).

2-2. Bioassay reagents

- Citrate, EDTA, and *p*-NPP were purchased from Sigma-Aldrich (USA).
- DTT was purchased from Roche Diagnostics (USA).
- PTP1B was obtained from BIOMOL International LP (USA).
- Sodium chloride was purchased from OCI Company (Korea).

- Sodium hydroxide was purchased from Junsei Chemical (Japan).

3. Experimental instruments

- Analytical balance: BSA 2245-CW from Sartorius (Germany).
- Autoclave: LAC-5080S from LAB Tech. (Korea).
- Centrifuge (for filtration): AVANTI J2 from Beckman Coulter (USA).
  (for bioassay): FLETA S from Hanil Science (Korea).
- Clean bench: Class II Biological Safety Cabinet from Esco (Korea).
- CO_2 incubator: Forma Series II water jacketed CO_2 incubator from THERMO (USA)
- Drying oven: WFO-700 from EYELA (Japan).
- ELISA Microplate reader: VersaMax from Molecular Devices (USA).
- ESIMS spectrometer: 6130 Quadrupole MS/Agilent, 1260 Infinity from Agilent (USA).
- ESIMS column: Inno C_{18} column (4.6 mm × 250 mm, 5μm particle size), Young Jin Biochrom (Korea).
- Evaporator: KSB-202 from EYELA (Japan).
- Fraction collector: Advantec 2120 from Waters (USA).
- HRESIMS/MS spectrometer: 6530 Q-TOF spectrometer from Agilent (USA).
- HPLC column: Optima Pak C_{18} column (10 × 250 mm, 5 μm particle size) from RS Tech (Korea).
- HPLC system : 321 pump and Gilson UV/VIS 155 detector from Gilson (USA).
- IR spectrometer: JASCO, FT/IR-4200 from Jasco (USA).
- NMR spectrometers
  - Varian Gemini 2000, 300 MHz spectrometer from Agilent (USA).
  - AVANCE digital 400 spectrometer from Bruker (Germany).
  - AVANCE digital 500 spectrometer from Bruker (Germany).
  - JNM-ECA-600 spectrometer from JEOL (USA).
  - AVANCE digital 800 spectrometer from Bruker (Germany).

- Polarimeter: P-2000 with a 10-mm cell from JASCO (USA).
- Shaking incubator: BF-60SIR from BioFree (Korea)
- Sonicator: Powersonic 420, Hwa Shin Tech. (Korea).
- UV lamp: VL-4.LC from Vilber Lourmat (France).
- Water purification system Direct-Q® & Direct-Q UV from Merck (Germany).

4. Extraction and isolation schemes

4-1. Extraction and fractionation of *C. operculatus* leaves

Air dried leaves of *C. operculatus* (2.5 kg) were ground and extracted with 50% aqueous EtOH for the three times at 60 °C for a period of eight hours ultra-sonication. The crude extract (478.7 g) was suspended in distilled water (2 L) and was completely partitioned with *n*-hexane and *n*-BuOH (each 2 L x 3 times) to obtain three fractions. Each fraction was evaporated under low pressure to dry, and 44.2 g of *n*-heaxane-soluble (1.77 % of dried leaves, w/w), 351.5 g of *n*-BuOH-soluble (14.06 % of dried leaves, w/w), and 65.3 g of water-soluble (2.61 % of dried leaves, w/w) fractions (See scheme 1).

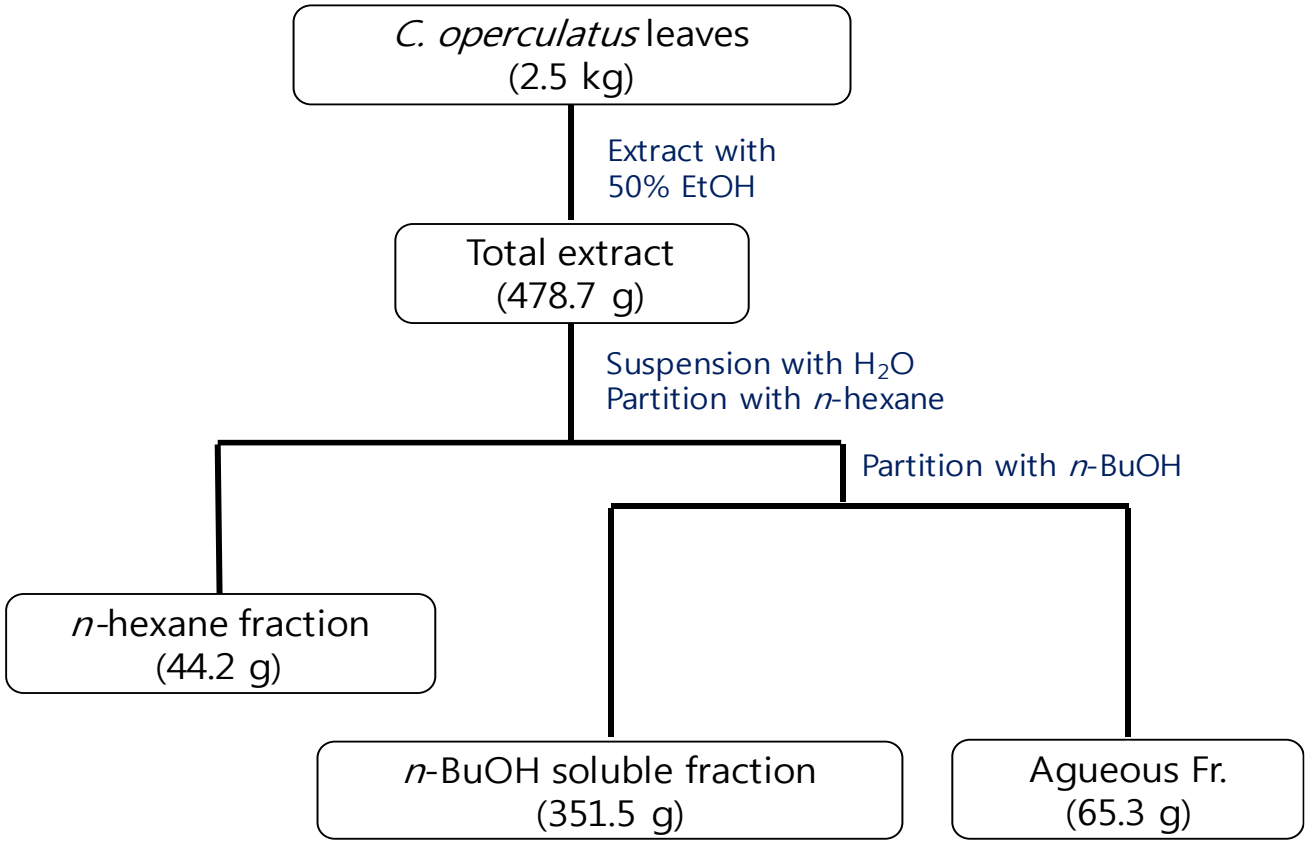

Scheme 1. Extraction and fractionation of *C. operculatus* leaves

4-2. Isolation scheme of *n*-BuOH-soluble fraction

n-BuOH residue (351.5 g) contains a large amount of mixed triterpenoids checked by RMD profiling. The further isolation steps were proceeded as dereplication processes monitored by LC-MS profile. This bioactive *n*-BuOH fraction was chromatographed on a NP silica gel (60-200 mesh) column with a stepwise gradients of *n*-hexane/EtOAc [9:1, 1:1, 0:1, MeOH100%; v/v] as eluant to yield 9 fractions (N1-9). By TLC and LC/MS profiles, the fractions from N1 to N5 contain numerous less oxygenated aglycones of chalcones, flavonoids, and triterpenoids. On the other hand, the more oxygenated compounds were included on the fractions from N6 to N9.

N4 has undergone recrystallization and filtered out by vacuum filtration. The crystal part was directly purified by HPLC [RS Tech Optima Pak C_{18} column (10 × 250 mm, 5 μm particle size)]; mobile phase MeCN in H_2O containing 0.1% HCO_2H (0−43 min: 85-100% MeCN, 43-54 min: 100% MeCN); flow rate 2 mL/min; UV detection at 205 and 254 nm] to yield compounds **6** (t_R = 27.0 min, 3.5 mg) and **7** (t_R = 32.0 min, 14.9 mg). The residue of N4 was also applied to the same system above to isolate compound **4** (t_R = 18.0 min, 11.3 mg), and **11** (t_R = 52.0 min, 5.3 mg) (See scheme 2).

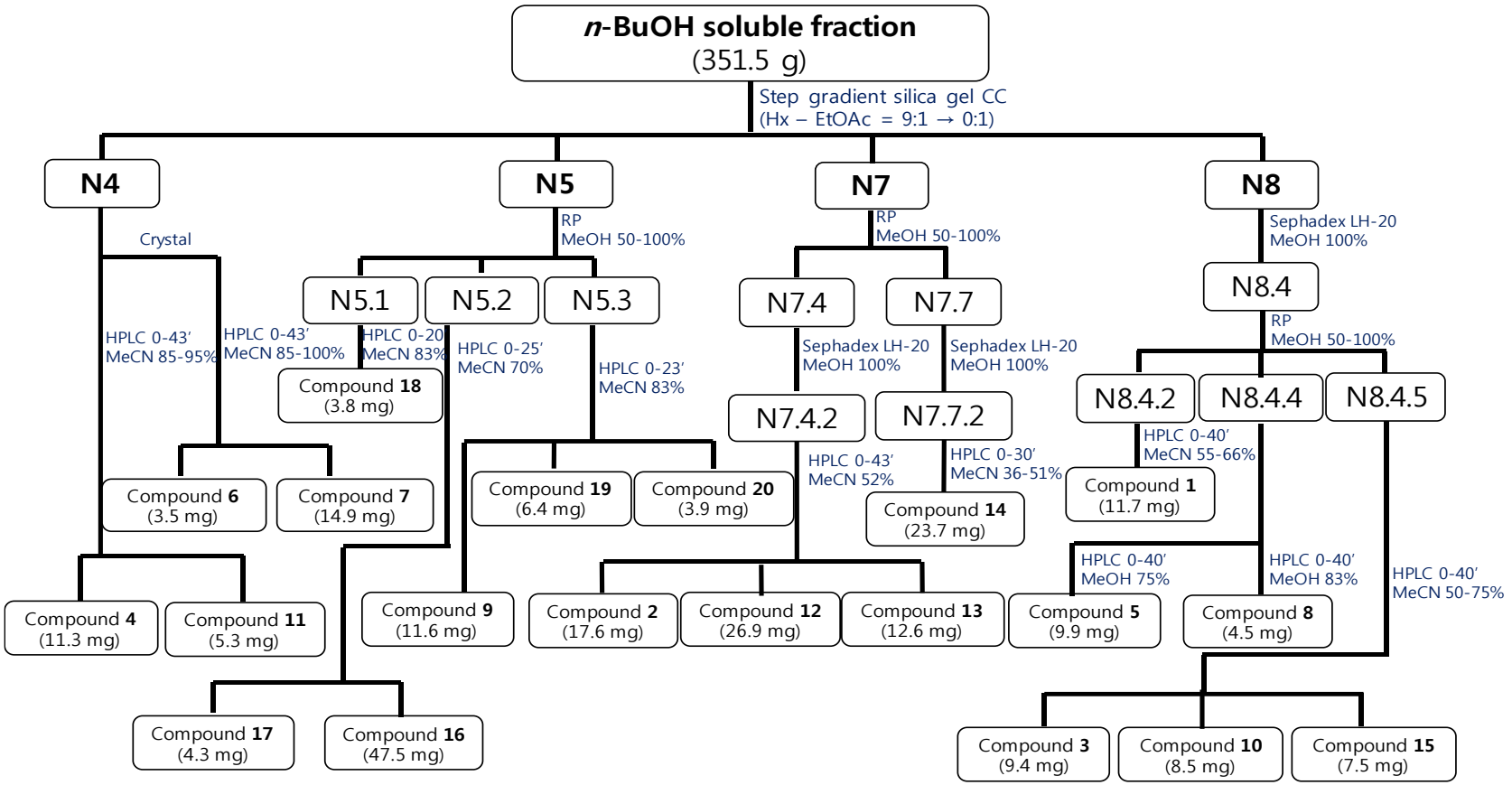

Scheme 2. Isolation scheme of *n*-BuOH fraction of *C. operculatus* leaves

Another fraction, N5, was chromatographed over a RP-C_{18} (4 × 40 cm; 75 μm particle size) Open CC and eluted with a stepwise gradient of MeOH/H_2O (1:1 to 1:0) to afford 4 subfractions (N5.1-N5.4). N5.1 was further applied to HPLC [RS Tech Optima Pak C_{18} column (10 × 250 mm, 5 μm particle size)]; mobile phase MeCN in H_2O containing 0.1% HCO_2H (0−23 min: 83% MeCN, 23-33 min: 100% MeCN); flow rate 2 mL/min; UV detection at 205 and 254 nm] to yield compound **18** (t_R = 12.0 min, 3.8 mg). N5.3 fraction was also purified by same method above to isolate compounds, **9** (t_R = 15.0 min, 11.6 mg), **19** (t_R = 19.0 min, 6.4 mg) and **20** (t_R = 16.5 min, 3.9 mg). N5.2 fraction was purified by HPLC [RS Tech Optima Pak C_{18} column (10 × 250 mm, 5 μm particle size)]; mobile phase MeCN in H_2O containing 0.1% HCO_2H (0−25 min: 70 % MeCN, 25-35 min: 100% MeCN); flow rate 2 mL/min; UV detection at 205 and 254 nm] to yield compounds **16** (t_R = 23.0 min, 47.5 mg) and **17** (t_R = 14.5 min, 4.3 mg) (See scheme 2).

Fraction N7 was further subjected to RP-C18 (4 × 40 cm; 75 μm particle size) Open CC and eluted with a stepwise gradient of MeOH/H_2O (1:1 to 1:0) to afford 9 subfractions (N7.1-N7.9). N7.4 fraction was applied to Sephadex LH-20 (18 – 111 μm) with MeOH/H_2O (1:1 to 1:0) to afford 3 fractions monitored by TLC and LC/MS profile. N7.4.2 as a rich triterpenoids' fraction further applied to semi-preparative HPLC [RS Tech Optima Pak C_{18} column (10 × 250 mm, 5 μm particle size)]; mobile phase MeCN in H_2O containing 0.1% HCO_2H (0−43 min: 52 % MeCN, 43-52 min: 100% MeCN); flow rate 2 mL/min; UV detection at 205 and 254 nm] to yield **2** (t_R = 28.0 min, 17.6 mg), **12** (t_R = 32.0 min, 26.9 mg), and **13** (t_R = 19.0 min, 12.6 mg). The compound **14** (t_R = 28.5 min, 23.7 mg) was isolated from N7.7 by HPLC [RS Tech Optima Pak C_{18} column (10 × 250 mm, 5 μm particle size)]; mobile

phase MeCN in H_2O containing 0.1% HCO_2H (0−30 min: 36-51 % MeCN, 30-40 min: 100% MeCN); flow rate 2 mL/min; UV detection at 205 and 254 nm] (See scheme 2).

The chromatographic purification of N8 fraction by Sephadex LH-20 (18 – 111 μm) with MC/MeOH (1:1 to 0:1) to obtain a rich triterpenoid fraction (N8.4). It was further subjected to ODS Open CC and eluted with a stepwise gradient of MeCN/H_2O (1:1 to 1:0) to afford 7 sub-fractions (N8.4.1-N8.4.7). Compound **3** (t_R = 34.0 min, 9.4 mg), **10** (t_R = 10.5 min, 8.5 mg), and **15** (t_R = 28.0 min, 7.5 mg) were purified by HPLC [RS Tech Optima Pak C_{18} column (10 × 250 mm, 5 μm particle size)]; mobile phase MeCN in H_2O containing 0.1% HCO_2H (0−40 min: 50-75 % MeCN, 40-50 min: 100% MeCN); flow rate 2 mL/min; UV detection at 205 and 254 nm] from N8.4.5 fraction. Fraction N8.4.4 was chromatographed over HPLC [RS Tech Optima Pak C_{18} column (10 × 250 mm, 5 μm particle size)]; mobile phase MeOH in H_2O containing 0.1% HCO_2H (0−40 min: 70-83 % MeOH, 41-50 min: 100% MeOH); flow rate 2 mL/min; UV detection at 205 and 254 nm] to yield the compound **5** (t_R = 16.0 min, 9.9mg) and compound **8** (t_R = 41.0 min, 4.5 mg). While compound **1** (t_R = 39.0 min, 11.7 mg) was purified from HPLC [RS Tech Optima Pak C_{18} column (10 × 250 mm, 5 μm particle size)]; mobile phase MeOH in H_2O containing 0.1% HCO_2H (0−40 min: 55-63 % MeOH, 41-50 min: 100% MeOH); flow rate 2 mL/min; UV detection at 205 and 254 nm] from N8.4.2 fraction (See scheme 2).

4-3. Chemical and spectral properties of isolated compounds

4-3-1. Compound **1**

Brownish gum; $[\alpha]_D^{20}$ -20.8 (c 0.3, MeOH); UV λ_{max} (MeOH) (log ε) (nm) 194 (2.95), 224 (1.96); IR (KBr) ν_{max} (cm^{-1}) 3364, 2946, 2871, 2359, 1706, 1697, 1451, 1389, 1219, 1032; ESIMS m/z 539.3 $[M+Na]^+$, 471.3 $[M-HCOO]^+$, 481.3 $[M-2H_2O+H]^+$, 515.3 $[M-H]^-$; HRESIMS m/z 515.3379 $[M-H]^-$ (calcd for $C_{31}H_{48}O_6$ 515.3378); see Table 1 for ^1H NMR (600 MHz, pyridine-d_5) and ^{13}C NMR (150 MHz, pyridine-d_5).

4-3-2. Compound **2**

White amorphous powder; $[\alpha]_D^{20}$ +81.9 (c 0.3, MeOH); UV λ_{max} (MeOH) (log ε) (nm) 196 (3.16); IR (KBr) ν_{max} (cm^{-1}) 3365, 2924, 1775, 1647, 1356, 1218, 1149, 1057, 1033; ESIMS m/z 469.3 $[M+H]^+$, 451.3 $[M-H_2O+H]^+$, 491.2 $[M+Na]^+$, 513.3 $[M+HCOO]^-$; HRESIMS m/z 513.2856 $[M+HCOO]^-$ (calcd for $C_{29}H_{40}O_5$ 513.2858); see Table 1 for ^1H NMR (600 MHz, pyridine-d_5) and ^{13}C NMR (150 MHz, pyridine-d_5).

4-3-3. Compound **3**

White amorphous powder; $[\alpha]_D^{20}$ +4.2 (c 0.3, MeOH); UV λ_{max} (MeOH) (log ε) (nm) 196 (2.85) 226 (2.28); IR (KBr) ν_{max} (cm^{-1}) 3245, 2934, 2889, 2359, 2342, 1718, 1680, 1641, 1452, 1212, 1167, 1033; ESIMS m/z 539.3 $[M+Na]^+$, 471.3 [M-

HCOO]$^+$, 453.3 [M-H_2O-HCOO]$^+$, 515.3 [M-H]$^-$; HRESIMS m/z 515.3381 [M-H]$^-$ (calcd for $C_{29}H_{40}O_5$ 515.3378); see Table 1 for ^{1}H NMR (600 MHz, pyridine-d_5) and ^{13}C NMR (150 MHz, pyridine-d_5).

4-3-4. Compound **4**

White amorphous powder; $[\alpha]_D^{20}$ +5.0 (c 0.3, MeOH); UV λ_{max} (MeOH) (log ε) (nm) 194 (2.17) 226 (2.33); IR (KBr) ν_{max} (cm^{-1}) 3388, 2966, 2873, 2359, 1704, 1680, 1658, 1643, 1641, 1453, 1165, 1015; ESIMS m/z 501.3 [M+H]$^+$, 483.3 [M-H_2O+H]$^+$, 455.3 [M-HCOO]$^+$, 437.3 [M-H_2O-HCOO]$^+$, 499.3 [M-H]$^-$, 567.3 [M-H+HCOONa]$^-$.

^{1}H NMR (800 MHz, pyridine-d_5, δ in ppm) : δ 5.05 (1 H, br s, H-29a), δ 4.83 (1 H, br s, H-29b), δ 3.77 (3 H, s, -OCH_3-28), δ 3.51 (1 H, td, *J*= 4.0, 11.8 Hz, H-19), δ 3.25 (1 H, dd, *J*= 4.7, 10.9 Hz, H-3), δ 2.12 (1 H, t, *J*= 11.0 Hz, H-18), δ 1.90 (3 H, s, CH_3-30), δ 1.18 (3 H, s, CH_3-26), δ 1.08 (3 H, s, CH_3-23), δ 1.01 (3 H, s, CH_3-24), δ 0.92 (3 H, s, CH_3-25).

^{13}C NMR (200 MHz, pyridine-d_5, δ in ppm) : δ 39.8 (C-1), δ 28.8 (C-2), δ 78.3 (C-3), δ 39.9 (C-4), δ 56.5 (C-5), δ 19.3 (C-6), δ 38.8 (C-7), δ 41.3 (C-8), δ 52.2 (C-9), δ 38.3 (C-10), δ 21.7 (C-11), δ 27.3 (C-12), δ 40.7 (C-13), δ 60.3 (C-14), δ 29.0 (C-15), δ 35.4 (C-16), δ 57.2 (C-17), δ 52.9 (C-18), δ 48.1 (C-19), δ 151.1 (C-20), δ 31.3 (C-21), δ 37.7 (C-22), δ 29.0 (C-23), δ 17.0 (C-24), δ 17.5 (C-25), δ 17.8 (C-26), δ 178.8 (C-27), δ 177.3 (C-28), δ 111.0 (C-29), δ 19.6 (C-30), δ 52.0 (OCH_3-28).

4-3-5. Compound **5**

White amorphous powder; $[\alpha]_D^{20}$ +14.4 (c 0.3, MeOH); UV λ_{max} (MeOH) (log ε) (nm) 208 (2.38); IR (KBr) ν_{max} (cm^{-1}) 3335, 2928, 2876, 2359, 1687, 1457, 1389, 1271, 1157, 1049, 1033; ESIMS m/z 527.3 $[M+Na]^+$, 469.3 $[M-2H_2O+H]^+$, 451.3 $[M-3H_2O+H]^+$, 503.3 $[M-H]^-$.

^{1}H NMR (600 MHz, pyridine-d_5, δ in ppm) : δ 5.60 (1 H, br s, H-12), δ 4.27 (1 H, td, *J*= 4.3, 9.7 Hz, H-2), δ 4.22 (1 H, m, H-3), δ 4.21 (1 H, d, *J*= 10.1 Hz, H-23b), δ 3.73 (1 H, d, *J*= 10.5 Hz, H-23a), δ 3.06 (1 H, s, H-18), δ 1.67 (3 H, s, CH_3-29), δ 1.43 (3 H, s, CH_3-27), δ 1.14 (3 H, s, CH_3-25), δ 1.13 (3 H, d, *J*= 6.6 Hz, CH_3-30) , δ 1.11 (3 H, s, CH_3-26) , δ 1.09 (3 H, s, CH_3-24).

^{13}C NMR (150 MHz, pyridine-d_5, δ in ppm) : δ 48.3 (C-1), δ 69.4 (C-2), δ 78.8 (C-3), δ 44.1 (C-4), δ 48.5 (C-5), δ 19.2 (C-6), δ 33.7 (C-7), δ 41.0 (C-8), δ 48.3 (C-9), δ 38.9 (C-10), δ 24.7 (C-11), δ 128.5 (C-12), δ 140.5 (C-13), δ 42.7 (C-14), δ 29.8 (C-15), δ 26.9 (C-16), δ 48.8 (C-17), δ 55.1 (C-18), δ 73.2 (C-19), δ 42.9 (C-20), δ 27.4 (C-21), δ 39.0 (C-22), δ 67.1 (C-23), δ 14.8 (C-24), δ 17.3 (C-25), δ 17.9 (C-26), δ 27.6 (C-27), δ 181.2 (C-28), δ 25.2 (C-29), δ 17.8 (C-30).

4-3-6. Compound **6**

White amorphous powder; $[\alpha]_D^{20}$ -4.3 (c 0.3, MeOH); UV λ_{max} (MeOH) (log ε) (nm) 196 (3.00); IR (KBr) ν_{max} (cm^{-1}) 3398, 2994, 2941, 2868, 2359, 2341,

1681, 1641, 1452, 1236, 1033, 1012; ESIMS m/z 439.3 $[M\text{-}H2O+H]^+$, 455.4 $[M\text{-}H]^-$.

^{1}H NMR (300 MHz, pyridine-d_5, δ in ppm) : δ 4.96 (1 H, br s, H-29a), δ 4.79 (1 H, br s, H-29b), δ 3.55 (1 H, m, H-19), δ 3.47 (1 H, dd, *J*= 8.7, 7.4 Hz, H-3), δ 2.75 (1 H, td, *J*= 2.9, 11.4 Hz, H-13), δ 1.81 (3 H, s, CH_3-30), δ 1.24 (3 H, s, CH_3-23), δ 1.09 (3 H, s, CH_3-27), δ 1.08 (3 H, s, CH_3-24), δ 1.03 (3 H, s, CH_3-26), δ 0.84 (3 H, s, CH_3-25).

^{13}C NMR (75 MHz, pyridine-d_5, δ in ppm) : δ 39.5 (C-1), δ 28.3 (C-2), δ 78.1 (C-3), δ 39.3 (C-4), δ 55.9 (C-5), δ 18.8 (C-6), δ 34.8 (C-7), δ 41.1 (C-8), δ 51.0 (C-9), δ 37.5 (C-10), δ 21.2 (C-11), δ26.1 (C-12), δ 38.6 (C-13), δ 42.8 (C-14), δ 30.3 (C-15), δ 32.9 (C-16), δ 56.6 (C-17), δ 49.7 (C-18), δ 47.8 (C-19), δ 151.3 (C-20), δ 31.2 (C-21), δ 37.6 (C-22), δ 28.7 (C-23), δ 16.4 (C-24), δ 16.4 (C-25), δ 16.3 (C-26), δ 14.9 (C-27), δ 178.9 (C-28), δ 109.9 (C-29), δ 19.5 (C-30).

4-3-7. Compound **7**

White amorphous powder; $[\alpha]_D^{20}$ +43.6 (c 0.3, MeOH); UV λ_{max} (MeOH) (log ε) (nm) 196 (2.56); IR (KBr) ν_{max} (cm^{-1}) 3393, 2937, 2865, 2359, 2348, 1688, 1460, 1386, 1048, 1033; ESIMS m/z 439.3 $[M\text{-}H2O+H]^+$, 455.4 $[M\text{-}H]^-$.

^{1}H NMR (400 MHz, chloroform-*d*, δ in ppm) : δ 5.27 (1 H, t-like s, H-12), δ 3.21 (1 H, dd, *J*= 3.8, 10.5 Hz, H-3), δ 2.82 (1 H, dd, *J*= 4.0, 14.1 Hz, H-18), δ 1.13 (3 H, s, CH_3-27), δ 0.98 (3 H, s, CH_3-23), δ 0.92 (3 H, s, CH_3-30), δ 0.91 (3 H, s, CH_3-29), δ 0.90 (3 H, s, CH_3-25), δ 0.77 (3 H, s, CH_3-24) , δ 0.74 (3 H, s, CH_3-26).

^{13}C NMR (100 MHz, chloroform-*d*, δ in ppm) : δ 38.5 (C-1), δ 28.2 (C-2), δ 79.2 (C-3), δ 38.9 (C-4), δ 55.3 (C-5), δ 18.4 (C-6), δ 32.6 (C-7), δ 39.4 (C-8), δ 47.8 (C-9), δ 37.2 (C-10), δ 23.5 (C-11), δ 122.8 (C-12), δ 143.8 (C-13), δ 41.1 (C-14), δ 27.3 (C-15), δ 23.0 (C-16), δ 46.7 (C-17), δ 41.7 (C-18), δ 46.0 (C-19), δ 30.8 (C-20), δ 33.9 (C-21), δ 33.2 (C-22), δ 27.8 (C-23), δ 15.7 (C-24), δ 15.5 (C-25), δ 17.3 (C-26), δ 26.1 (C-27), δ 183.6 (C-28), δ 32.7 (C-29), δ 23.7 (C-30).

4-3-8. Compound **8**

White amorphous powder; $[\alpha]_D^{20}$ +9.3 (c 0.3, MeOH); UV λ_{max} (MeOH) (log ε) (nm) 190 (1.99) 224 (0.99); IR (KBr) ν_{max} (cm^{-1}) 3366, 2937, 2864, 2360, 1748, 1049, 1033; ESIMS m/z 489.3 $[M+H]^+$, 511.3 $[M+Na]^+$, 533.4 $[M+HCOO]^-$.

^{1}H NMR (600 MHz, pyridine-d_5, δ in ppm) : δ 4.20 (1 H, br s, H-12), δ 4.13 (1 H, td, *J*= 4.5, 11.2 Hz, H-2), δ 3.38 (1 H, d, *J*= 9.4 Hz, H-3), δ 1.61 (3 H, s, CH_3-27), δ 1.35 (3 H, s, CH_3-26), δ 1.29 (3 H, s, CH_3-23), δ 1.12 (3 H, s, H-24) , δ 1.02 (3 H, s, CH_3-25), δ 0.92 (3 H, s, CH_3-30), δ 0.82 (3 H, s, CH_3-29).

^{13}C NMR (125 MHz, pyridine-d_5, δ in ppm) : δ 48.6 (C-1), δ 69.2 (C-2), δ 84.2 (C-3), δ 40.4 (C-4), δ 56.4 (C-5), δ 18.9 (C-6), δ 34.9 (C-7), δ 43.2 (C-8), δ 45.6 (C-9), δ 38.6 (C-10), δ 30.0 (C-11), δ 76.2 (C-12), δ 92.0 (C-13), δ 43.3 (C-14), δ 28.8 (C-15), δ 22.2 (C-16), δ 45.5 (C-17), δ 52.1 (C-18), δ 40.0 (C-19), δ 32.1 (C-20), δ 35.0 (C-21), δ 28.8 (C-22), δ 29.7 (C-23), δ 17.9 (C-24), δ 18.4 (C-25), δ 19.6 (C-26), δ 19.2 (C-27), δ 180.2 (C-28) , δ 24.3 (C-29), δ 33.7 (C-30).

4-3-9. Compound **9**

White amorphous powder; $[\alpha]_D^{20}$ +32.3 (c 0.3, MeOH); UV λ_{max} (MeOH) (log ε) (nm) 196 (2.83); IR (KBr) ν_{max} (cm^{-1}) 3392, 2940, 2864, 2359, 1704, 1688, 1052, 1033; ESIMS m/z 495.3 $[M+Na]^+$, 409.3 $[M-H_2O-HCOO]^+$, 471.3 $[M-H]^-$.

^{1}H NMR (400 MHz, pyridine-d_5, δ in ppm) : δ 5.49 (1 H, t, *J*= 3.2 Hz, H-12), δ 4.12 (1 H, m, H-2), δ 3.42 (1 H, d, *J*= 9.4 Hz, H-3), δ 3.31 (1 H, dd, *J*= 3.8, 13.6 Hz, H-18), δ 1.29, 1.28, 1.10, 1.04, 1.02, 1.01, 0.97 (each 3 H, s).

^{13}C NMR (100 MHz, pyridine-d_5, δ in ppm) : δ 48.2 (C-1), δ 69.1 (C-2), δ 84.3 (C-3), δ 40.3 (C-4), δ 56.4 (C-5), δ 19.3 (C-6), δ 33.8 (C-7), δ 40.4 (C-8), δ 48.6 (C-9), δ 39.0 (C-10), δ 24.4 (C-11), δ 123.0 (C-12), δ 145.3 (C-13), δ 42.7 (C-14), δ 28.8 (C-15), δ 24.2 (C-16), δ 47.2 (C-17), δ 42.5 (C-18), δ 46.9 (C-19), δ 31.4 (C-20), δ 34.7 (C-21), δ 33.7 (C-22), δ 29.8 (C-23), δ 17.3 (C-24), δ 18.0 (C-25), δ 18.2 (C-26), δ 26.7 (C-27), δ 180.7 (C-28), δ 33.7 (C-29), δ 24.2 (C-30).

4-3-10. Compound **10**

White amorphous powder; $[\alpha]_D^{20}$ -5.8 (c 0.3, MeOH); UV λ_{max} (MeOH) (log ε) (nm) 196 (2.81) 226 (2.26); IR (KBr) ν_{max} (cm^{-1}) 3384, 2943, 2868, 2845, 2359, 2842, 1705, 1689, 1508, 1375, 1052, 1033; ESIMS m/z 495.3 $[M+Na]^+$, 409.3 $[M-H_2O-HCOO]^+$, 471.3 $[M-H]^-$.

^{1}H NMR (800 MHz, pyridine-d_5, δ in ppm) : δ 4.92 (1 H, br s, H-29b), δ 4.75 (1 H, br s, H-29a), δ 4.08 (1 H, td, *J*= 4.4, 9.6 Hz, H-2), δ 3.51 (1 H, td, *J*=

5.4, 10.9 Hz, H-19), δ 3.38 (1 H, d, *J*= 9.4 Hz, H-3), δ 2.70 (1 H, td, *J*= 3.4, 12.4 Hz , H-13), δ 2.60 (1 H, dt, *J*= 3.0, 12.7 Hz , H-16), δ 2.30 (1 H, dd, *J*= 4.6, 12.5 Hz , H-1), δ 1.76 (3 H, s, CH_3-30), δ 1.24 (3 H, s, CH_3-23) , δ 1.04 (3 H, s, CH_3-24) , δ 1.03 (3 H, s, CH_3-26) , δ 1.03 (3 H, s, CH_3-27), δ 0.89 (3 H, s, CH_3-25).

^{13}C NMR (200 MHz, pyridine-d_5, δ in ppm) : δ 48.7 (C-1), δ 69.3 (C-2), δ 84.3 (C-3), δ 40.4 (C-4), δ 56.5 (C-5), δ 19.3 (C-6), δ 35.2 (C-7), δ 41.6 (C-8), δ 51.4 (C-9), δ 38.1 (C-10), δ 21.8 (C-11), δ 26.5 (C-12), δ 39.2 (C-13), δ 43.3 (C-14), δ 30.7 (C-15), δ 33.3 (C-16), δ 57.1 (C-17), δ 50.2 (C-18), δ 48.2 (C-19), δ 151.8 (C-20), δ 31.6 (C-21), δ 39.0 (C-22), δ 29.7 (C-23), δ 18.0 (C-24), δ 18.1 (C-25), δ 16.9 (C-26), δ 15.3 (C-27), δ 179.3 (C-28), δ 110.5 (C-29), δ 19.9 (C-30).

4-3-11. Compound **11**

White amorphous powder; $[\alpha]_D^{20}$ +53.6 (c 0.3, MeOH); UV λ_{max} (MeOH) (log ε) (nm) 198 (2.58) 228 (1.86); IR (KBr) ν_{max} (cm^{-1}) 3335, 2923, 2862, 2359, 2342, 1460, 1362, 1047, 1033, 1006.

^{1}H NMR (600 MHz, chloroform-*d*, δ in ppm) : δ 5.20 (1 H, t, *J*= 3.6 Hz, H-12), δ 3.56 (1 H, d, *J*= 10.9 Hz, H-28), δ 3.23 (1 H, dd, *J*= 11.3 Hz, H-3), δ 3.21 (1 H, d, *J*= 10.9 Hz, H-28), δ 1.98 (1 H, dd, *J*= 4.3, 13.4 Hz, H-18), δ 1.16 (3 H, s, H-27), δ 0.99 (3 H, s, CH_3-23), δ 0.94 (3 H, s, CH_3-26), δ 0.93 (3 H, s, H-25), δ 0.89 (3 H, s, CH_3-29) , δ 0.87 (3 H, s, CH_3-30) , δ 0.79 (3 H, s, CH_3-24).

^{13}C NMR (150 MHz, chloroform-*d*, δ in ppm) : δ 38.7 (C-1), δ 27.4 (C-2), δ 79.2 (C-3), δ 38.9 (C-4), δ 55.3 (C-5), δ 18.5 (C-6), δ 32.7 (C-7), δ 39.9 (C-8), δ 47.7 (C-9), δ 37.1 (C-10), δ 23.7 (C-11), δ 122.5 (C-12), δ 144.4 (C-13), δ 41.9 (C-

14), δ 25.7 (C-15), δ 22.2 (C-16), δ 37.1 (C-17), δ 42.5 (C-18), δ 46.6 (C-19), δ 31.1 (C-20), δ 34.2 (C-21), δ 31.2 (C-22), δ 28.2 (C-23), δ 15.7 (C-24), δ 15.7 (C-25), δ 16.9 (C-26), δ 26.1 (C-27), δ 69.9 (C-28), δ 33.3 (C-29), δ 23.7 (C-30).

4-3-12. Compound **12**

White amorphous powder; $[\alpha]_D^{20}$ +54.0 (c 0.3, MeOH); UV λ_{max} (MeOH) (log ε) (nm) 194 (3.00); IR (KBr) ν_{max} (cm^{-1}) 3388, 2870, 2843, 2359, 1772, 1761, 1650, 1451, 1360, 1137, 1057, 1017; ESIMS m/z 471.3 $[M+H]^+$, 493.2 $[M+Na]^+$, 515.4 $[M+HCOO]^-$.

^{1}H NMR (800 MHz, pyridine-d_5, δ in ppm) : δ 5.88 (1 H, br s, H-23b), δ 4.98 (1 H, br s, H-23a), δ 4.36 (1 H, dt, *J*= 1.9, 8.8 Hz, H-3), δ 4.12 (1 H, m, H-2), δ 3.33 (1 H, dd, *J*= 2.4, 3.4 Hz, H-11), δ 3.11 (1 H, d, *J*= 3.8 Hz, H-12), δ 2.62 (1 H, dd, *J*= 4.9, 12.6 Hz, H-1b), δ 1.85 (1 H, d, *J*= 11.7 Hz, H-18), δ 1.78 (1 H, m, H-5), δ 1.70 (1 H, m, H-1a), δ 1.34 (3 H, d, *J*= 6.2 Hz, H-29), δ 1.18 (3 H, s, CH_3-26), δ 1.17 (3 H, s, CH_3-27), δ 0.92 (3 H, d, *J*= 6.5 Hz, H-30), , δ 0.91 (3 H, s, CH_3-25).

^{13}C NMR (200 MHz, pyridine-d_5, δ in ppm) : δ 48.2 (C-1), δ 73.7 (C-2), δ 79.9 (C-3), δ 151.9 (C-4), δ 50.3 (C-5), δ 21.2 (C-6), δ 30.5 (C-7), δ 42.2 (C-8), δ 50.2 (C-9), δ 38.6 (C-10), δ 55.5 (C-11), δ 56.9 (C-12), δ 89.5 (C-13), δ 42.3 (C-14), δ 27.5 (C-15), δ 23.5 (C-16), δ 45.7 (C-17), δ 60.9 (C-18), δ 40.8 (C-19), δ 38.0 (C-20), δ 31.2 (C-21), δ 32.4 (C-22), δ 105.7 (C-23), δ 16.3 (C-25), δ 20.8 (C-26), δ 16.9 (C-27), δ 179.3 (C-28), δ 18.1 (C-29), δ 20.0 (C-30).

4-3-13. Compound **13**

White amorphous powder; $[\alpha]_D^{20}$ +51.4 (c 0.3, MeOH); UV λ_{max} (MeOH) (log ε) (nm) 196 (3.15); IR (KBr) ν_{max} (cm^{-1}) 3392, 2966, 2934, 2866, 2359, 1688, 1054, 1033, 1016; ESIMS m/z 495.3 $[M+Na]^+$, 455.3 $[M-H_2O+H]^+$, 437.2 $[M-2H_2O+H]^+$, 471.3 $[M-H]^-$.

^{1}H NMR (500 MHz, pyridine-d_5, δ in ppm) : δ 5.85 (1 H, br s, H-23b), δ 5.61 (1 H, br s, H-12), δ 5.07 (1 H, br s, OH-19), δ 4.95 (1 H, br s, H-23a), δ 4.36 (1 H, d, *J*= 8.75 Hz, H-3), δ 4.05 (1 H, m, H-2), δ 3.13 (1 H, td, *J*= 3.9, 12.8 Hz, H-16b), δ 3.07 (1 H, s, H-18), δ 2.07 (1 H, m, H-16a), δ 1.87 (1 H, t, *J*= 8.75, H-5), δ 1.54 (1 H, m, H-20), δ 1.75 (3 H, s, H-27), δ 1.46 (3 H, s, CH_3-29), δ 1.15 (3 H, s, CH_3-26), δ 1.14 (3 H, d, *J*= 6.0 Hz, H-30), δ 0.85 (3 H, s, CH_3-25).

^{13}C NMR (125 MHz, pyridine-d_5, δ in ppm) : δ 48.6 (C-1), δ 74.0 (C-2), δ 80.0 (C-3), δ 153.0 (C-4), δ 51.2 (C-5), δ 22.1 (C-6), δ 32.5 (C-7), δ 40.9 (C-8), δ 45.7 (C-9), δ 39.3 (C-10), δ 25.5 (C-11), δ 128.6 (C-12), δ 140.7 (C-13), δ 42.8 (C-14), δ 29.7 (C-15), δ 26.9 (C-16), δ 48.8 (C-17), δ 55.2 (C-18), δ 73.2 (C-19), δ 42.9 (C-20), δ 27.4 (C-21), δ 39.0 (C-22), δ 105.1 (C-23), δ 15.6 (C-25), δ 17.7 (C-26), δ 25.2 (C-27), δ 181.2 (C-28), δ 27.6 (C-29), δ 17.3 (C-30).

4-3-14. Compound **14**

White amorphous powder; $[\alpha]_D^{20}$ +20.9 (c 0.3, MeOH); UV λ_{max} (MeOH) (log ε) (nm) 194 (2.49); IR (KBr) ν_{max} (cm^{-1}) 3384, 2980, 2942, 1688, 1679, 1640, 1052, 1033; ESIMS m/z 471.3 $[M\text{-}H_2O+H]^+$, 511.3 $[M+Na]^+$, 487.3 $[M-H]^-$.

^{1}H NMR (500 MHz, pyridine-d_5, δ in ppm) : δ 5.45 (1 H, t-like s, H-12), δ 4.20 (1 H, m, H-2), δ 4.20 (1 H, m, H-23b), δ 3.71 (1 H, d, *J*= 10.3 Hz, H-23a), δ 3.28 (1 H, d, *J*= 10.6 Hz, H-3), δ 1.18, 1.06, 1.06, 1.03, 0.97, 0.89 (each 3 H, s).

^{13}C NMR (125 MHz, pyridine-d_5, δ in ppm) : δ 48.2 (C-1), δ 69.3 (C-2), δ 78.7 (C-3), δ 44.1 (C-4), δ 48.7 (C-5), δ 19.0 (C-6), δ 33.4 (C-7), δ 40.3 (C-8), δ 48.4 (C-9), δ 38.9 (C-10), δ 24.4 (C-11), δ 123.0 (C-12), δ 145.3 (C-13), δ 42.7 (C-14), δ 28.8 (C-15), δ 24.1 (C-16), δ 47.1 (C-17), δ 42.4 (C-18), δ 46.9 (C-19), δ 31.4 (C-20), δ 34.7 (C-21), δ 33.7 (C-22), δ 67.0 (C-23), δ 14.8 (C-24), δ 18.0 (C-25), δ 17.8 (C-26), δ 26.6 (C-27), δ 180.7 (C-28), δ 33.7 (C-29), δ 24.2 (C-30).

4-3-15. Compound **15**

White amorphous powder; $[\alpha]_D^{20}$ +38.6 (c 0.3, MeOH); UV λ_{max} (MeOH) (log ε) (nm) 196 (2.55); IR (KBr) ν_{max} (cm^{-1}) 3389, 2950, 2844, 2359, 2341, 1688, 1644, 1054, 1033, 1015; ESIMS m/z 479.3 $[M+Na]^+$, 455.3 $[M-H]^-$.

^{1}H NMR (800 MHz, pyridine-d_5, δ in ppm) : δ 5.86 (1 H, br s, H-23b), δ 5.50 (1 H, br s, H-12), δ 4.95 (1 H, br s, H-23a), δ 4.36 (1 H, d, *J*= 8.8 Hz, H-3), δ 4.05 (1 H, m, H-2), δ 2.64 (1 H, br d, *J*= 11.4 Hz , H-18), δ 1.22 (3 H, s, CH_3-27), δ 1.09 (3 H, s, CH_3-26), δ 1.00 (3 H, d, *J*= 6.4 Hz, CH_3-29), δ 0.97 (3 H, d, *J*= 6.4 Hz, H-30), δ 0.83 (3 H, s, CH_3-25).

^{13}C NMR (200 MHz, pyridine-d_5, δ in ppm) : δ 48.7 (C-1), δ 73.9 (C-2), δ 80.0 (C-3), δ 153.0 (C-4), δ 51.1 (C-5), δ 21.9 (C-6), δ 32.4 (C-7), δ 39.9 (C-8), δ 45.9 (C-9), δ 39.2 (C-10), δ 25.4 (C-11), δ 126.2 (C-12), δ 140.0 (C-13), δ 43.2 (C-14), δ 29.0 (C-15), δ 25.1 (C-16), δ 48.5 (C-17), δ 54.1 (C-18), δ 39.9 (C-19), δ 40.5 (C-20), δ 31.5 (C-21), δ 37.9 (C-22), δ 105.1 (C-23), δ 15.7 (C-25), δ 17.9 (C-26), δ 24.3 (C-27), δ 180.4 (C-28), δ 18.0 (C-29), δ 21.9 (C-30).

4-3-16. Compound **16**

Yellowish amorphous powder; $[\alpha]_D^{20}$ -4.0 (c 0.3, MeOH); UV λ_{max} (MeOH) (log ε) (nm) 200 (3.25) 340 (3.13); IR (KBr) ν_{max} (cm^{-1}) 3445, 3419, 2936, 2359, 1628, 1611, 1564, 1350, 1167, 991, 970; ESIMS m/z 299.1 $[M+H]^+$, 297.1 $[M-H]^-$.

^{1}H NMR (800 MHz, chloroform-*d*, δ in ppm) : δ 13.63 (1 H, br s, OH-4'), δ 8.00 (1 H, d, *J*= 15.6 Hz, H-α), δ 7.85 (1 H, d, *J*= 15.7 Hz, H-β), δ 7.65 (2 H, dd, *J*= 1.2, 7.9 Hz, H-2 and H-6), δ 7.41 (3 H, m, H-3, H-4 and H-5), δ 5.56 (1 H, br s, OH-4'), δ 3.66 (3 H, s, OCH_3-5), δ 2.16 (3 H, s, CH_3-5'), δ 2.14 (3 H, s, CH_3-3').

^{13}C NMR (200 MHz, chloroform-*d*, δ in ppm) : δ 135.5 (C-1), δ 128.5 (C-2), δ 129.1 (C-3), δ 130.4 (C-4), δ 129.1 (C-5), δ 128.5 (C-6), δ 126.8 (C-α), δ 143.1 (C-β), δ 193.5 (C=O), δ 109.2 (C-1'), δ 159.0 (C-2'), δ 109.1 (C-3'), δ 159.4 (C-4'), δ 106.8 (C-5'), δ 162.2 (C-6'), δ 62.5 (OCH_3-5), δ 8.4 (CH_3-5'), δ 7.7 (CH_3-3').

4-3-17. Compound **17**

Brownish gum; $[\alpha]_D^{20}$ +6.6 (c 0.3, MeOH); UV λ_{max} (MeOH) (log ε) (nm) 198 (3.29) 216 (3.21) 296 (3.17); IR (KBr) ν_{max} (cm^{-1}) 3398, 2981, 2952, 2842, 1658, 1639, 1451, 1116, 1018; ESIMS m/z 285.1 $[M+H]^+$, 283.2 $[M-H]^-$.

^{1}H NMR (800 MHz, DMSO-d_6, δ in ppm) : δ 12.36 (1 H, br s, OH-5), δ 7.51 (2 H, d, *J*= 7.4 Hz, H-2’ and H-6’), δ 7.43 (2 H, t, *J*= 7.4 Hz, H-3’ and H-5’), δ 7.37 (1 H, t, *J*= 7.4 Hz, H-4’), δ 5.55 (1 H, dd, *J*= 3.1, 12.2 Hz, H-2), δ 3.18 (1 H, dd, *J*= 12.3, 17.0 Hz, H-3α), δ 2.84 (1 H, dd, *J*= 3.3, 17.0 Hz, H-3β), δ 1.97 (3 H, s, CH_3-6), δ 1.96 (3 H, s, CH_3-8).

^{13}C NMR (200 MHz, DMSO-d_6, δ in ppm) : δ 77.9 (C-2), δ 42.2 (C-3), δ 196.6 (C-4), δ 101.8 (C-4a), δ 158.5 (C-5), δ 103.4 (C-6), δ 162.6 (C-7) , δ 102.7 (C-8), δ 157.2 (C-8a), δ 139.2 (C-1’), δ 126.3 (C-2’), δ 128.6 (C-3’), δ 128.4 (C-4’), δ 128.6 (C-5’), δ 126.3 (C-6’), δ 8.3 (CH_3-6), δ 7.7 (CH_3-8).

4-3-18. Compound **18**

Brownish gum; $[\alpha]_D^{20}$ -2.9 (c 0.3, MeOH); UV λ_{max} (MeOH) (log ε) (nm) 192 (3.05) 218 (2.91) 284 (2.70); IR (KBr) ν_{max} (cm^{-1}) 3398, 2954, 2843, 1648, 1535, 1109, 1017; ESIMS m/z 299.2 $[M+H]^+$, 297.2 $[M-H]^-$.

^{1}H NMR (400 MHz, chloroform-*d*, δ in ppm) : δ 7.46 (2 H, d, *J*= 7.2 Hz, H-2’ and H-6’), δ 7.42 (1 H, t, *J*= 7.4 Hz, H-3’ and H-5’), δ 7.37 (1 H, t, *J*= 7.0 Hz, H-4’), δ 5.42 (1 H, dd, *J*= 2.5, 12.8 Hz, H-2), δ 3.81 (3 H, s, OCH_3-5), δ 2.97 (1 H,

dd, *J*= 13.0, 16.7 Hz, H-3α), δ 2.84 (1 H, dd, *J*= 2.8, 16.6 Hz, H-3β), δ 2.13 (3 H, s, CH_3-6), δ 2.13 (3 H, s, CH_3-8).

^{13}C NMR (100 MHz, chloroform-*d*, δ in ppm) : δ 78.6 (C-2), δ 45.8 (C-3), δ 189.9 (C-4), δ 109.2 (C-4a), δ 157.8 (C-5), δ 111.4 (C-6), δ 159.0 (C-7) , δ 107.1 (C-8), δ 159.7 (C-8a), δ 139.4 (C-1'), δ 126.0 (C-2'), δ 128.9 (C-3'), δ 128.6 (C-4'), δ 128.9 (C-5'), δ 126.0 (C-6'), δ 8.0 (CH_3-6) , δ 8.3 (CH_3-8), δ 61.4 (OCH_3-5).

4-3-19. Compound **19**

White amorphous powder; $[\alpha]_D^{20}$ +26.2 (c 0.3, MeOH); UV λ_{max} (MeOH) (log ε) (nm) 192 (2.86) 210 (2.80) 224 (2.73) 310 (3.02); IR (KBr) ν_{max} (cm^{-1}) 3391, 2972, 2950, 2844, 1688, 1640, 1516, 1452, 1050, 1033, 1016; ESIMS m/z 619.3 $[M+H]^+$, 617.4 $[M-H]^-$.

^{1}H NMR (800 MHz, pyridine-d_5, δ in ppm) : δ 8.04 (1 H, d, *J*= 15.8 Hz, H-3'), δ 7.58 (2 H, d, *J*= 8.6 Hz, H-5' and H-9'), δ 7.19 (2 H, d, *J*= 8.6 Hz, H-6' and H-8'), δ 6.72 (1 H, d, *J*= 15.9 Hz, H-2'), δ 5.49 (1 H, t, *J*= 3.2 Hz, H-12), δ 5.28 (1 H, d, *J*= 9.4 Hz, H-3), δ 4.33 (1 H, m, H-2), δ 3.33 (1 H, dd, *J*= 3.7, 14.1 Hz, H-18), δ 1.29, 1.08, 1.08, 1.06, 1.03, 1.02, 0.98 (each 3 H, s).

^{13}C NMR (200 MHz, pyridine-d_5, δ in ppm) : δ 48.5 (C-1), δ 66.9 (C-2), δ 85.5 (C-3), δ 40.3 (C-4), δ 56.0 (C-5), δ 19.1 (C-6), δ 33.7 (C-7), δ 40.3 (C-8), δ 48.9 (C-9), δ 38.9 (C-10), δ 24.4 (C-11), δ 122.9 (C-12), δ 145.3 (C-13), δ 42.7 (C-14), δ 28.8 (C-15), δ 24.2 (C-16), δ 47.1 (C-17), δ 42.4 (C-18), δ 46.9 (C-19), δ 31.4 (C-20), δ 34.7 (C-21), δ 33.7 (C-22), δ 29.5 (C-23), δ 17.2 (C-24), δ 17.9 (C-

25), δ 18.7 (C-26), δ 26.7 (C-27), δ 180.7 (C-28), δ 33.5 (C-29) , δ 24.2 (C-30), δ 168.4 (C-1'), δ 116.6 (C-2'), δ 145.5 (C-3'), δ 126.8 (C-4'), δ 131.1 (C-5'), δ 117.3 (C-6'), δ 161.8 (C-7'), δ 117.3 (C-8'), δ 131.1 (C

4-3-20. Compound **20**

White amorphous powder; $[\alpha]_D^{20}$ +20.9 (c 0.3, MeOH); UV λ_{max} (MeOH) (log ε) (nm) 192 (2.79) 304 (2.50); IR (KBr) ν_{max} (cm^{-1}) 3394, 2981, 2949, 2844, 1705, 1658, 1646, 1053, 1033, 1014; ESIMS m/z 619.3 $[M+H]^+$, 617.4 $[M-H]^-$.

^{1}H NMR (600 MHz, pyridine-d_5, δ in ppm) : δ 8.15 (2 H, d, *J*= 8.6 Hz, H-5' and H-9'), δ 7.17 (2 H, d, *J*= 8.6 Hz, H-6' and H-8'), δ 6.95 (1 H, d, *J*= 12.9 Hz, H-3'), δ 6.14 (1 H, d, *J*= 12.8 Hz, H-2'), δ 5.47 (1 H, t, *J*= 3.1 Hz, H-12), δ 5.21 (1 H, d, *J*= 9.8 Hz, H-3), δ 4.26 (1 H, m, H-2), δ 3.31 (1 H, dd, *J*= 4.3, 13.7 Hz, H-18), δ 1.25, 1.06, 1.03, 1.01, 0.99, 0.98, 0.97 (each 3 H, s).

^{13}C NMR (150 MHz, pyridine-d_5, δ in ppm) : δ 48.5 (C-1), δ 66.8 (C-2), δ 85.4 (C-3), δ 40.2 (C-4), δ 56.0 (C-5), δ 19.1 (C-6), δ 33.7 (C-7), δ 40.1 (C-8), δ 48.9 (C-9), δ 38.9 (C-10), δ 24.4 (C-11), δ 122.7 (C-12), δ 143.2 (C-13), δ 42.7 (C-14), δ 28.8 (C-15), δ 24.3 (C-16), δ 47.2 (C-17), δ 42.4 (C-18), δ 46.9 (C-19), δ 31.4 (C-20), δ 34.7 (C-21), δ 33.7 (C-22), δ 29.4 (C-23), δ 17.2 (C-24), δ 17.9 (C-25), δ 18.6 (C-26), δ 26.6 (C-27), δ 180.7 (C-28), δ 33.5 (C-29) , δ 24.2 (C-30), δ 167.7 (C-1'), δ 117.6 (C-2'), δ 144.0 (C-3'), δ 127.2 (C-4'), δ 134.2 (C-5'), δ 116.4 (C-6'), δ 160.9 (C-7'), δ 116.4 (C-8'), δ 134.2 (C-9').

Table 1. ^{1}H (600 MHz) and ^{13}C (150 MHz) NMR data of compounds **1-3.**

no.	**1**		**2**		**3**	
	δ_H (*J* in Hz)	δ_C	δ_H (*J* in Hz)	δ_C	δ_H (*J* in Hz)	δ_C
1	1.73 d (13.1) 0.99 m	39.8	2.62 dd (5.0, 12.7) 1.72 m	48.2	1.75 m 1.08 m	39.6
2	1.86 m 1.80 m	28.8	4.13 m	73.7	1.92 m 1.86 m	28.3
3	3.27 dd (4.7, 11.3)	78.3	4.38 d (8.8)	79.9	4.05 dd (4.0, 11.3)	74.0
4		39.9		151.9		43.3
5	0.88 m	56.5	50.4 br d (12.2)	50.4	1.54 m	49.6
6	1.62 m 1.42 m	19.3	1.64 m 1.50 m	21.1	1.68 m 1.45 m	19.2
7	3.01 m 1.93 m	38.8	1.28 m 1.06 m	30.5	2.15 m 1.87 m	38.6
8		41.3		42.3		41.3
9	1.93 m	52.2	1.90 br s	50.1	2.03 m	52.2
10		38.3		38.7		38.2
11	1.57 m 1.31 m	21.7	3.32 dd (2.4, 3.1)	55.3	1.60 m 1.35 m	21.7
12	2.79 m 1.89 m	28.1	3.07 d (3.7)	56.8	2.70 m 2.01 m	27.4
13	2.79 m	40.7		89.7	2.71 m	40.7
14		60.3		42.2		60.4
15	2.50 d (13.4) 1.57 m	29.1	1.73 m 1.03 m	27.5	2.47 d (13.4) 1.56 m	29.0
16	2.68 m 1.93 m	35.3	2.31 m 1.42 m	23.5	2.65 m 1.88 m	35.4
17		57.3		45.7		57.3
18	2.33 t (11.1)	53.0	1.88 m	61.6	2.13 m	52.9
19	3.53 td (4.7, 11.3)	44.2	2.71 m	36.6	3.51 td (4.2, 10.9)	48.2
20		156.5		152.4		151.2
21	2.20 m 1.63 m	33.0	2.23 m 2.29 m	32.4	2.03 m 1.46 m	31.3
22	2.01 m 1.57 m	37.5	1.96 dt (3.1, 12.9) 1.62 m	33.8	2.02 m 1.45 m	37.7
23	1.08 s	29.0	5.89 br s 4.99 br s	105.7	4.10 d (10.3) 3.59 d (10.3)	68.5
24	1.01 s	17.0			1.06 s	13.5
25	0.91 s	17.5	0.91 s	16.3	0.99 s	17.8
26	1.18 s	17.9	1.17 s	20.7	1.20 s	17.9
27		178.8	1.18 s	16.7		178.8
28		177.3		178.6		177.4
29	5.61 br s 5.38 br s	107.3	1.45 d (6.3)	16.9	5.04 br s 4.81 br s	111.0
30	4.73 d (15.0) 4.56 d (15.0)	64.7	4.87 br s 4.81 br s	108.7	1.89 s	19.7
OCH_3	3.77 s	51.9			3.77 s	52.0

pyridine-d_5 used as solvent.

5. Bioassay procedures

5-1. PTP1B enzyme assay

PTP1B inhibition assay procedure was followed by previously described literature (Bruke et al., 1996). Briefly, ursolic acid, a famous dominant PTP1B inhibitor, was operated as a positive control. the enzyme activity was measured using 0.05 – 0.1 μg of PTP1B, 4 mM *p*-NPP as a substrate in buffer containing 1 mM DTT, 0.1 M NaCl, 1 mM EDTA, and 50 mM citrate (pH 6.0) with or without the isolates to make the final volume 100 μL in 96-well plates. After the reaction mixture was incubated at 37 °C for 30 min, 10 M NaOH was added to quench the reaction. The enzyme activity was measured by the amount of produced *p*-nitrophenol using the absorbance at 405 nm by VersaMax. The nonenzymatic hydrolysis of 4 mM *p*-NPP was corrected by measuring the control, which did not contain PTP1B enzyme.

5-2. Statistical analysis

The results are presented as the mean ± SD of duplicate experiments. Characteristics were compared between groups, and their differences were tested by the unpaired student's t-test. All statistical analyses were performed using SAS version 9.4.0 (SAS Institute, Cary, NC, USA). A p-value < 0.05 was considered to be statistically significant at two-tailed test.

III. Results and Discussion

1. Structural elucidation of isolated compounds (1-20)

1-1. Compound **1**

Compound **1** was obtained as brownish gum. Its molecular formula was assigned as $C_{31}H_{48}O_6$ by $[M-H]^-$ ion peak at m/z 515.3379 (calcd. 515.3378) by HR-ESIMS. The IR spectrum indicated the presence of hydroxyl (3364 cm^{-1}), ester (1706 and 1219 cm^{-1}), and carboxylic acid (2946 and 1697 cm^{-1}) functionalities. The ^1H NMR spectrum (Table 1) revealed two olefinic protons at δ_H 5.61 (1H, br s) and 5.38 (1H, br s), one methoxy group at δ_H 3.77 (3H, s), one oxygenated methine proton at δ_H 3.27 (1H, dd, J = 4.7, 11.3 Hz). Also, there are signals of two hydroxyl methylene protons at δ_H 4.73 and 4.56 (2H, d, J = 15.0 Hz) and four methyl singlets at δ_H 1.18, 1.08, 1.01, and 0.91 (3H, s). The ^{13}C NMR spectrum showed 31 signals, including two carboxylic groups in the downfield region at δ_C 178.8 and 177.3, one exocyclic methylene at δ_C 107.3 and 156.5, one oxygenated carbon at δ_C 78.3, a methoxy group at δ_C 51.9, a hydroxyl methylene carbon at δ_C 64.7, and four methyl groups at δ_C 29.0, 17.0, 17.5, and 17.9. From the above signals, one more carbon was added to a common triterpenoid. The NMR data of compound **1** was very similar to that of Melaleucic acid 28-O-methyl ester (Kaneta et al., 2017). The major difference between compound **1** and Melaleucic acid 28-O-methyl ester was the presence of a hydroxyl methylene (δ_C 64.7) in lieu of a methyl (δ_C 19.0) in the former at C-30. The signals (C-30) at δ_H 4.73 and 4.56 were recognized as the attachment of a hydroxyl group by the HSQC. HMBC correlation confirmed the interactions of the hydroxyl methylene protons (C-30) at δ_H 4.73 and 4.56 to the double bond moiety (C-20 and C-29) at δ_C 156.5 and 107.3, C-19 at δ_C 44.2 attached to a pentacyclic ring. Also, the

correlations from H-22 at δ_H 2.01 and 1.57, and H-16 at δ_H 1.93 to methyl ester carbon of C-28 (δ_C 177.3), and from H-13 (δ_H 2.79) and H-15 (δ_H 1.57) to C-27 (δ_C 178.8) finally established the positions of methyl ester (C-28) and carboxylic acid (C-27). NOESY correlations were observed for H-3α/CH_3-23, H-3α/H-5α, H-5α/H-9α, CH_3-24/CH_3-25, CH_3-25/CH_3-26, CH_3-26/H-13β, and H-13β/H-19β. Therefore, the chemical structure of compound **1** was completely determined as cleistocalyxic acid L. This compound was firstly announced from the nature.

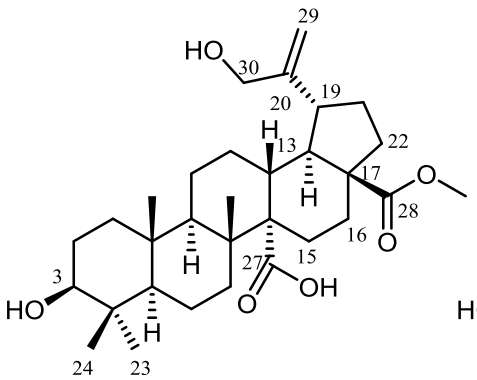

compound **1**

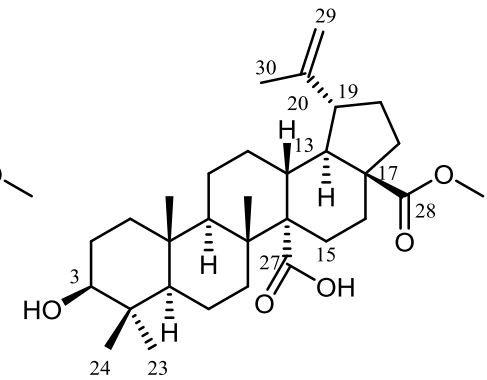

Melaleucic acid 28-O-methyl ester

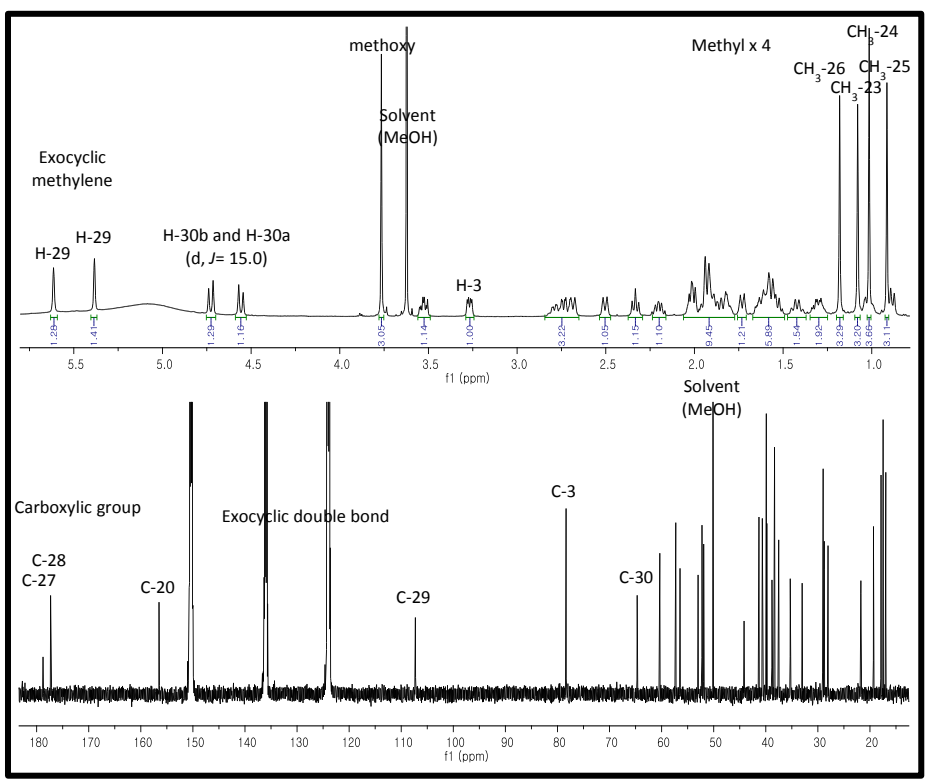

Figure 2. ^{1}H and ^{13}C NMR spectra of compound **1**

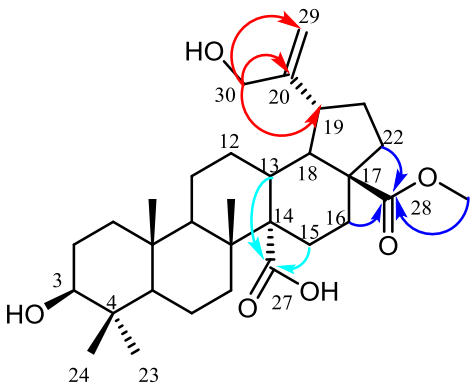

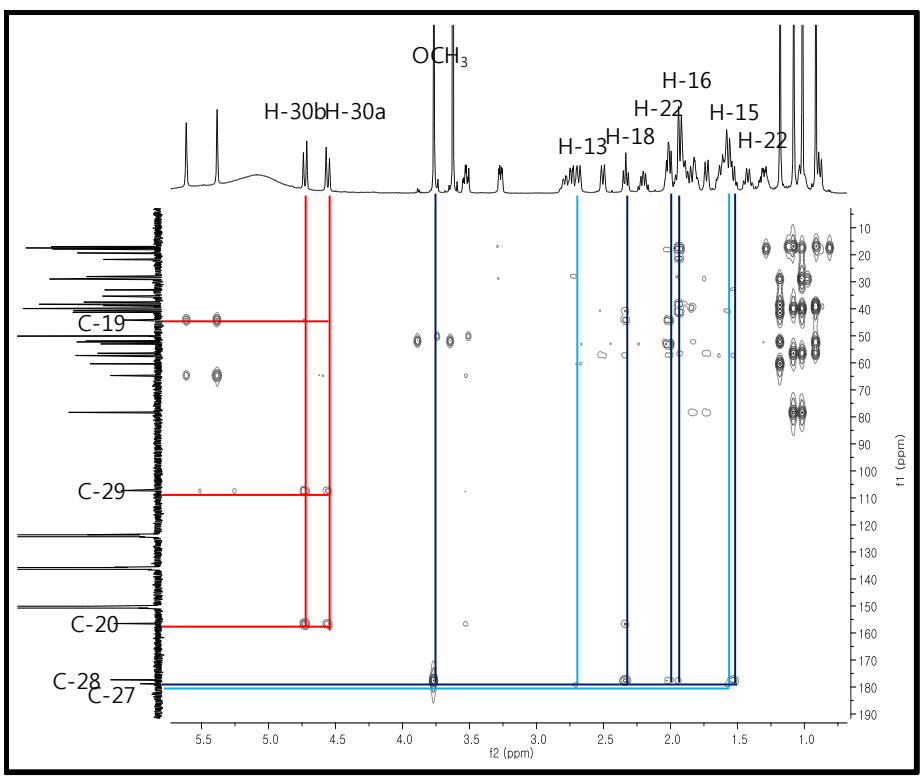

Figure 3. HMBC spectrum of compound **1**

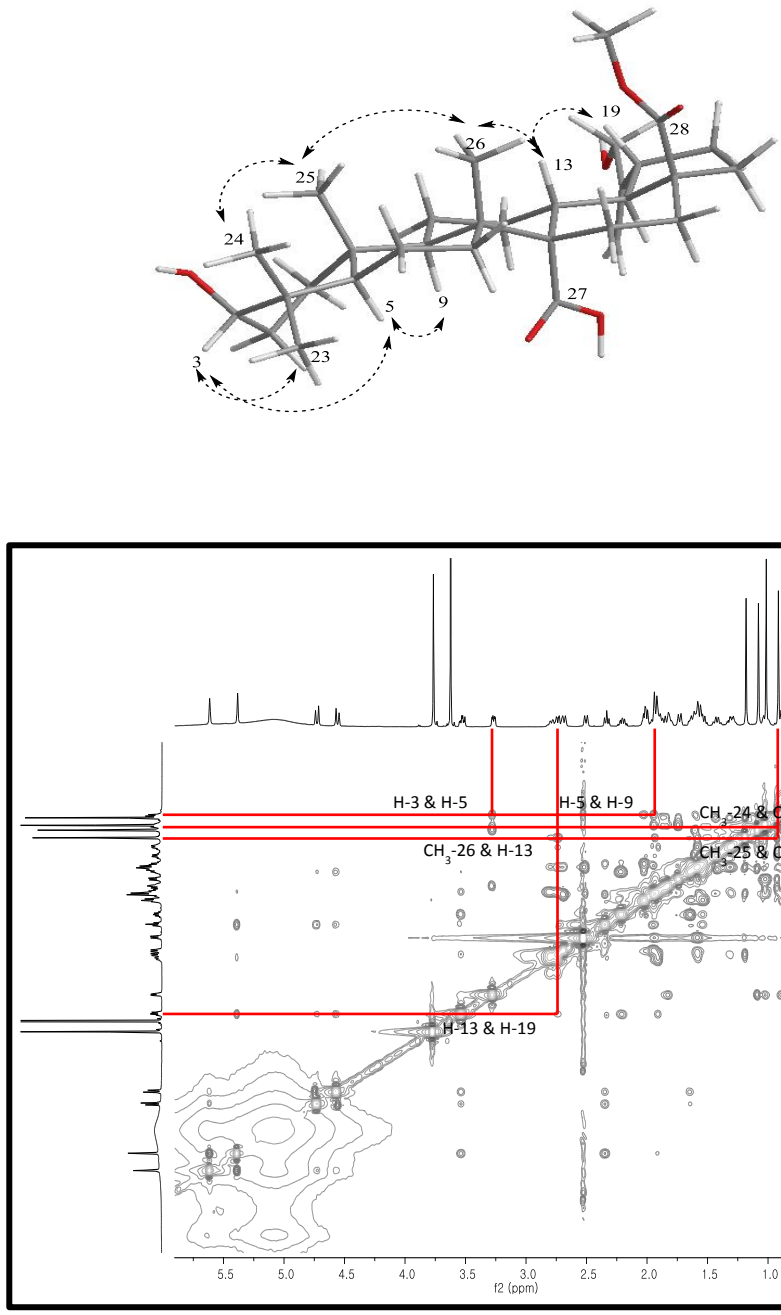

Figure 4. NOESY spectrum of compound **1**

1-2. Compound **2**

Compound **2**, a white amorphous powder, was determined to have a molecular formula of $C_{29}H_{40}O_5$ by HR-ESIMS (m/z 513.2856 $[M+HCOO]^-$, calcd. 513.2858). The IR spectrum indicated the presence of hydroxyl groups (broad 3365 cm^{-1}) and ester group (1775 and 1149 cm^{-1}). The ^1H NMR spectrum of compound **2** (Table 1) revealed two pairs of exomethylene protons, δ_H 5.89 (1H, br s, H-23) and 4.99 (1H, br s, H-23), and δ_H 4.87 (1H, br s, H-30) and 4.81 (1H, br s, H-30), and four oxygenated protons at δ_H 4.38 (1H, d, J = 8.8 Hz, H-3), 4.13 (1H, m, H-2), 3.32 (1H, dd, J = 2.4, 3.1 Hz, H-11), and 3.07 (1H, d, J = 3.7 Hz, H-12). Three singlet signals were shown for methyl groups at δ_H 0.91 (H-25), 1.17 (H-26) and 1.18 (H-27), and one doublet signal was detected at δ_H 1.45 (3H, d, J = 6.3 Hz, H-29). The ^{13}C NMR spectrum of compound **2** was observed 29 signals represented as a nor-type triterpenoid. There are also signals of one carboxylic group at δ_C 178.6, two exocyclic methylenes at δ_C 152.4, 151.9, 108.7 and 105.7, five oxygenated carbons at δ_C 89.7, 79.9, 73.7, 56.8 and 55.3, and four methyl groups at δ_C 20.7, 16.9, 16.7, and 16.3. The NMR data of compound **2** were very similar to those of ulmoidol isolated from *Ilex kudincha* (Nishimura et al., 1999). The major difference between compound **2** and ulmoidol was replaced a methyl group C-30 (δ_C 19.5) to a double bond (δ_C 108.6 and 151.3). The HMBC correlation analysis supported that the structure has ulmoidol moiety. The signal δ_H 2.71 at H-19 had correlations with C-29 (δ_C 16.9), C-30 (δ_C 108.7), C-18 (δ_C 61.6), and C-20 (δ_C 152.4). The interactions of a remarkable proton signal δ_H 1.88 at H-18 had many correlations such as C-28 (δ_C 178.6), C-29 (δ_C 16.9), C-17 (δ_C 45.7), C-13 (δ_C 89.7), and C-12 (δ_C 56.8) because of its position on the structure (Figure 5). It is supported to have the presence

of lactone ring. HMBC correlation from a methyl group δ_H 1.18 (CH_3-27) to quaternary carbon δ_C 89.7 (C-13) supported the formation of lactone moiety connected to C-13, C-17, and C-28. Lastly, the correlations of δ_H 4.38 at H-3 to C-2 (δ_C 73.7), C-4 (δ_C 151.9) and C-23 (δ_C 105.7) made the position of 23-nor-triterpenoid. NOESY correlations was performed to confirm the stereochemistry of the structure with the correlations H-3α/H-5α, H-5α/H-9α, H-9α/CH_3-27, CH_3-27/H-19α, H-2β/CH_3-25, CH_3-25/CH_3-26, CH_3-25/H-11β, H-11β/H-12β, CH_3-26/H-12β, H-12β/H-18β, and H-18β/CH_3-29. Therefore, the compound **2** was firstly proposed to cleistocalyxolide C as a new compound.

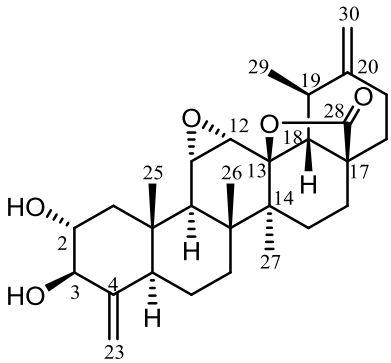

compound 2

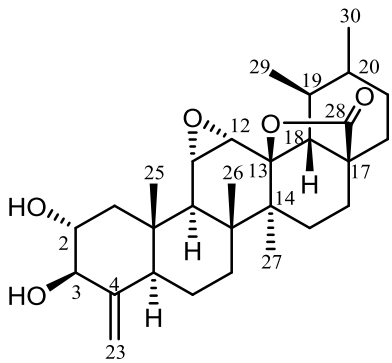

Ulmoidol

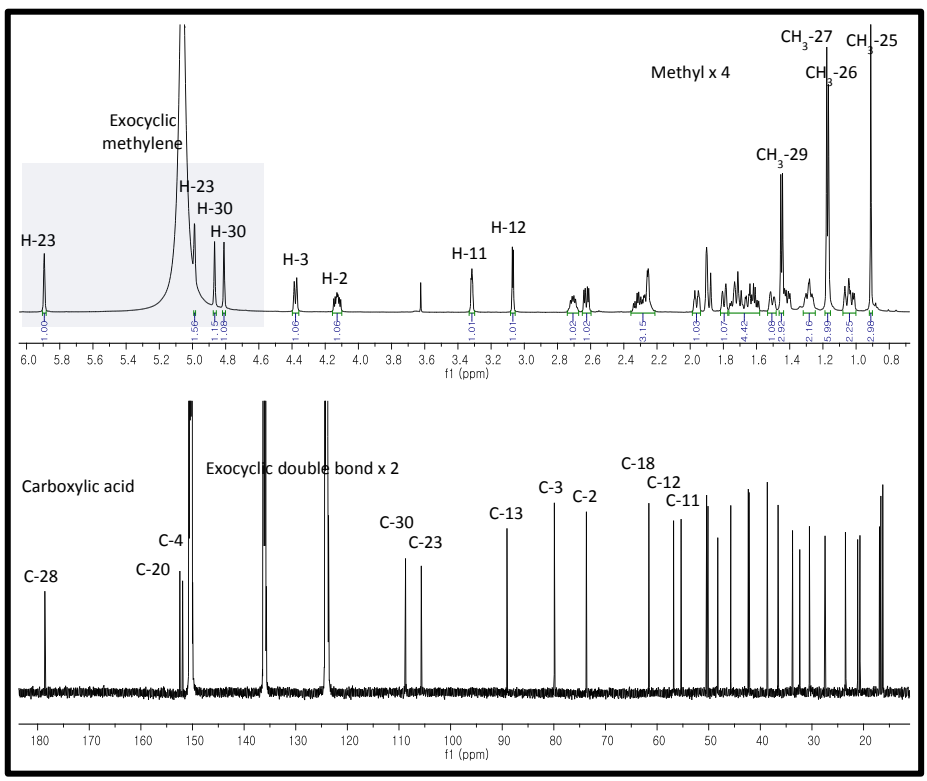

Figure 5. ^{1}H and ^{13}C NMR spectra of compound **2**

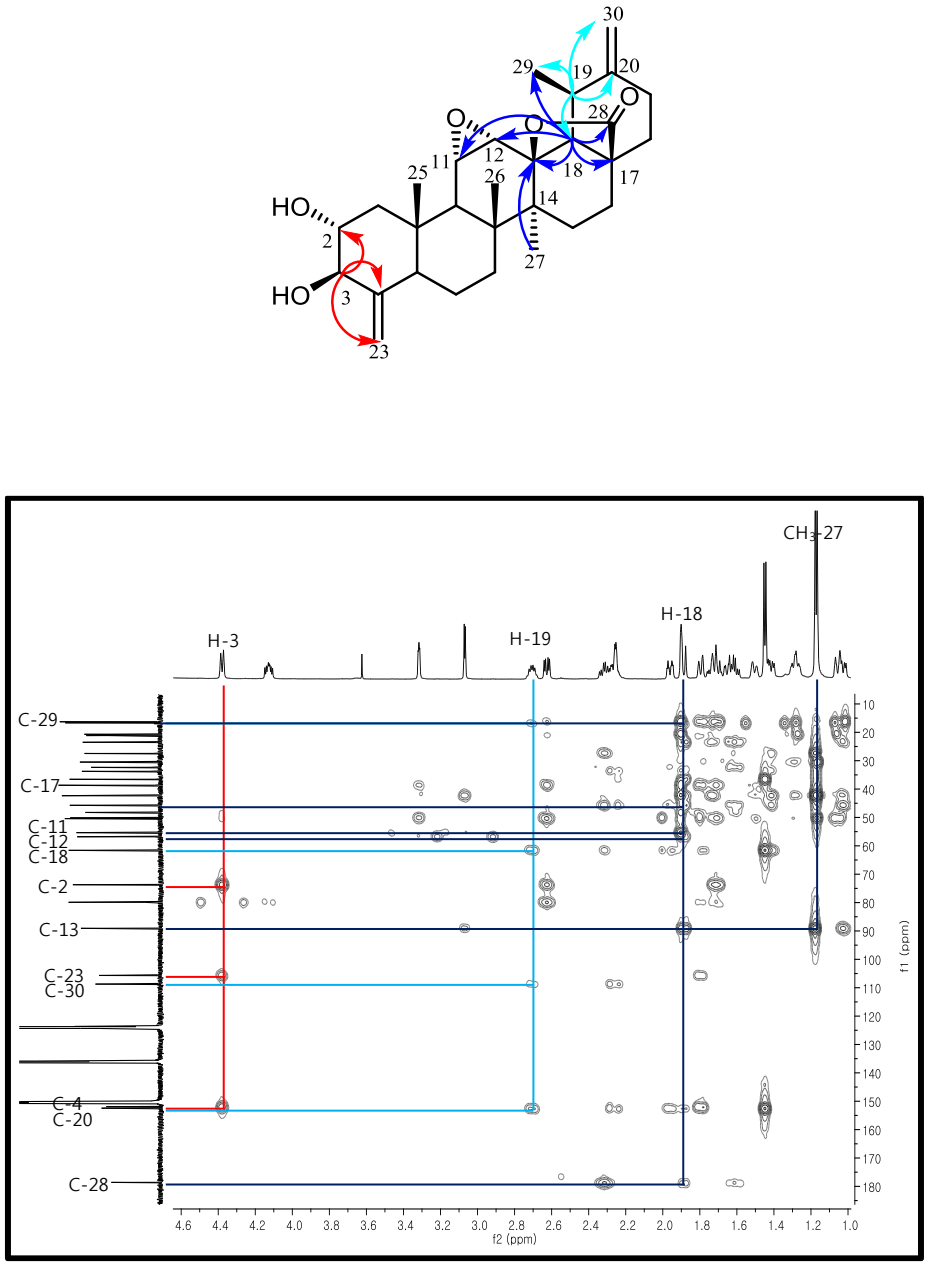

Figure 6. HMBC spectrum of compound **2**

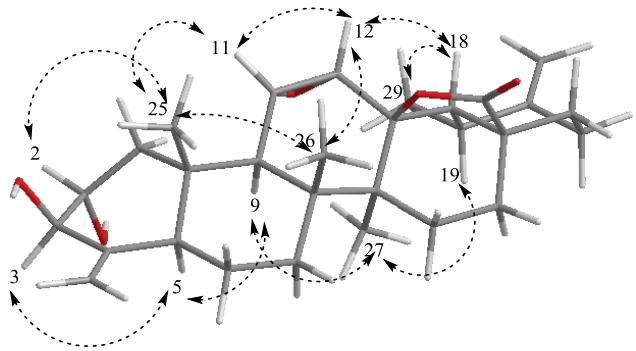

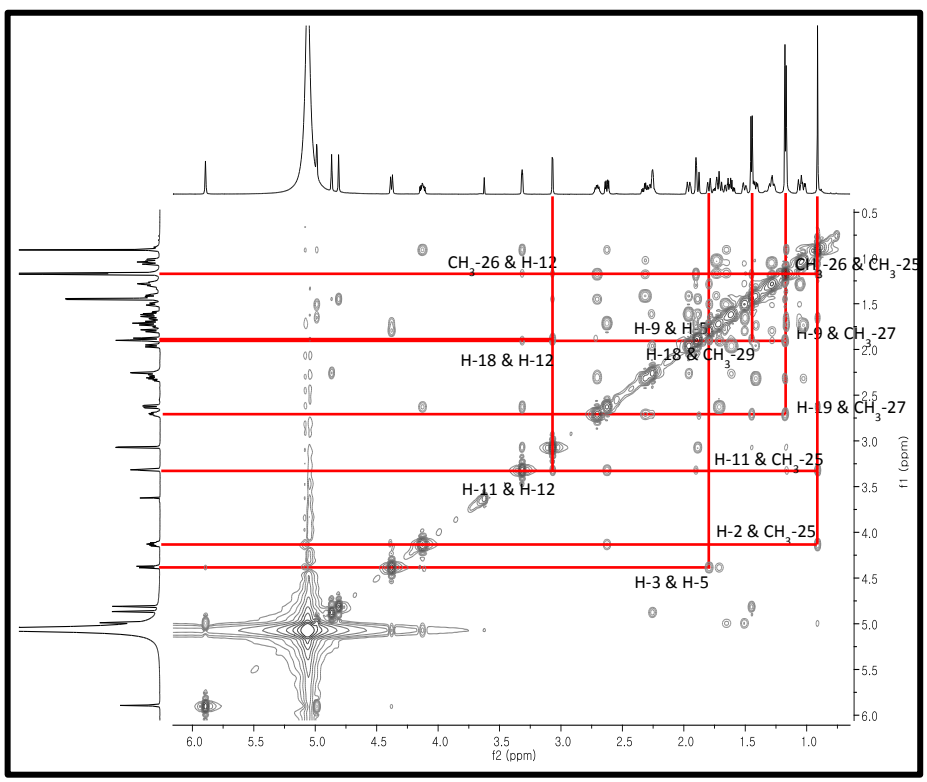

Figure 7. NOESY spectrum of compound **2**

1-3. Compound **3**

Compound **3** was obtained as white amorphous powder. Its molecular formula was assigned as $C_{31}H_{48}O_6$ from the HRESIMS data (m/z 515.3381 $[M-H]^-$, calcd. 515.3378). In the IR spectrum, absorption bands showed the presence of hydroxyl (3245 cm^{-1}), ester (1718 and 1212 cm^{-1}), and carboxyl (2934 and 1680 cm^{-1}) groups. The ^1H NMR spectrum and ^{13}C NMR spectra (Table 1) were closely identical to those of **1** with the only difference being the change of a hydroxyl group position from δ_H 4.73 and 4.56 at the C-30 in compound **1** to δ_H 4.10 and 3.59 at the C-23 in compound **3**. Based on HSQC, two correlations from δ_C 68.5 at C-23 to δ_H 4.10 and 3.59 at H-23α and H-23β were assumed to have a hydroxyl group at C-23. HMBC signals of H-23α and H-23β clearly set the position as the correlations were seen at δ_C 74.0 at C-3, δ_C 43.3 at C-4, δ_C 49.6 at C-5, and δ_C 13.5 at C-24. The correlations from H-22 at δ_H 2.02 and 1.45, and H-16 at δ_H 1.88 to the methyl ester carbon of C-28 (δ_C 177.3) were also confirmed where its location is. Other correlations from H-13 (δ_H 2.71) to H-15 (δ_H 1.56) and C-27 (δ_C 178.8) finally established the position of carboxylic acid (C-27). NOESY correlations were observed for H-3α/CH_3-23, H-3α/H-5α, H-5α/H-9α, CH_3-24/CH_3-25, CH_3-25/CH_3-26, CH_3-26/H-13β, and H-13β/H-19β to determine the configuration of **3**. It is consistent with **1** by interpretation of its NOESY spectrum. Therefore, the structure of **3** as a new compound was firstly reported the name as clesitocalyxic acid M.

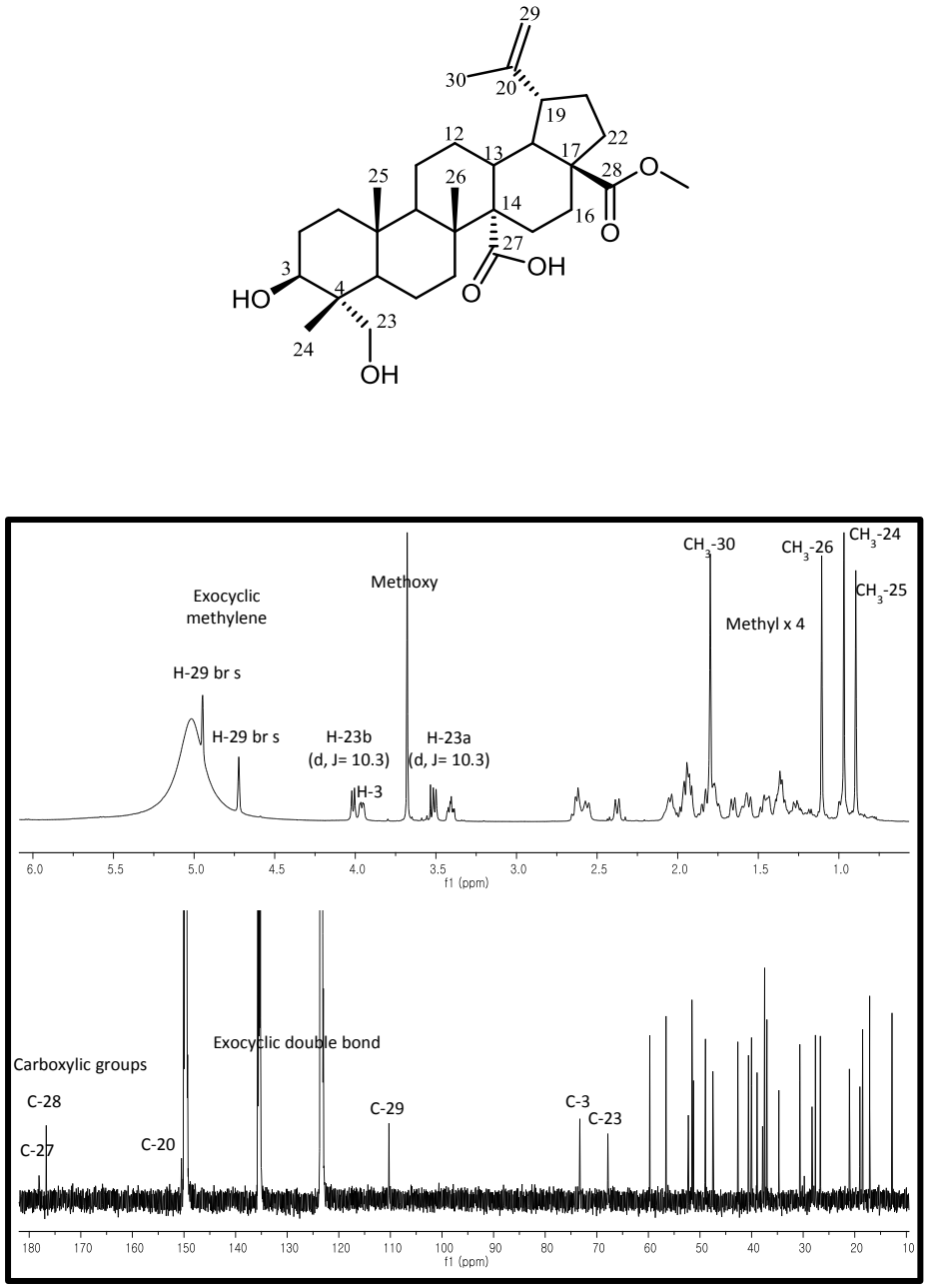

Figure 8. ^{1}H and ^{13}C NMR spectra of compound **3**

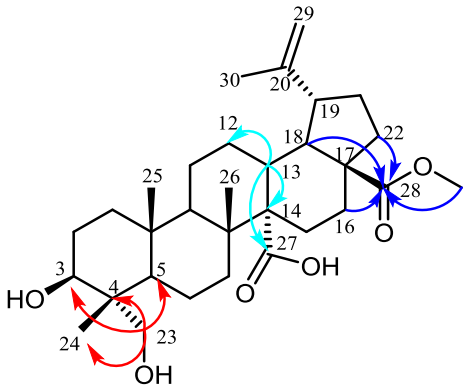

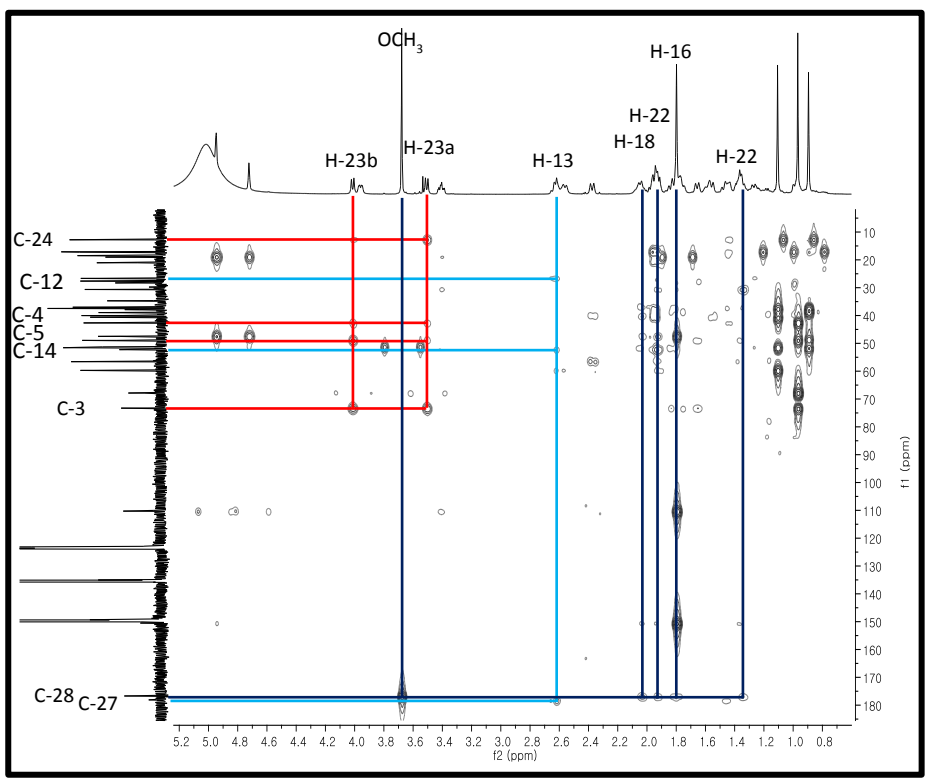

Figure 9. HMBC spectrum of compound **3**

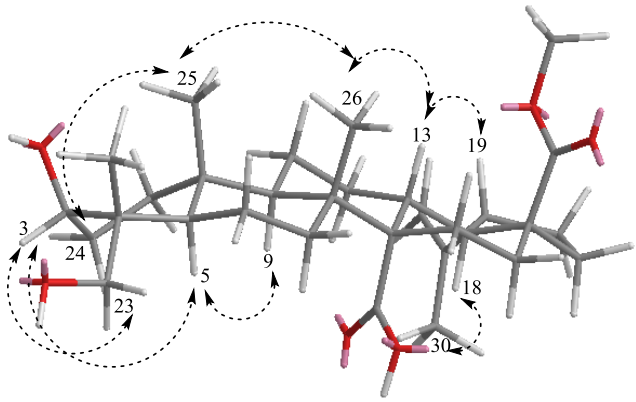

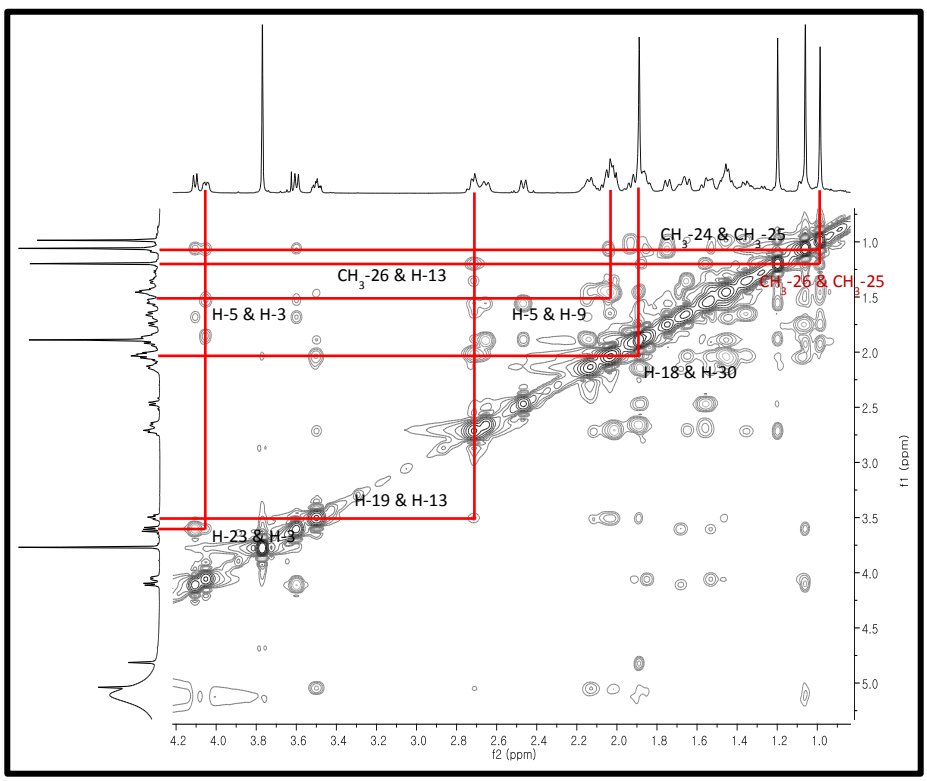

Figure 10. NOESY spectrum of compound **3**

1-4. Compound **4**

Compound **4** was isolated as white amorphous powder with $[\alpha]_D^{20}$ = +5.0 (c, 0.3, MeOH). The IR spectrum showed the presence of hydroxyl (3388 cm^{-1}), ester (1704 and 1165 cm^{-1}), and carboxyl (2966 and 1680 cm^{-1}) groups. ^{1}H and ^{13}C NMR data of **4** intended the structure as an Melaleucic 28-methyl ester, indicating the presence of five methyl groups at δ_H 1.08 (CH_3-23), 1.01 (CH_3-24), 0.92 (CH_3-25), 1.18 (CH_3-26), and 1.90 (CH_3-30). Here, δ_H 1.90 is a notable methyl group next to a double bond, C-20 and C-29 in a betulinic moiety. Also, two olefinic protons at δ_H 5.05 (br s, H-29) and δ_H 4.83 (br s, H-29) with two olefinic carbons δ_C 151.1 (C-20) and δ_C 111.0 (C-29) and two carboxylic groups at δ_C 178.8 (C-27) and δ_C 177.4 (C-28) were confirmed as closely consistent the compound **1** without only one hydroxyl group.

Based on the above deductions and comparing spectrums with reference (Kaneta et al., 2017), compound **4** was elucidated as Melaleucic 28-methyl ester.

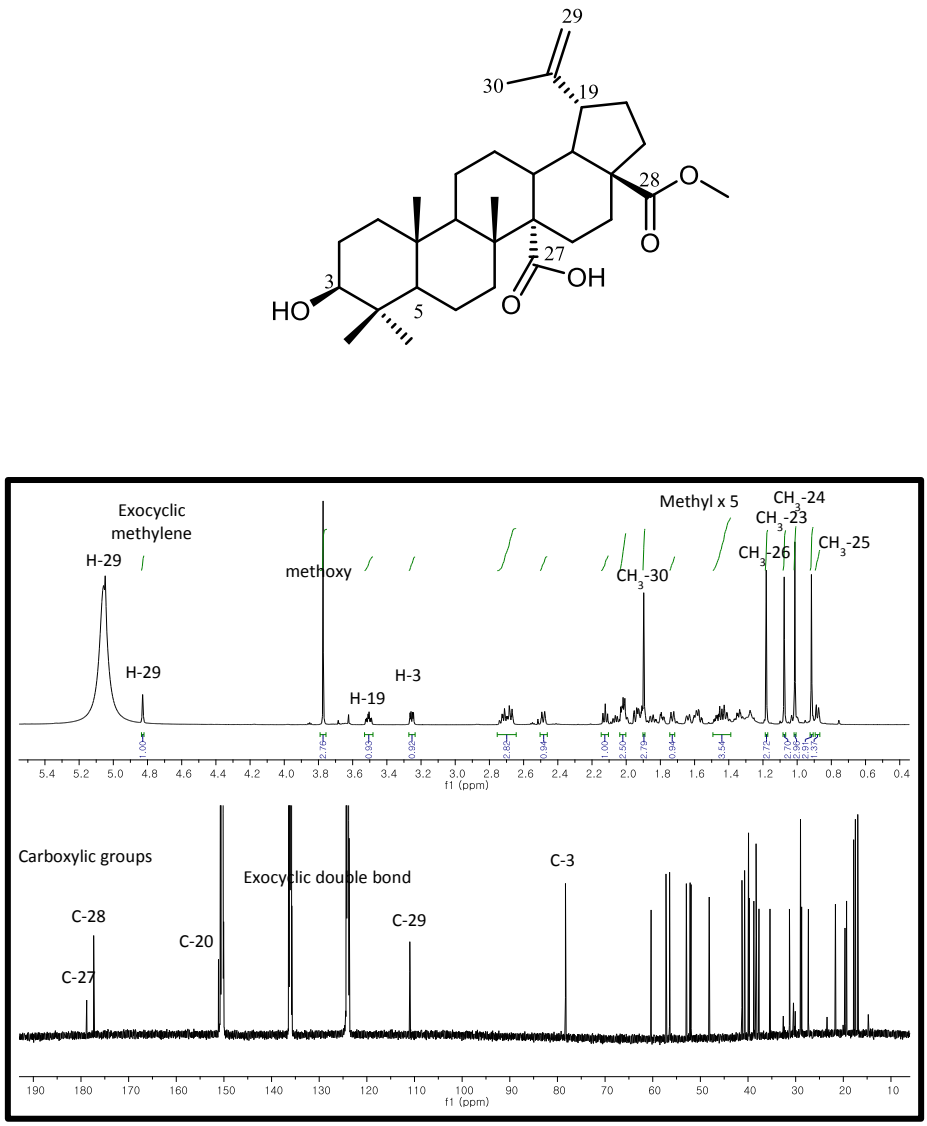

Figure 11. ^{1}H and ^{13}C NMR spectra of compound **4**

1-5. Compound **5**

Compound **5** was purified as white amorphous powder, with the $[\alpha]_D^{20}$ +14.4 (c 0.3, MeOH). IR spectrum represented the existence of hydroxyl (3335 cm^{-1}) and carboxyl (2928 and 1687 cm^{-1}) groups. ^{1}H and ^{13}C NMR spectra showed the signals as six methyl groups, δ_H 1.09 (CH_3-24), 1.14 (CH_3-25), 1.11 (CH_3-26), 1.43 (CH_3-27), 1.67 (CH_3-29), and 1.13 (CH_3-30), as well as a hydroxymethyl group at δ_H 3.73 and 4.21 (C-23, d, *J*= 10.5). One carboxylic acid (δ_C 181.2) and two olefinic carbons (δ_c 128.5 and 140.5) also detected, and four oxygenated carbons, at δ_C 69.4 (C-2), 78.8 (C-3), 67.1 (C-23), and 73.2 (C-19), supported to construct what the structure it is. One of the proton, δ_C 3.06 (s, H-18) recognized as a singlet where no protons presented right next to its position.

With rational analysis of the above information, 1D NMR data were consistent to those of known compound 19α-hydroxyasiatic acid (Hiroshi et al., 2007). This was further supported by ESI-MS, 527.3 $[M+Na]^+$ and 503.3 $[M-H]^-$.

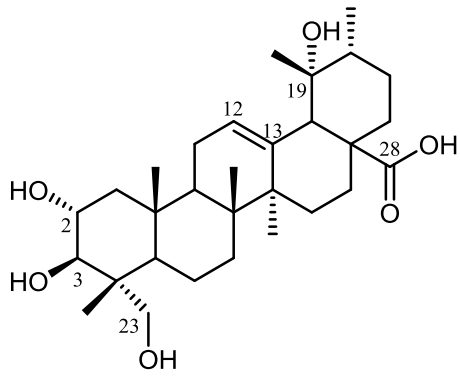

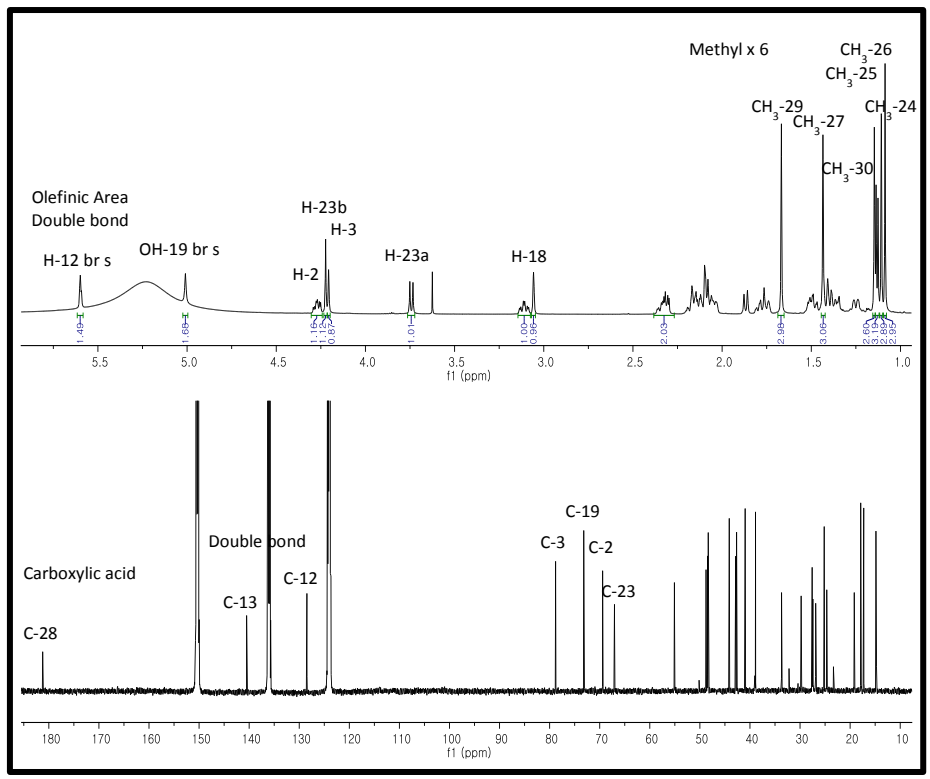

Figure 12. ^{1}H and ^{13}C NMR spectra of compound **5**

1-6. Compound **6**

Compound **6**, white amorphous powder, was yielded. The optical rotation values was $[\alpha]_D^{20}$ -4.3 (c 0.3, MeOH). The IR spectrum revealed the hydroxyl (3398 cm^{-1}) and carbonyl (1681 cm^{-1}) functionalities in the structure. The 1D NMR spectra indicated the presence of one exocyclic double bond, H-29 (δ_H 4.96 and 4.79), C-20 (δ_C 151.3), and C-29 (δ_C 109.9). Six methyl groups were in this structure, and one of them noticeably showed an unexpected deshield methyl peak at δ_H 1.81 (s, H-30) because of its location right next to double bond such as compound **4**.

Based on the above notable peaks, the NMR data of **6** were identical to those of previously reported compound betulinic acid (Kang et al., 2016). ESI-MS data also confirmed the structure of **6** by the ion peaks at *m/z* 439.3 $[M\text{-}H_2O+H]^+$ and 455.4 $[M\text{-}H]^-$, corresponding to the molecular weight of 456.

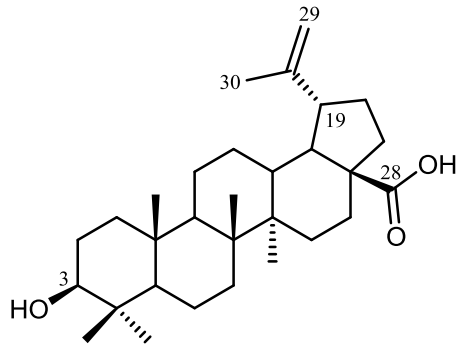

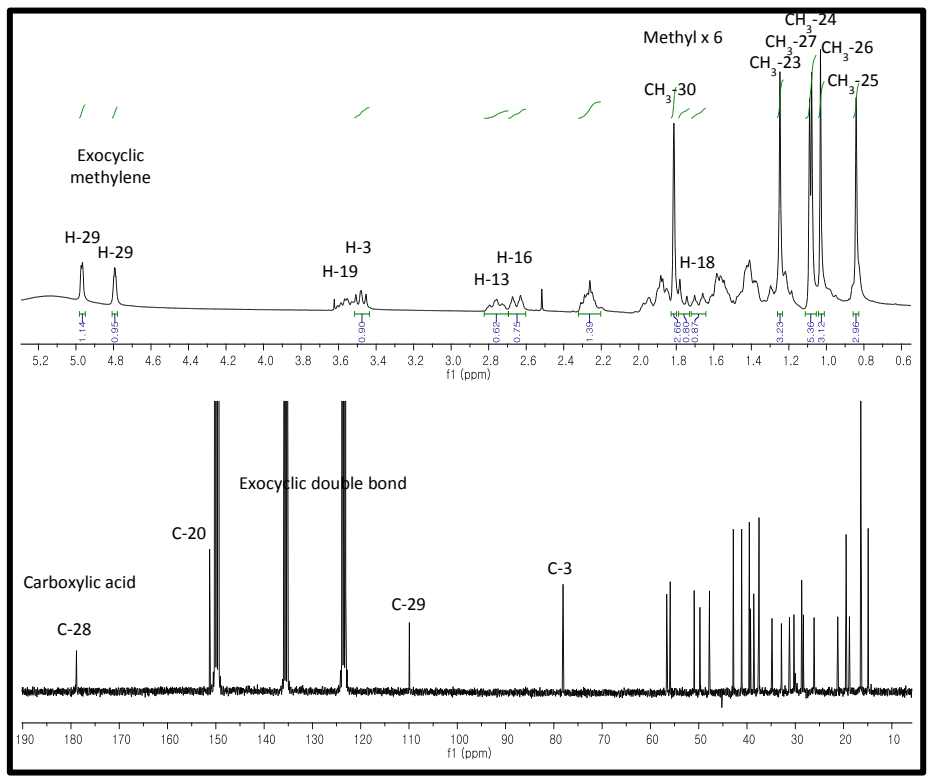

Figure 13. ^{1}H and ^{13}C NMR spectra of compound **6**

1-7. Compound **7**

Compound **7** was isolated as white amorphous powder with $[\alpha]_D^{20}$ +43.6 (c 0.3, MeOH). The IR spectral analysis showed the presence of hydroxyl (3393 cm^{-1}) and carboxylic acid (1688 and 1460 cm^{-1}) groups. The ion peaks at *m/z* 439.3 $[M-H_2O+H]^+$ and 455.4 $[M-H]^-$ offered the molecular weight of 456 on ESI-MS. From 1D NMR, there is one oxygenated proton δ_H 3.21 at H-3 and seven singlet methyls as common triterpenoid moiety. An olefinic proton signal of δ_H 5.27 (t-like s) at H-12 usually indicated to endocyclic double bond. From the carbon signals, δ_C 143.8 (C-13) and δ_C 122.8 (C-12) supported that the structure has a double bond inside of the ring system. There is also one carboxylic acid δ_C 183.6 (C-28). All of them represented that the compound is identical as oleanolic acid (Srivedavyasasri et al., 2017).

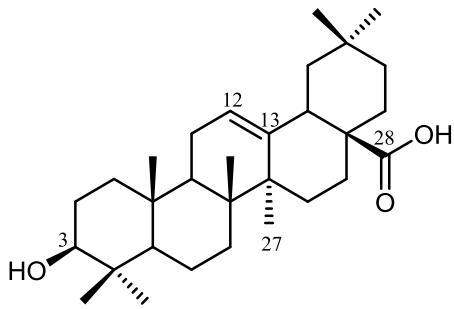

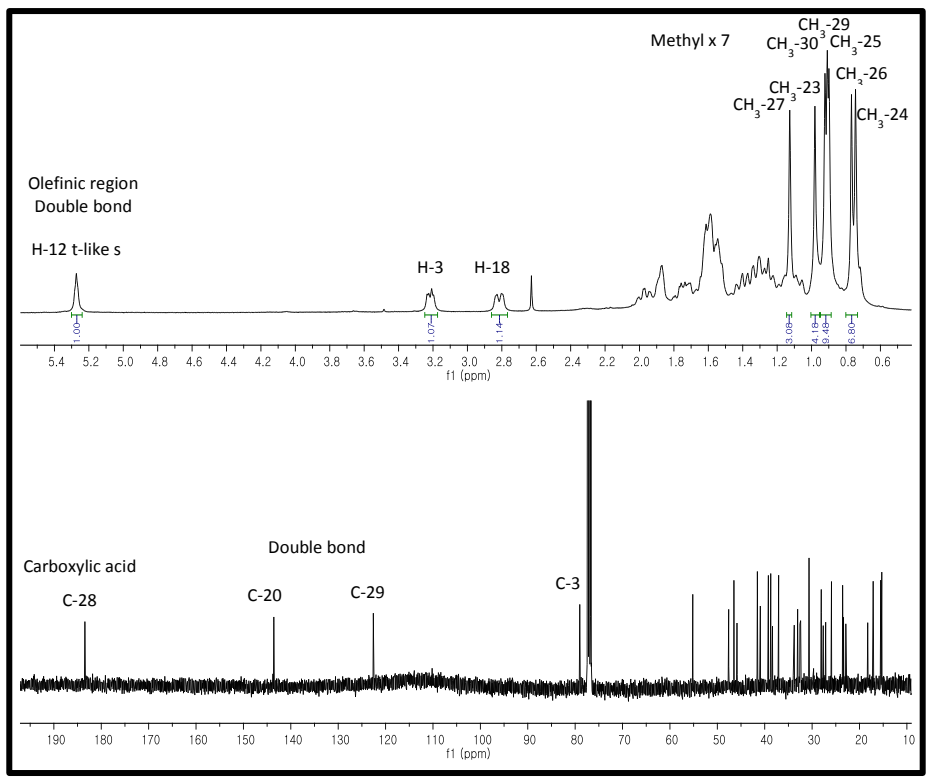

Figure 14. ^{1}H and ^{13}C NMR spectra of compound **7**

1-8. Compound **8**

Compound **8** was obtained as white amorphous powder. Its specific rotation was measured, $[\alpha]_D^{20}$ +9.3 (c 0.3, MeOH). IR spectrum showed the absorption bands at 3366, 2937, 1748, and 1049 cm^{-1} referred as hydroxyls and ester functionalities. The ^{1}H and ^{13}C NMR showed the presence of lactone ring because of the carbon signal, δ_C 92.0 at C-13, usually shared an ester bridge, δ_C 180.2 at C-28. The meaning of three oxygenated protons, δ_H 4.20 at H-12, δ_H 4.13 at H-2, and δ_H 3.38 at H-3,was substitutions of three hydroxyl groups. Seven methyl groups for δ_H 1.29, 1.12, 1.02, 1.35, 1.61, 0.82, and 0.92 also signified a common skeleton of triterpenoid.

Spectral data of **8** were observed to be consistent with those of known compound, (2α, 3β, 12α) 2, 3, 12-Trihydroxy-olean-28-oic acid 28, 13-lactone (Siewert et al., 2014). ESI-MS data further supported to the structure with *m/z* 489.3 $[M+H]^+$ and *m/z* 533.4 $[M+HCOO]^-$.

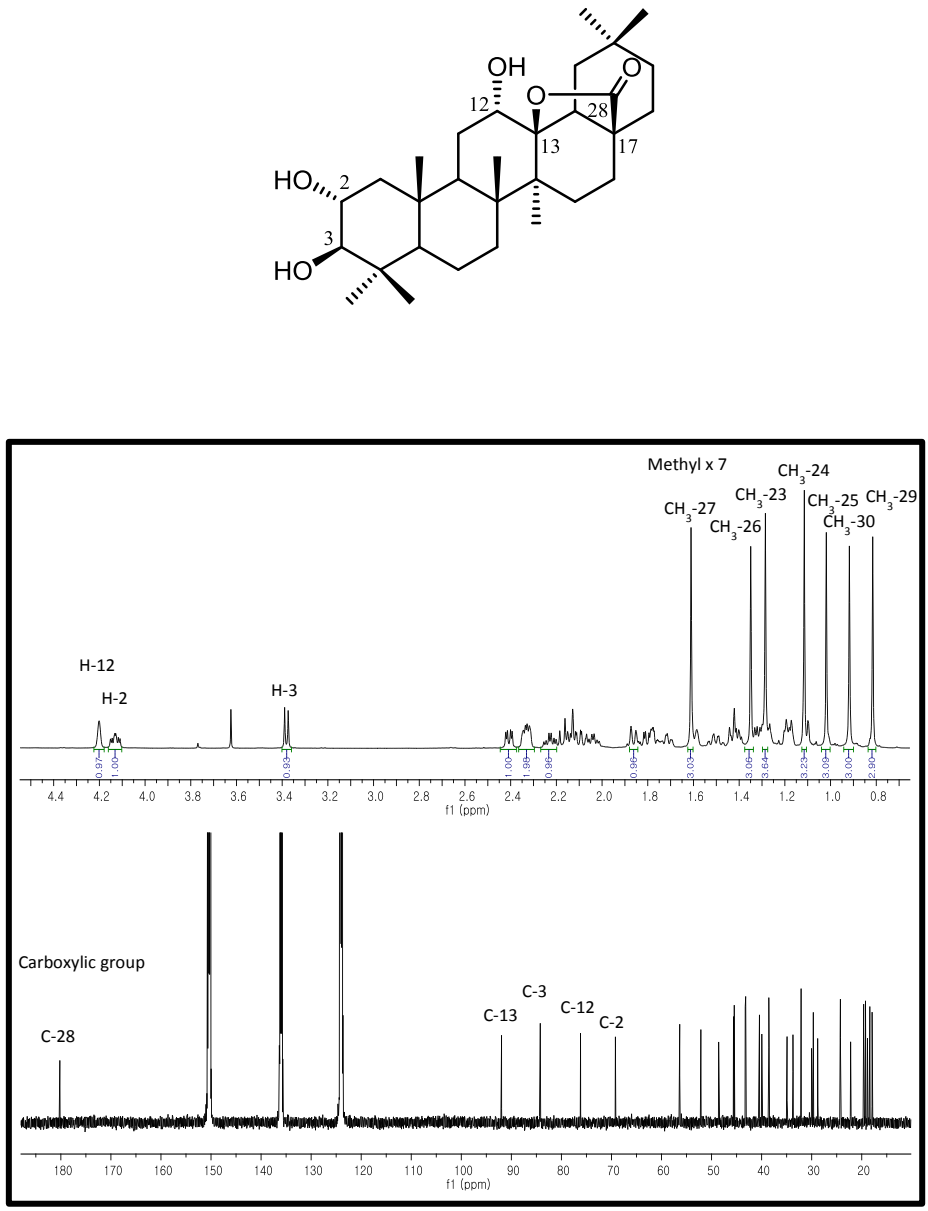

Figure 15. ^{1}H and ^{13}C NMR spectra of compound **8**

1-9. Compound **9**

Compound **9**, white amorphous powder, had the specific rotation of $[\alpha]_D^{20}$ +32.3 (c 0.3, MeOH). The IR absorption band at 3392 cm^{-1} indicated the presence of hydroxyl group while a carboxylic acid band showed at 1704 cm^{-1}. The ^{1}H NMR and ^{13}C NMR revealed it is really similar to the compound **7** without only one hydroxyl substitution at δ_H 4.12 (H-2) and δ_C 69.2 (C-2).

All of the above information has led to the compound **9** was structurally deduced as maslinic acid (Taniguchi et al., 2002). Futhermore, ESI-MS spectra, 495.3 $[M+Na]^+$ and 471.3 $[M-H]^-$, supported the proposal of compound **9** as maslinic acid.

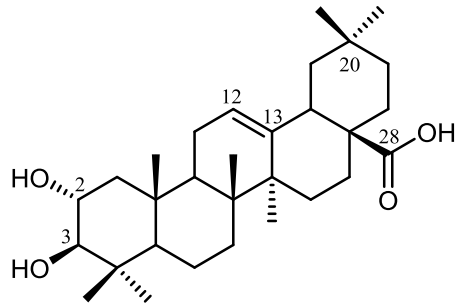

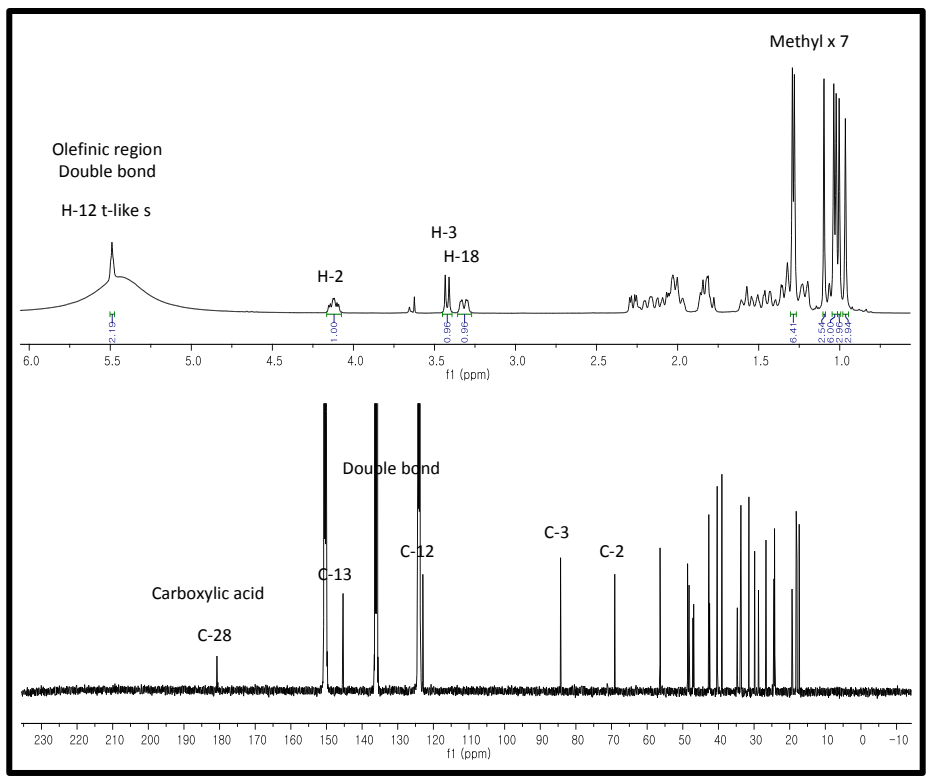

Figure 16. ^{1}H and ^{13}C NMR spectra of compound **9**

1-10. Compound **10**

Compound **10** was isolated as white amorphous powder with $[\alpha]_D^{20}$ -5.8 (c 0.3, MeOH). The IR spectral analysis showed the presence of hydroxyls (3384 cm^{-1}) and one carboxylic acid (1705 and 1375 cm^{-1}) in the structure. With the 1D NMR data of **10** exhibited the similar patterns to compound **6** except for one hydroxyl group attachment on C-2 (δ_H 4.08 and δ_C 69.1). The ^{1}H and ^{13}C NMR data were identical to those of previously reported compound, alphitolic acid (Kang et al., 2016). This was further supported by the co-appearance of protonated and deprotonated peaks on ESI-MS spectrums (*m/z* 495.3 $[M+Na]^+$ and 471.3 $[M-H]^-$, verifying to molecular weight as 472).

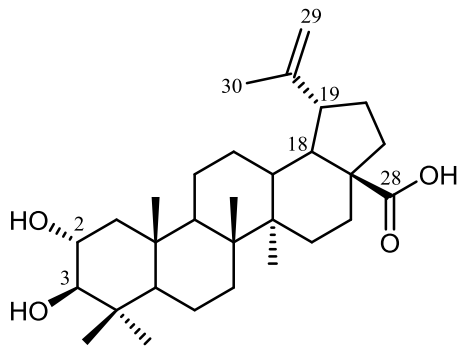

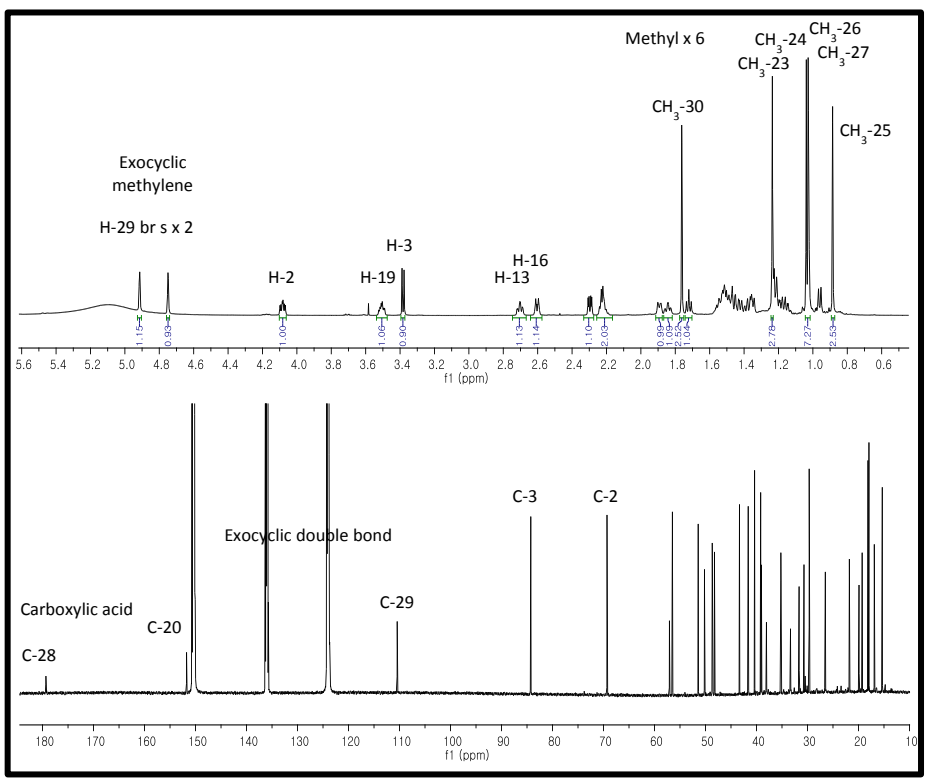

Figure 17. ^{1}H and ^{13}C NMR spectra of compound **10**

1-11. Compound **11**

Compound **11**, white amorphous powder, was obtained, and the optical rotation value was calculated $[\alpha]_D^{20}$ +53.6 (c 0.3, MeOH). The IR spectral analysis showed the existence of hydroxyl group (3335 cm^{-1}). This compound is closely identical to the ^{1}H and ^{13}C NMR spectra of compound **7**. It displayed the signals of δ_H 3.56 and 3.21 (d, 11.0) at H-28 and δ_C 69.9 at C-28 which meant by absence of carboxylic acid and appearance of hydroxymethyl group. Based on the above spectral observation and comparison to the reference, compound **11** was structurally proposed as erythrodiol (Jin et al., 2012).

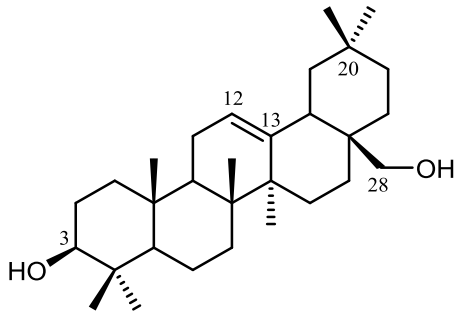

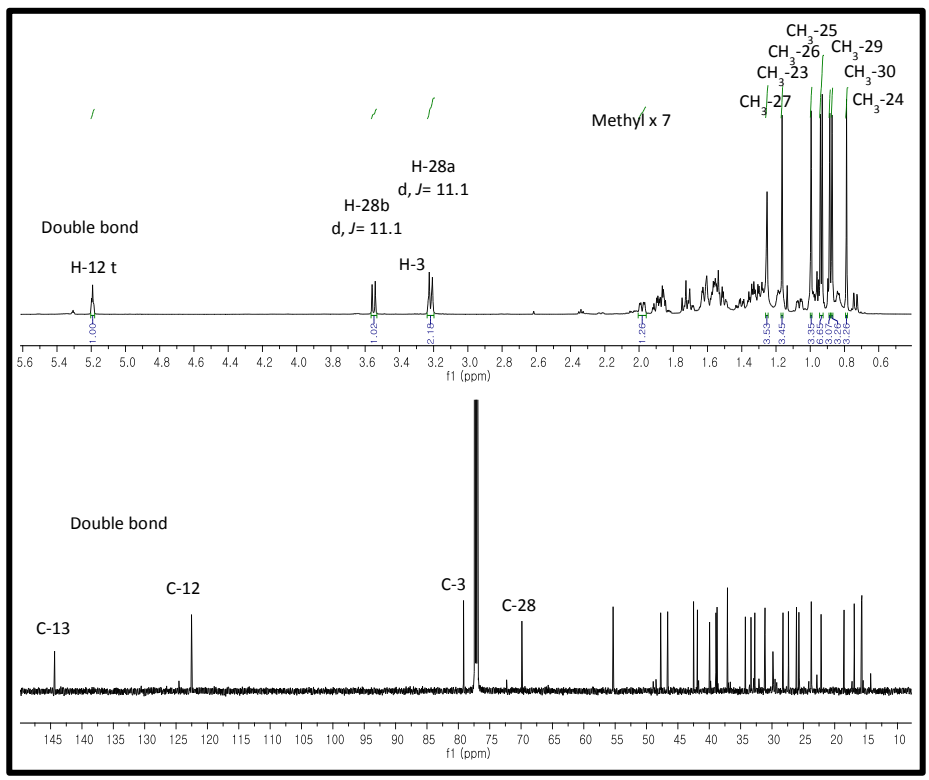

Figure 18. ^{1}H and ^{13}C NMR spectra of compound **11**

1-12. Compound **12**

Compound **12** was purified as white amorphous powder with the optical rotation $[\alpha]_D^{20}$ +54.0 (c 0.3, MeOH). The IR spectrum showed bands at 3388 cm^{-1} (hydroxyl) and 2870 and 1772 cm^{-1} (carbonyl). The protonated peak $[M+H]^+$ at *m/z* 471.3 and deprotonated peak $[M+HCOO]^-$ at *m/z* 515.4 indicated the molecular weight as 470 with the molecular formula, $C_{29}H_{42}O_5$. The 1D NMR spectra was closely consistent to those of compound **2** with disappearing one exocyclic double bond δ_H 0.92 (3H, d, *J*= 6.5 Hz) and δ_C 20.2 at C-30 position. All NMR spectra were consistent with previously reported compound, ulmoidol (Nishimura et al., 1999). Therefore, its structure was fully elucidated.

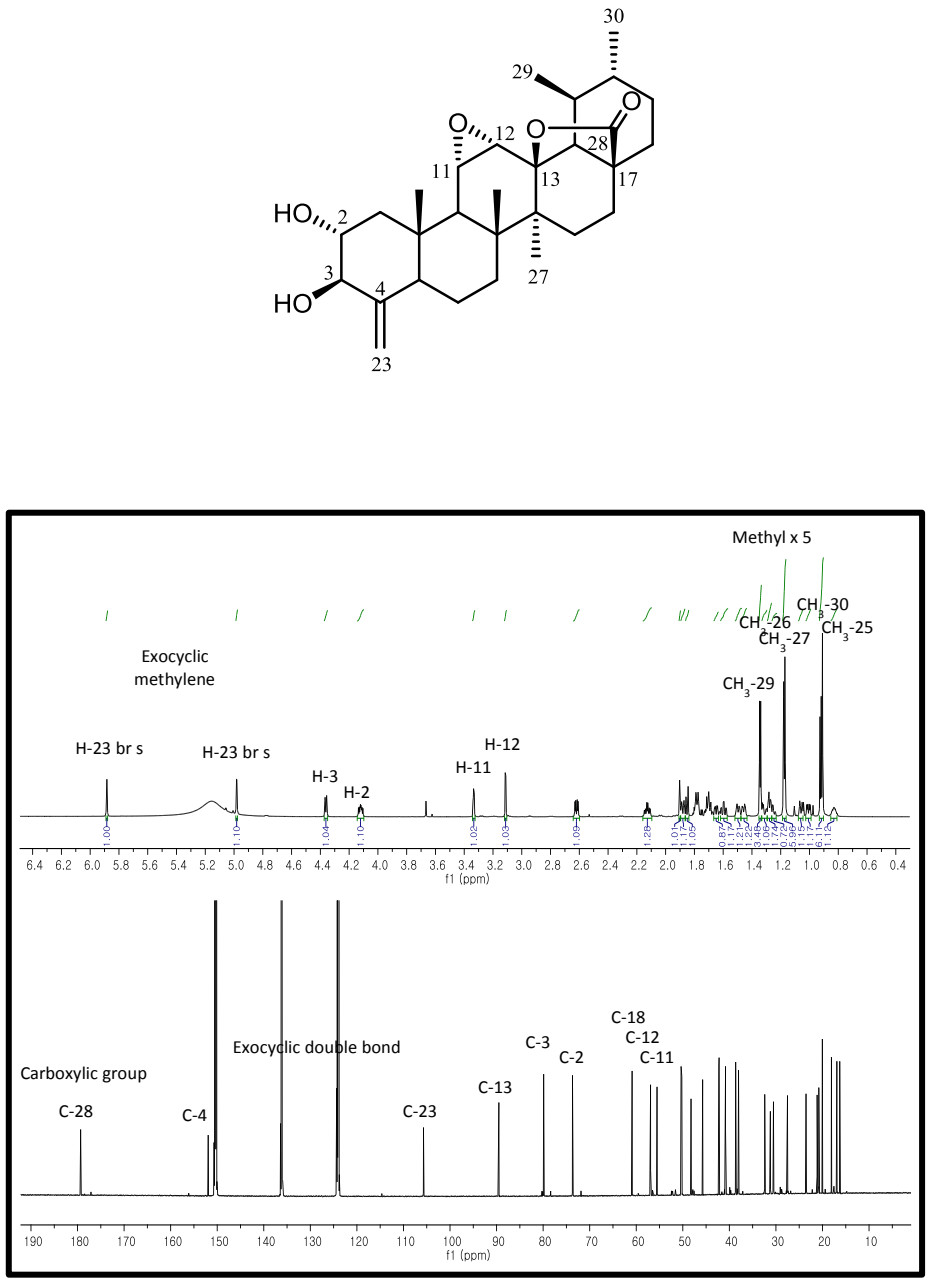

Figure 19. ^{1}H and ^{13}C NMR spectra of compound **12**

1-13. Compound **13**

Compound **13** was yielded as white amorphous powder with $[\alpha]_D^{20}$ +51.4 (c 0.3, MeOH). The IR spectrum showed absorption bands at 3392 and 1688 cm^{-1}, representing to hydroxyl and carbonyl groups, respectively. ^1H NMR data displayed the characteristics of two double bonds (δ_H 4.95, 5.85, and 5.61), two hydroxyl groups (δ_H 4.05 and 4.36) and five methyls (δ_H 0.85, 1.15, 1.75, 1.46, and 1.14). The ^{13}C NMR supported all of these functionalities in the structure; however, one more oxygenated carbon δ_C 73.2 at C-19 was showed. Based on the above spectral dedeuction and comparison to the data of reference, compound **13** was fully elucidated as 2α,3β,19α-Trihydroxy-24-norurs- 4(23),12-dien-28-oic acid (Jang et al., 2005 & Ekon et al. 2015).

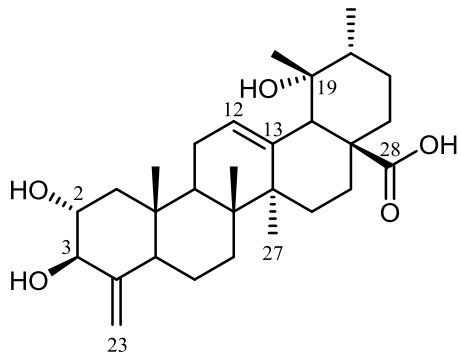

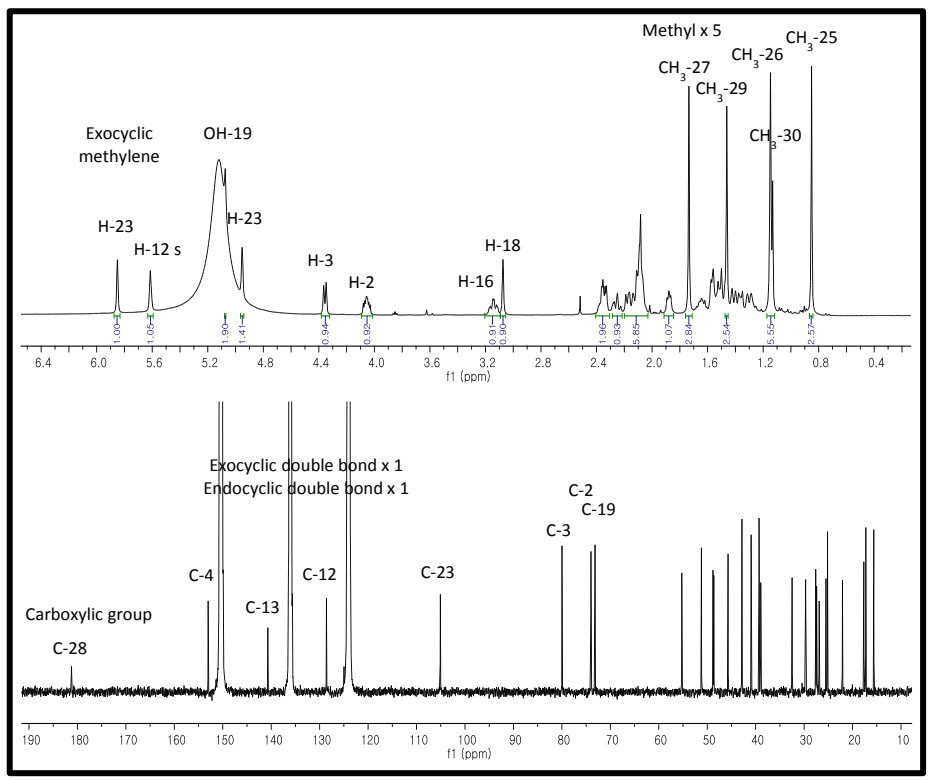

Figure 20. ^{1}H and ^{13}C NMR spectra of compound **13**

1-14. Compound **14**

Compound **14** as white amorphous powder has the optical rotation value of $[\alpha]_D^{20}$ +20.9 (c 0.3, MeOH). IR spectrum showed 3384 cm^{-1} as the hydroxyl and 1688 cm^{-1} as the carboxyl. The 1D NMR patterns of **14** were observed to be similar to those of **9**, indicating one double bond, one carboxylic acid, and two hydroxyl groups. However, it is suggested that **14** possessed the hydroxymethyl group through the peaks of H-23 (δ_H 3.71 and 4.20) and C-23 (δ_C 67.0) because of comparing the chemical shifts difference with compound **9**. As a result, the structure of **14** was characterized as arjunolic acid (Li et al., 2009) by comparison of the physical and spectral data with the reported data.

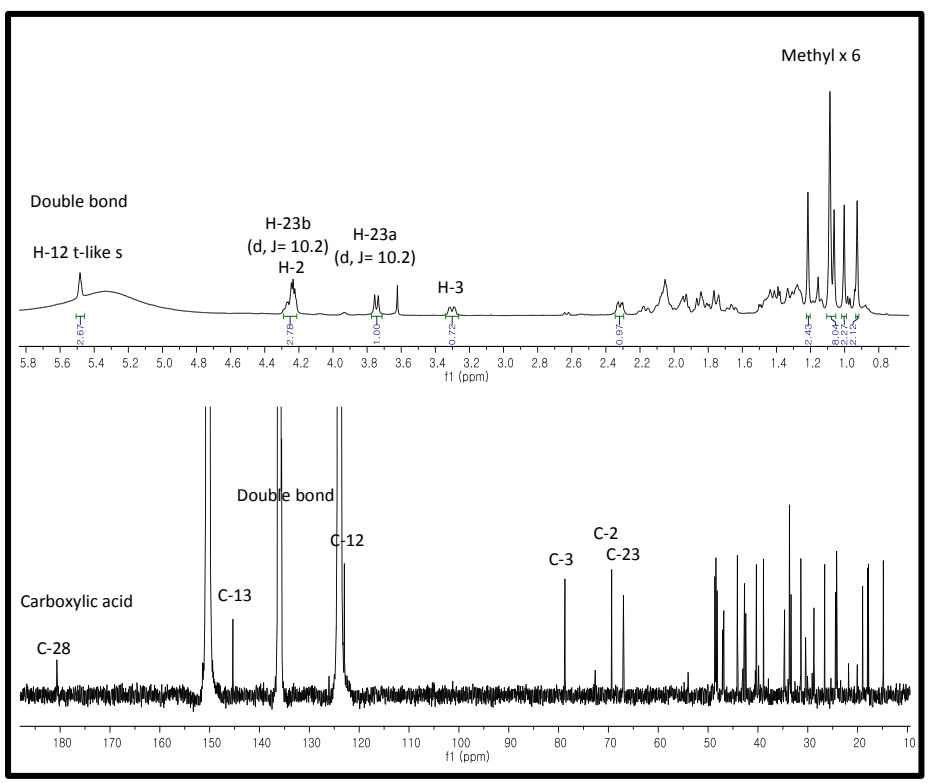

Figure 21. ^{1}H and ^{13}C NMR spectra of compound **14**

1-15. Compound **15**

Compound **15** was gained as white amorphous powder. The optical rotation was $[\alpha]_D^{20}$ +38.6 (c 0.3, MeOH). The absorption bands at 3389 cm^{-1} and 1688 cm^{-1} in IR spectrum represented the existence of hydroxyl group and carbonyl function, respectively. The ^{1}H NMR data of **15** showed the diagnostic resonances corresponding to a nor-triterpenoid type, including 29 total carbon peaks. Two oxygenated protons, δ_H 4.05 at H-2 and δ_H 4.36 at H-3, two olefinic double bonds, δ_H 5.50 at H-12 and δ_H 4.95 and 5.86 at H-23, and five methyl groups, δ_H 0.83, 1.09, 1.22, 1.00 and 0.97. The ^{13}C NMR data supported those evidence of two oxygenated carbons, δ_C 73.9 at C-2 and 80.0 at C-3, two double bond carbons, δ_C 153.0 at C-4, δ_C 105.1 at C-23, δ_C 126.2 at C-12, δ_C 140.0 at C-13, and five methyl groups for δ_C 15.7, 17.9, 24.3, 18.0, and 21.9. Therefore, the deduction of all the NMR data could be established the compound **15** as Ilekudinol B by comparison of reported literature (Nishimura et al., 1999). ESI-MS data also assisted to confirm the structure (*m/z* 479.3 $[M+Na]^+$ and 455.3 $[M-H]^-$, MW 456).

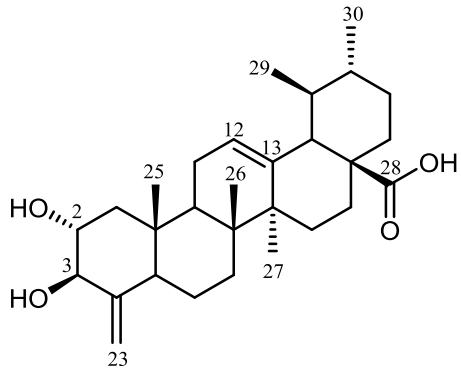

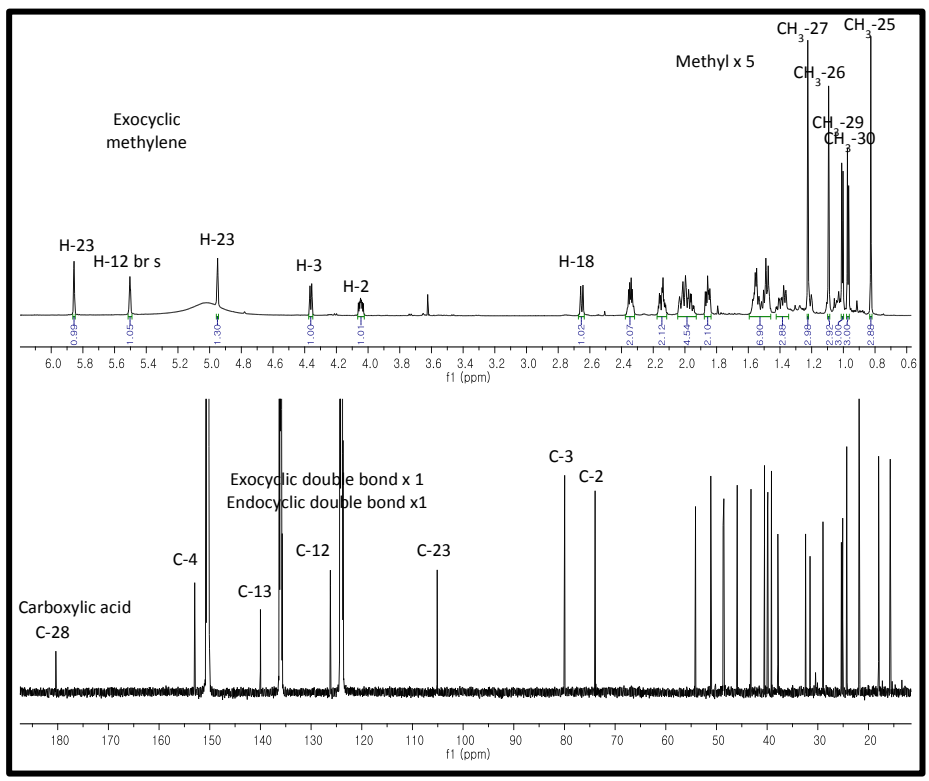

Figure 22. ^{1}H and ^{13}C NMR spectra of compound **15**

1-16. Compound **16**

Compound **16** was obtained as yellowish amorphous powder form. The optical rotation value is -4.0 at 20 degrees Celsius. The IR spectrum showed the presence of two hydroxyl groups at 3445 and 3419 cm^{-1} and a ketone at 1628 cm^{-1}.

The ^{1}H NMR spectra of **16** showed a benzene moiety for δ_H 7.62 and 7.41 with 5 protons, a double bond for δ_H 7.85 (d, J= 15.7) and δ_H 8.00 (d, J= 15.6), one methoxy at δ_H 3.66 (s), and two methyl groups for δ_H 2.16 (s) and 2.14 (s). The ^{13}C NMR also supported those above functionalities with showing one more functional group, ketone at δ_C 193.5. With a logically deduction by comparing spectral data, compound **16** was fully elucidated as 2',4'-dihydroxy-6′-methoxy-3',5'-dimethylchalcone by literature data (Salem et al., 2005). This was further supported by the co-appearance of protonated and deprotonated peaks on ESI-MS spectrums (*m/z* 299.1 $[M+H]^+$ and 297.1 $[M-H]^-$, matching with molecular weight as 298).

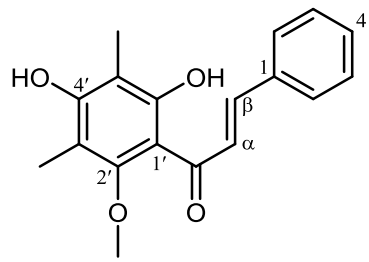

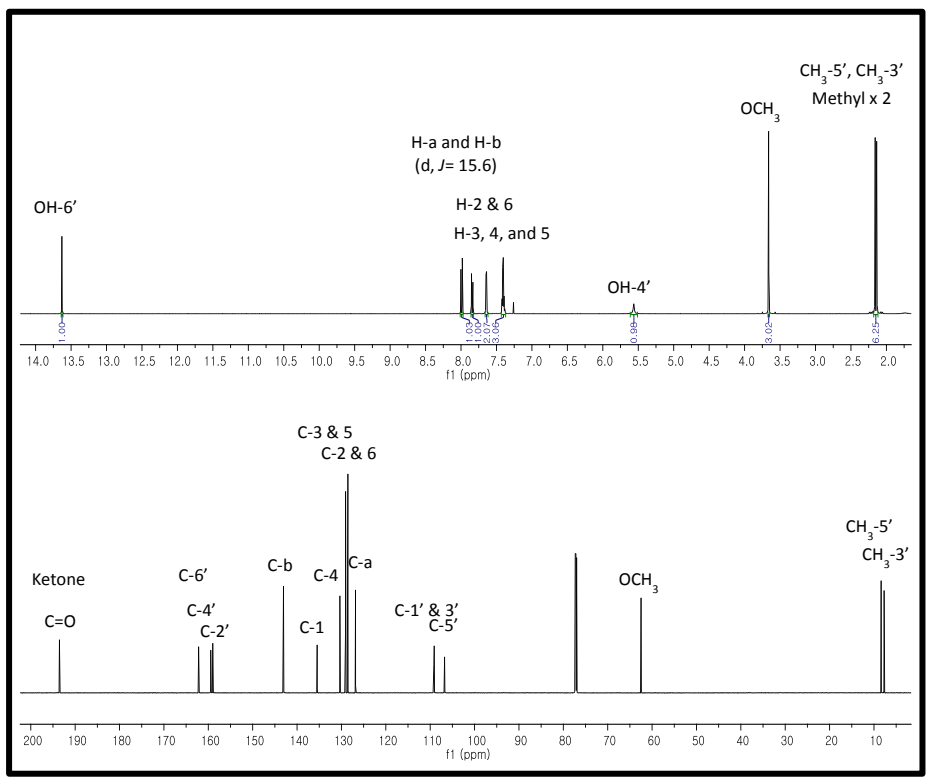

Figure 23. ^{1}H and ^{13}C NMR spectra of compound **16**

1-17. Compound **17**

Compound **17**, a brownish gum, possessed a dimethyl flavanone skeleton where the characteristic proton signals existed a benzene ring (δ_H 7.51, 7.43, and 7.37), a ketone group (δ_C 196.6), two methyl groups (δ_H 1.97 and 1.96), and a hydroxyl group 5-OH (δ_H 12.36) affected by hydrogen bond interaction with ketone. This skeleton is also reported as one of the major constituents in this plant. Noticeably, all of the NMR data led to deduce the structure as Demethoxymatteucinol by previously reported paper (Basnet et al., 1993). The ESI-MS data showed the protonated peak $[M+H]^+$ at *m/z* 285 and the deprotonated peak $[M-H]^-$ at *m/z* 283, corresponding to the molecular weight 284. In conclusion, compound **17** was fully determined.

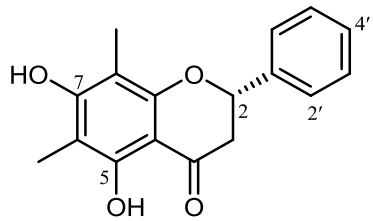

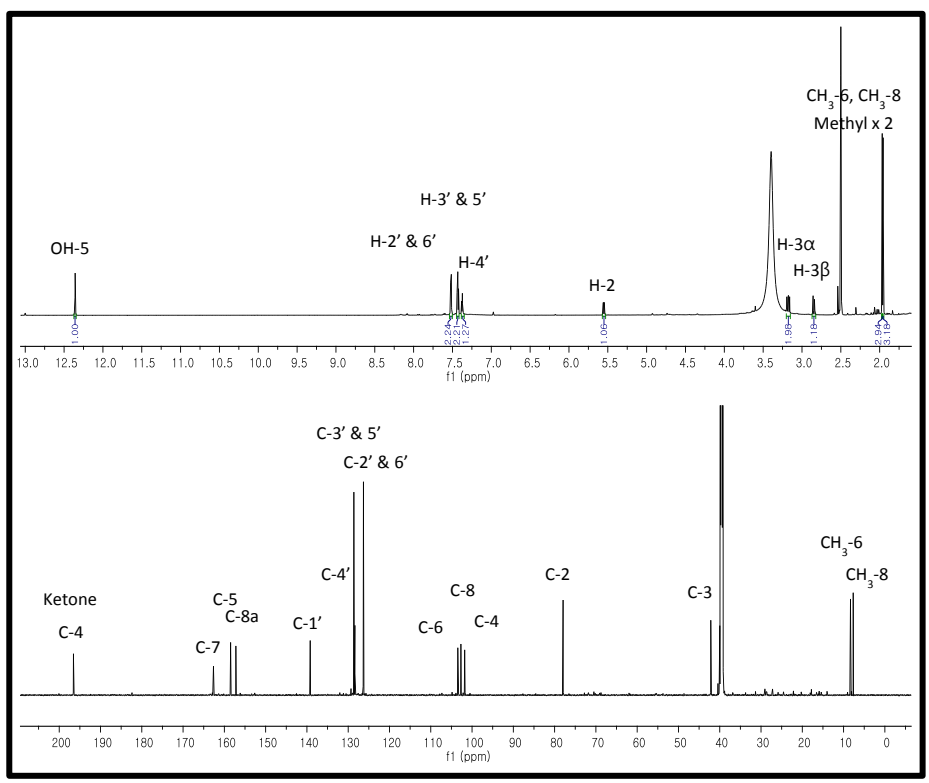

Figure 24. ^{1}H and ^{13}C NMR spectra of compound **17**

1-18. Compound **18**

Compound **18** was purified as brownish gum with the optical rotation, $[\alpha]_D^{20}$ -2.9 (c 0.3, MeOH). The IR peaks at 3398 and 1648 cm^{-1} indicated the existence of hydroxyl and carbonyl functionalities. By the logical interpretation of ^{1}H and ^{13}C NMR, compound **18** was closely identical to those of compound **17** without only the disappearance of hydroxyl group peak at 5-OH in **17**, and a methoxy peak is formed at δ_H 3.81 (s). The reliable assumption could be appeared 5-OCH_3. By comparing the NMR data to previous paper, compound **18** is structurally determined as 7-hydroxy-5-methoxy-6,8-dimethylflavanone (Peralta et al., 2014). The ESI-MS analysis also supported the MW is 298 with the values of *m/z* 299.2 $[M+H]^+$ and *m/z* 297.2 $[M-H]^-$.

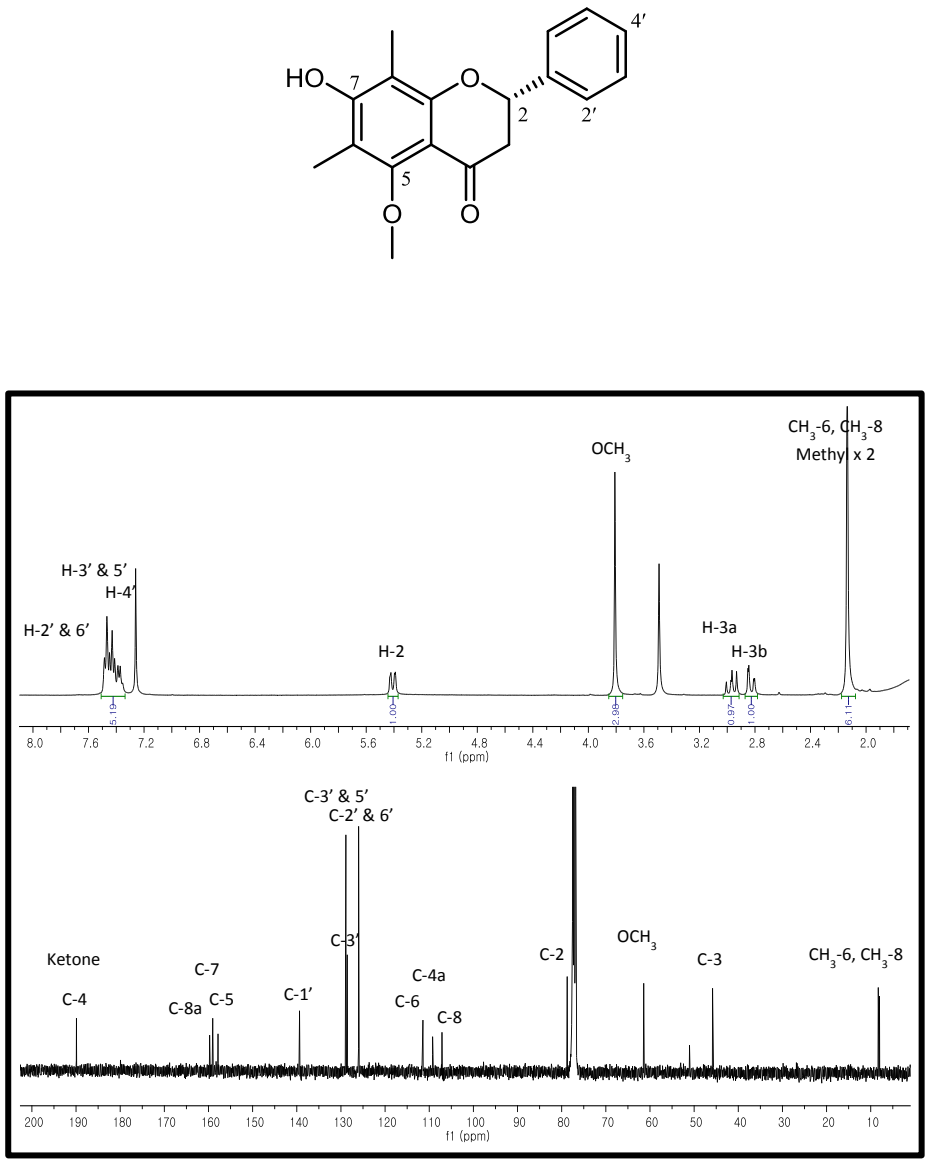

Figure 25. ^{1}H and ^{13}C NMR spectra of compound **18**

1-19. Compound **19**

Compound **19** was obtained under white amorphous powder with $[\alpha]_D^{20}$ +26.2 (c 0.3, MeOH). From the IR spectrum, the existence of hydroxyl (3391 cm^{-1}) and carbonyl (1688 cm^{-1}) functionalities were observed. Compound **19** similarly shared NMR patterns to those of **9** about the signals, δ_H 5.49 (1H, t, *J*= 3.2 Hz), δ_H 3.42 (1H, d, *J*= 9.3 Hz), and δ_H 4.12 (1H, td, *J*= 4.2, 11.0 Hz). However, the changes between two oxygenated protons, from δ_H 3.42 in **9** to δ_H 5.28 in **19**, led to determine the compound attached a functional group on C-3 position. From the ^{13}C NMR, δ_C 168.4, 116.6, 145.5, 126.8, 131.1, 117.3, 161.8, 117.3, and 131.1 recognized as the moiety of *–O-(E)-p*-coumaroyl by the reported paper (Liao et al., 2014). As a result, 3*–O-(E)-p*-coumaroyl maslinic acid structurally determined. The protonated peak $[M+H]^+$ at *m/z* 619.3 and deprotonated peak $[M-H]^-$ at *m/z* 617.4 (MW 618) also supported the structure.

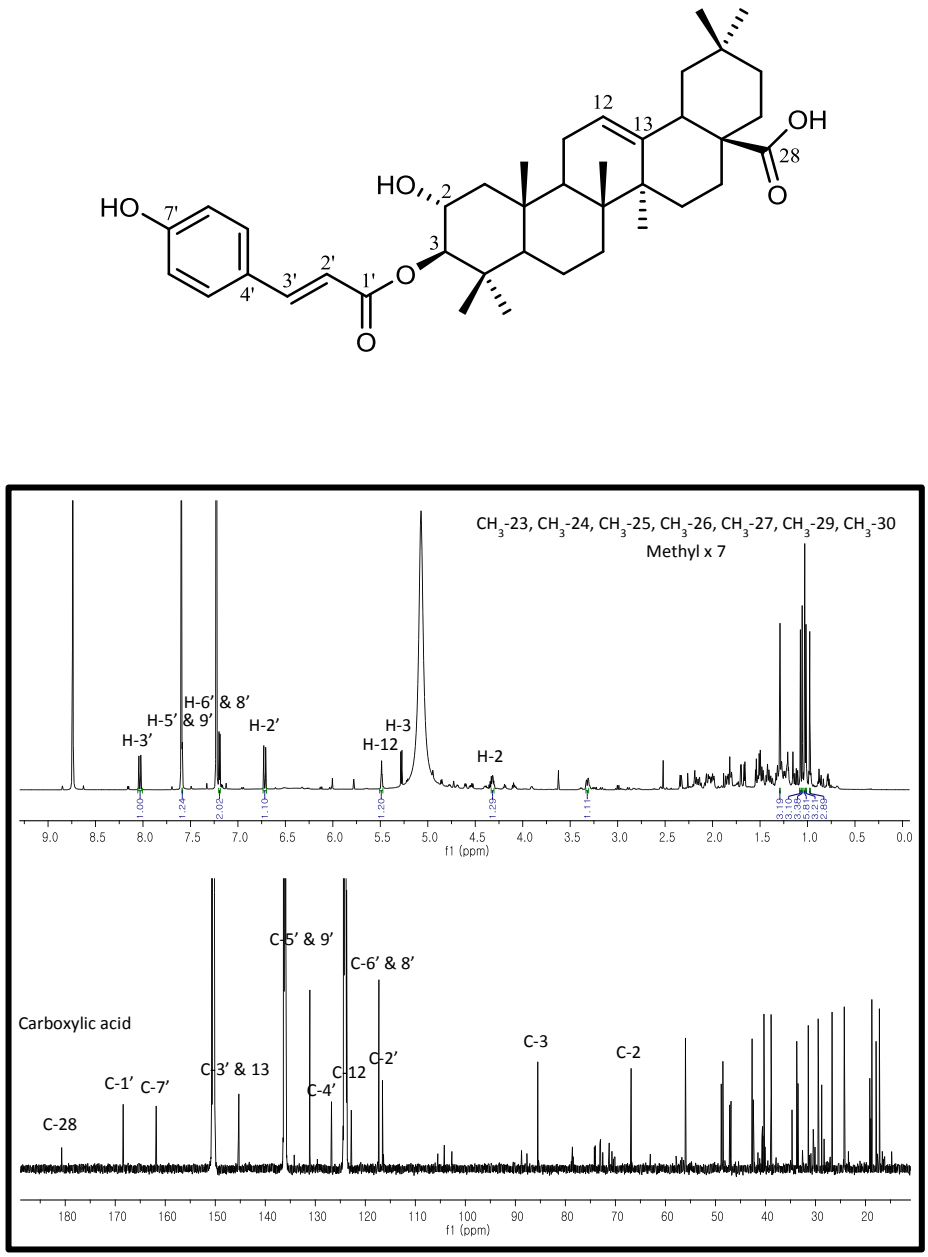

Figure 26. ^{1}H and ^{13}C NMR spectra of compound **19**

1-20. Compound **20**

Compound **20** was isolated as white amorphous powder, with $[\alpha]_D^{20}$ +20.9 (c 0.3, MeOH). The IR spectrum showed strong absorption bands at 3394 and 1705 cm^{-1}, indicating the presence of hydroxyl and ketone groups. Compound **20** is approximately equal to compound **19**, but difference is the only characteristics of a coumaroyl configuration. It is represented trans to cis form from the chemical shifts of δ_H 6.14 (1H, d, *J*= 12.8 Hz), 6.95 (1H, d, *J*= 12.9 Hz), 8.15 (2H, d, *J*= 8.6 Hz), and 7.17 (2H, d, J= 8.6 Hz). Based on the comparing to literature values, the compound is proposed as 3–*O-(Z)-p*-coumaroyl maslinic acid (Liao et al., 2014). The protonated peak $[M+H]^+$ at *m/z* 619.3 and deprotonated peak $[M-H]^-$ at *m/z* 617.4 (MW 618) also supported the structure.

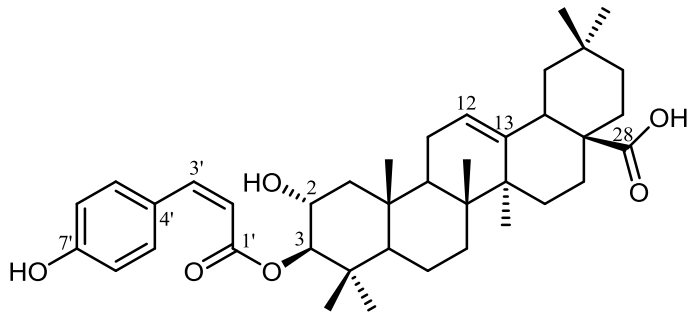

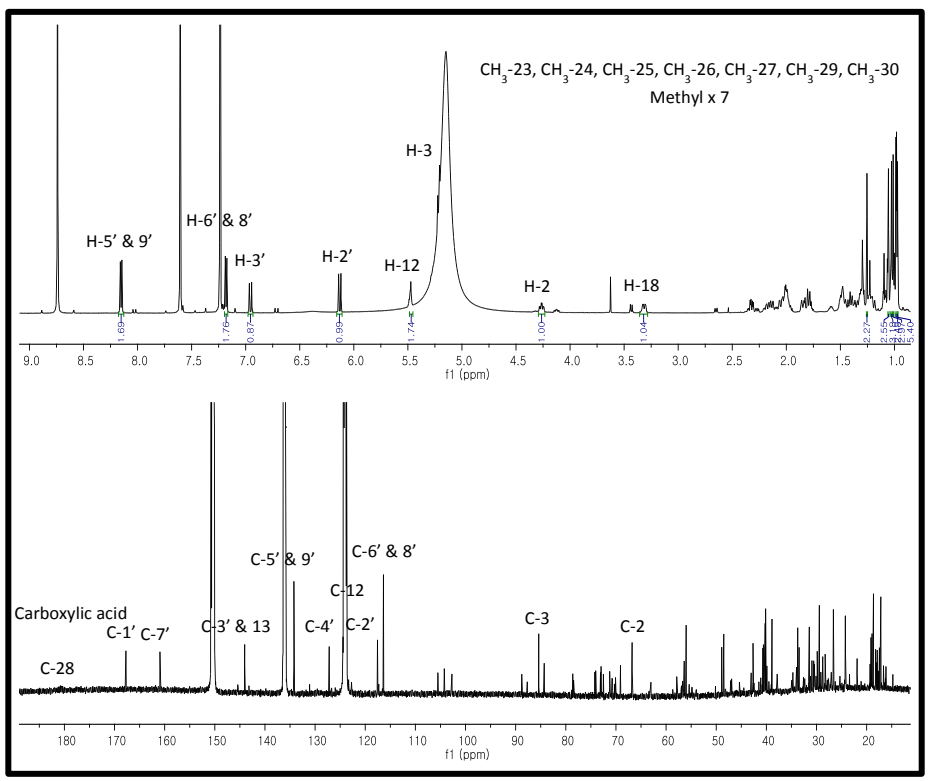

Figure 27. ^{1}H and ^{13}C NMR spectra of compound **20**

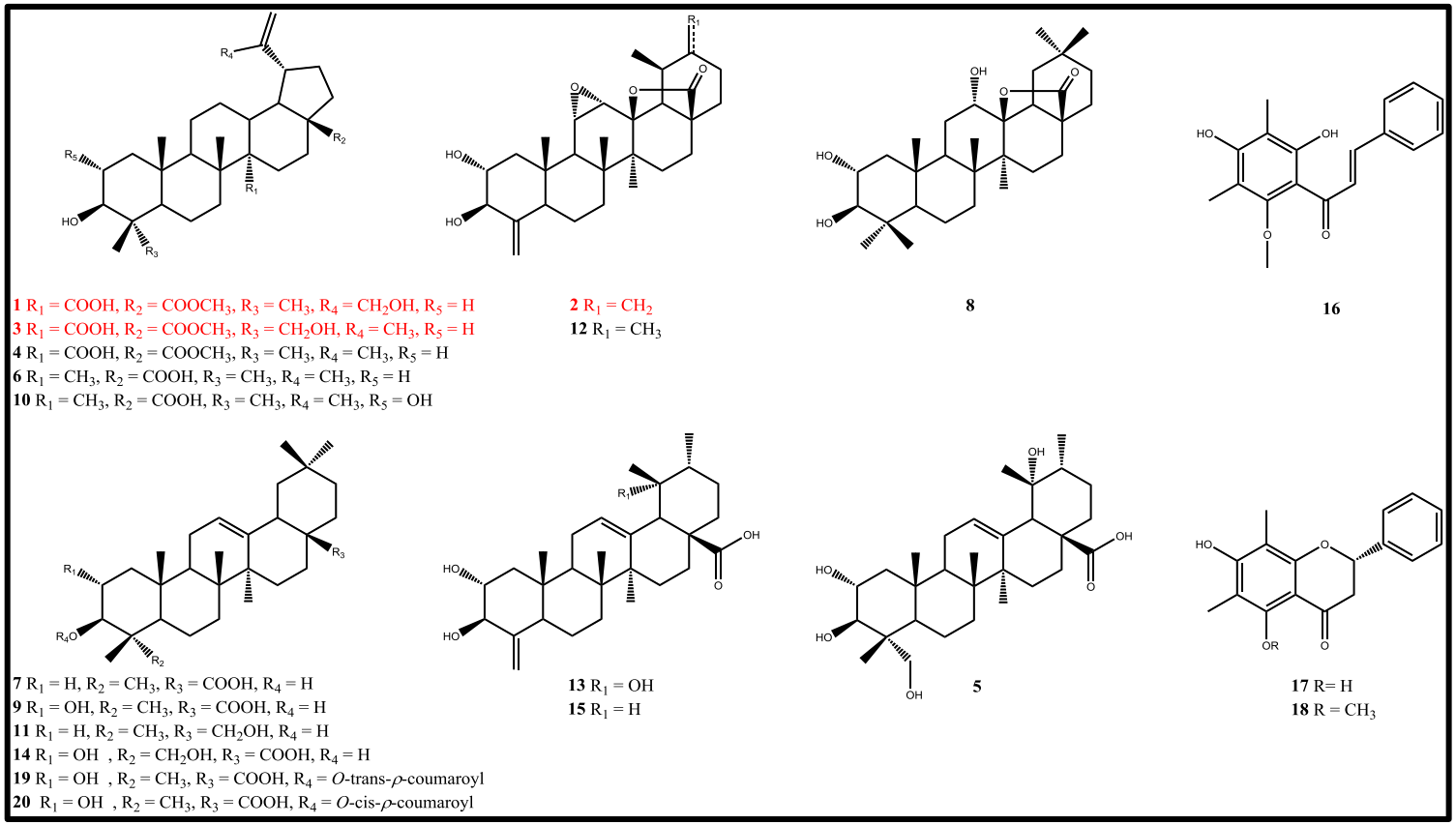

Figure 28. Structures of compounds isolated from *C. operculatus* leaves

2. Relative mass defects (RMDs) analysis.

RMD analysis was performed to isolate target compounds. First, web-databased library of compounds from leaf extracts of *C. operculatus* was built by Scifinder. Next, molecular weights were recalculated using Matlab's *in silico* program to acquire better accuracy to four decimal places. RMD values were calculated by dividing the mass defect by the measured monoisotopic mass and multiplying it by 10^6 to be expressed in ppm. After the processing of RMD calculations, the subsequent graphs (See Figure 29) could be obtained. The graphs clearly showed the division of specific metabolite classes in the plant. Among the classes, the fractionations containing potential PTP1B inhibitors were traced to be the n-BuOH-soluble fraction with a large quantity of triterpenoids. By analyzing the RMD values and the molecular weights, purification was successfully performed through several isolation steps to result in 20 compounds, among which 3 compounds were new. As shown in Table 2, the RMD values for triterpenoids were closely fixed in the range between the minimum, 614.1525, and the maximum, 861.4744, with the exact mass range from 442.3811 to 618.3920.

Table 2. The calculations of relative mass defects (**1-20**) based on the MS/MS spectra.

Theoretical Exact mass based on Negative Ion Mode Fragment Ion	**RMD**	**Chemical Formula**	**Types**
516.3451	668.3515	$C_{31}H_{48}O_6$	Lupane
468.2876	614.1525	$C_{29}H_{40}O_5$	Ursane
516.3451	668.3515	$C_{31}H_{48}O_6$	Lupane
500.3502	699.9098	$C_{31}H_{48}O_5$	Lupane
504.3451	684.2537	$C_{30}H_{48}O_6$	Ursane
456.3603	789.5078	$C_{30}H_{48}O_3$	Lupane
456.3603	789.5078	$C_{30}H_{48}O_3$	Oleanane
488.3502	717.1083	$C_{30}H_{48}O_5$	Oleanane
472.3553	752.188	$C_{30}H_{48}O_4$	Oleanane
472.3553	752.188	$C_{30}H_{48}O_4$	Lupane
442.3811	861.4744	$C_{30}H_{50}O_2$	Oleanane
470.3032	644.6905	$C_{29}H_{42}O_5$	Ursane
472.3189	675.1794	$C_{29}H_{44}O_5$	Ursane
488.3502	717.1083	$C_{30}H_{48}O_5$	Oleanane
456.3240	710.0218	$C_{29}H_{44}O_4$	Ursane
298.1205	404.199	$C_{18}H_{18}O_4$	Dimethylchalcone
284.1049	369.2298	$C_{17}H_{16}O_4$	Dimethylflavanone
298.1205	404.199	$C_{18}H_{18}O_4$	Dimethylflavanone
618.3920	633.9021	$C_{39}H_{54}O_6$	Oleanane
618.3920	633.9021	$C_{39}H_{54}O_6$	Oleanane

(a) (b) (c)

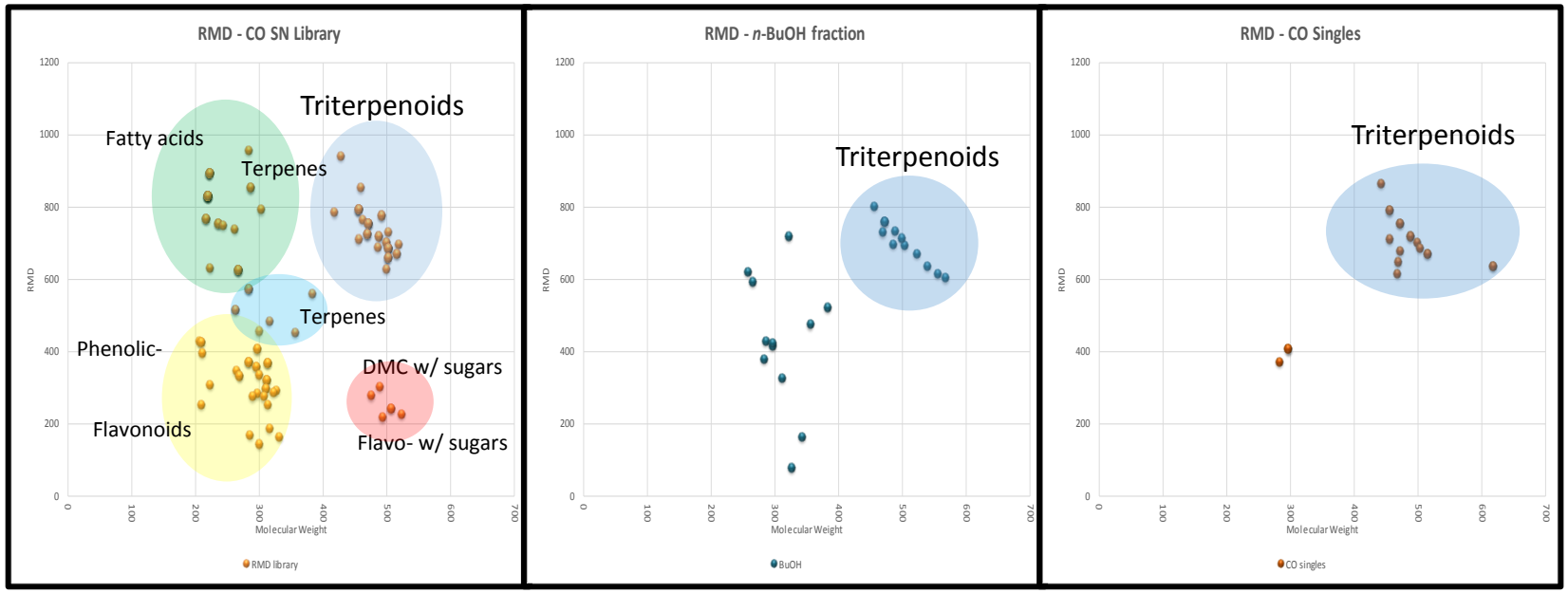

Figure 29. Relative Mass defects (RMDs) calculations: a) *C. operculatus* leaves library based on scifinder search. b) *n*-BuOH fraction by MS/MS. c) Total isolates (**1**-**20**) by MS/MS.

3. PTP1B inhibitory activities of isolated compounds

PTP1B has been demonstrated as a brilliant drug target for the treatment of diabetes mellitus type 2 and obesity (Na et al., 2007). PTP1B enzyme assay was performed to all isolated compounds (**1**-**20**) for their inhibitory activities. The procedure is clearly described in section II.5-1. As shown in Figure 30, among all the isolated constituents, compounds **3**, **6**, **7**, **9**, **10**, **19**, and **20** significantly inhibited the activity against PTP1B while compound **6** had especially strong inhibitory effect on the enzyme.

The structure activity relationships (SARs) were searched based on the PTP1B assay by the previously described literature (Jiang et al., 2012). It suggested that the presence of hydroxyl group and lipophilic functionalities had a significant PTP1B inhibitory effect among triterpenoids. For example, hydroxylation of C-2, C-19, C-23, or C-6 decreased the activity whereas formation of double bond on C-12 and C-13 enhanced the inhibitory effect. Moreover, the existence of C-28 as a free carboxylic acid instead of a lactone ring improved the activity. The position of methyls at C-29 and C-30 in case of ursane- and oleanane- types left the activity unchanged. Isolated triterpenoids, **1**-**15**, **19**, and **20**, were satisfied with the above rules. Betulinic acid and oleanolic acid moiety usually have great chance to inhibit the effect for reference as shown in Figure 28.

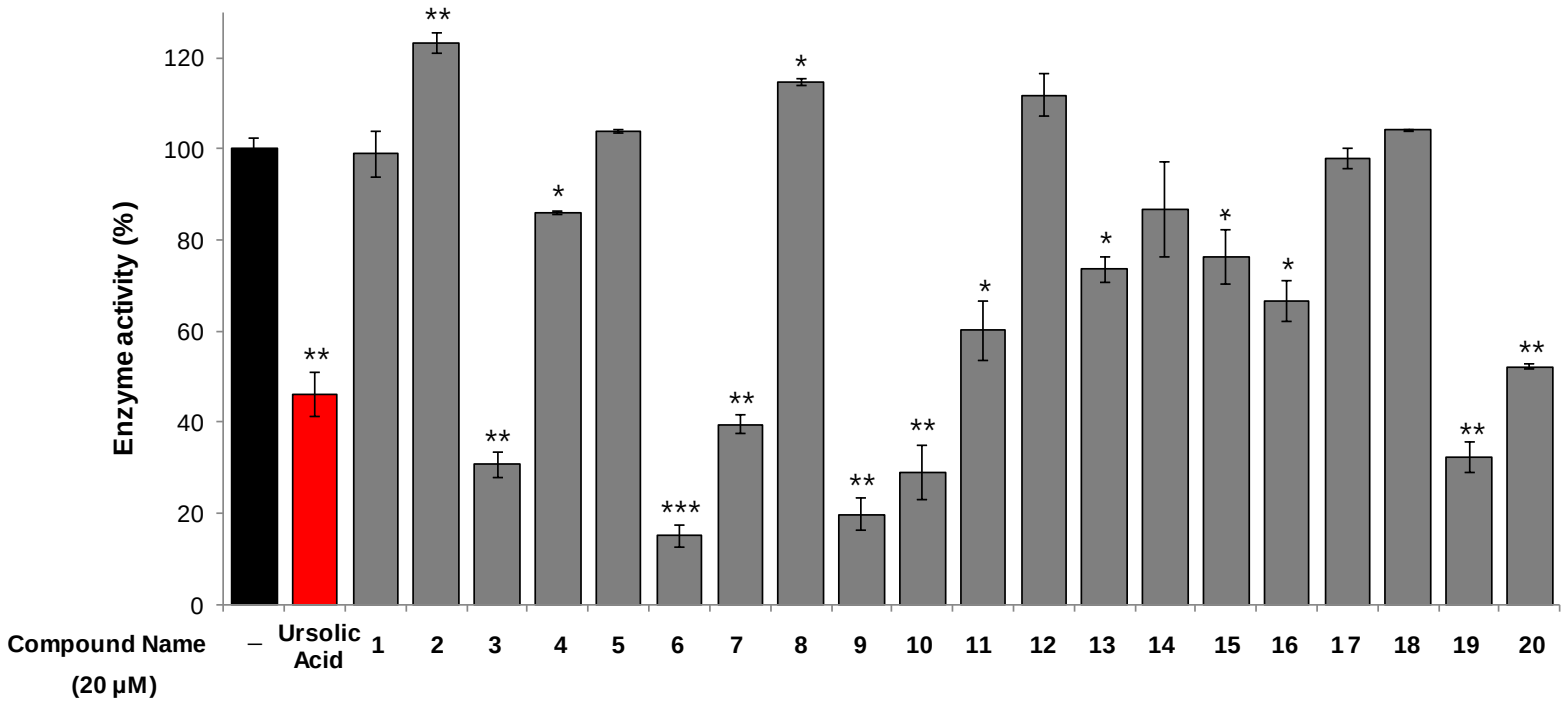

Figure 30. PTP1B Inhibitory activities of isolated compounds **1-20**.

Data were evaluated as the mean ± SD (n= 2). Characteristics were compared between groups, $^{*}p < 0.05$, $^{**}p < 0.01$ and $^{***}p < 0.001$ compared only to the DMSO blank. Ursolic acid was used as positive control.

IV. Conclusions

The purpose of this research was the investigation of the triterpenoids from leaves of *Cleistocalyx operculatus* by mining LC-MS metabolites profile with dereplication isolating process. In addition, this research was performed exploration the bioactive compounds as PTP1B inhibitors to determine their inhibition properties.

After this promising approach for specific metabolite classes is accomplished by determining RMDs, the purification was successfully performed. As shown in Table 2, the fixed range of triterpenoids in RMD values was fully understood because of the isoprene as triterpene building block. The RMD of 600-800 ppm reflects its high hydrogen content. This range stays at the constant for the structures, shared the same fractional hydrogen content. This plant consists of a large amount of triterpenoids and was discovered the presence of highly modified and oxygenated triterpenoids. As a result, it has been succeeded for isolating total 20 compounds, including three new triterpenoids (**1**-**3**) and seventeen known compounds (**4**-**20**).

All isolated constituents were analyzed for their PTP1B inhibitory activities. Among the tested compounds, the triterpenoids (**3**, **6**, **7**, **9**, **10**, **19**, and **20**) showed moderate effects on the inhibition activities while the compound **6** showed the most potent inhibitory activity.

References

An J.P., Ha T.K.Q., Kim J.W., Cho T.O. & Oh W.K. (**2016**) Protein Tyrosine Phosphatase 1B Inhibitors from the Stems of *Akebia quinata*. *Molecules*, 21, pp. 1091-1101.

Basnet P., Kadota S., Shimizu M., Xu H.X. & Namba T. (**1993**) 2'-Hydroxymatteucinol, a new C-methyl flavanone derivative from Matteccia orientalis; potent hypoglycemic activity in streptozotocin (STZ)-induced diabetic rat. *Chemical and Pharmaceutical Bulletin*, 41(10), pp.1790-1795.

Bruke T.R.J., Ye B., Yan X., Wang S., Jia Z., Chen L., Zhang Z.Y. & Barford D. (**1996**) Small Molecule Interactions with Protein-Tyrosine Phosphatase PTP1B and Their Use in Inhibitor Design. *Biochemistry*, 35, pp.15989-15996.

Diabetes. (n.d.) (**2017**) Data from the 2017 World Health Organization Fact Sheet. http://www.who.int/mediacentre/factsheets/fs312/en/.

Dung N.T., Bajpai V.K., Yoon J.I. & Kang S.C. (**2009**) Anti-inflammatory effects of essential oil isolated from the buds of *Cleistocalyx operculatus* (Roxb.) Merr and Perry. *Food Chemical Toxicology*, 47, pp.449-453.

Ekanayaka E.A.P., Celiz M.D. & Jones A.D. (**2015**) Relative Mass Defect Filtering of Mass Spectra: A Path to Discovery of Plant Specialized Metabolites. *Plant physiology*, 167, pp.1221-1232.

Ekon J.P.L., Bissoue A.N., Fomani M., Toze F.A.A., Kamdem A.F.W., Sewald N. & Wansi J.D. (**2015**) Cytotoxic 24-nor-ursane-type triterpenoids from the twigs of

Mostuea hirsute. *Zeitschrift für Naturforschung Section B-A Journal of Chemical Sciences*, 70(11), pp.837-842.

Ha T.K.Q., Dao T.T., Nguyen N.H., Kim J.W., Kim E.H., Cho T.O. & Oh W.K. (**2016**) Antiviral phenolics from the leaves of *Cleistocalyx operculatus*. *Fitoterapia*, 110, pp.135-141.

Hiroshi S., Orihara Y., Tansakul P., Kang Y.H., Shibuya M. & Ebizuka Y. (**2007**) Production of Triterpene Acids by Cell Suspension Cultures of *Olea europaea*. *Chemical and Pharmaceutical Bulletin*, 55(5), pp.784-788.

Jang D.S., Kim J.M. Kim J.H. & Kim J.S. (**2005**) 24-nor-Ursane Type Triterpenoids from the Stems of *Rumex japonicas*. *Chemical and Pharmaceutical Bulletin*, 53(12), pp.1594-1596.

Jiang C.S., Liang L.F. & Guo Y.W. (**2012**) Natural products possessing protein tyrosine phosphatase 1B (PTP1B) inhibitory activity found in the last decades. *Acta Pharmacologica Sinica*, 33, pp.1217-1245.

Jin Q., Jin H.G., Kim A.R. & Woo E.R. (**2012**) A New Megastigmane Palmitate and a New Oleanane Triterpenoid from *Aster yomena* Makino. *Helvetica Chimica Acta*, 95, pp.1455-1460.

Kaneta Y., Arai M. A., Ishikawa N., Toume K., Koyano T., Kowithayakorn T., Chiba T., Iwama A. & Ishibashi M. (**2017**) Identification of BMI1 Promoter Inhibitors from *Beaumontia murtonii* and *Eugenia operculata*. *Journal of Natural Products*, 80, pp.1853-1859.

Kang K.B., Kim J.W. Oh W.K., Kim J.W., Sung S.H. (**2016**) Cytotoxic Ceanothane- and Lupane-Type Triterpenoids from the Roots of *Ziziphus jujuba*. *Journal of Natural Products*, 79, pp.2364−2375.

Koren S. & Fantus I.G. (**2007**) Inhibition of the protein tyrosine phosphatase PTP1B: potential therapy for obesity, insulin resistance and type-2 diabetes mellitus. *Best Practice & Research: Clinical Endocrinology & Metabolism*, 21(4), pp.621-640.

Li E.N., Zhou G.D. & Kong L.Y. (**2009**) Chemical Constituents from the Leaves of *Eriobotrya japonica*. *Chinese Journal of Natural Medicines*, 7(3), pp.190-192.

Liao C.R., Kuo Y.H., Wang C.Y., Yang C.S., Lin C.W. & Chang Y.S. (**2014**) Studies on Cytotoxic Constituents from the Leaves of *Elaeagnus oldhamii* Maxim. in Non-Small Cell Lung Cancer A549 Cells. *Molecules, 19,* pp.9515-9534.

Mathers C.D. & Loncar D. (**2006**). Projections of Global Mortality and Burden of Disease from 2002 to 2030. *PLOS Medicine*, 3(11): e442.

Montalibet J. & Kennedy B.P. (**2005**) Therapeutic strategies for targeting PTP1B in diabetes. *Drug Discovery Today: Therapeutic Strategies*. 2(2), pp.129-135.

Morris J. M., Beilharz E. J., Maniam J., Reichelt C. A. & Westbrook F. R. (**2015**). Why is obesity such a problem in the 21st century? The intersection of palatable food, cues and reward pathways, stress, and cognition. *Neuroscience & Biobehavioral Reviews*, 58, pp.36-45.

Na M.K., Kim K.A., Oh H.C., Kim B.Y., Oh W.K. & Ahn J.S. (**2007**). Protein Tyrosine Phosphatase 1B Inhibitory Activity of Amentoflavone and Its Cellular

Effect on Tyrosine Phosphorylation of Insulin Receptors. *Biological and Pharmaceutical Bulletin*, 30(2), pp.379-381.

NCD Risk Factor Collaboration. (**2016**). Worldwide trends in diabetes since 1980: a pooled analysis of 751 population-based studies with 4·4 million participants. *The Lancet*, 387, pp.1513-1530.

Nguyen P.H., Yang J.L., Uddin M.N., Park S.L., Lim S.I., Jung D.W., Williams D.R. & Oh W.K. (**2013**). Protein Tyrosine Phosphatase 1B (PTP1B) Inhibitors from *Morinda citrifolia* (Noni) and Their Insulin Mimetic Activity. *Journal of Natural Products*, 76, pp.2080-2087.

Nishimura K., Fukuda T., Miyase T., Noguchi H. & Chen X.M. (**1999**) Activity-Guided Isolation of Triterpenoid Acyl CoA Cholesteryl Acyl Transferase (ACAT) Inhibitors from *Ilex kudincha*. *Journal of Natural Products*, 62, pp.1061-1064

Peralta M.A., Santi M.D., Agnese A.M. Cabrera J.L. & Ortega M.G. (**2014**) Flavanoids from Dalea elegans: Chemical reassignment and determination of kinetics parameters related to their anti-tyrosinase activity. *Phytochemistry Letters*, 10, pp.260-267.

Salem M.M. & Werbovetz K.A. (**2005**) Antiprotozoal Compounds from *Psorothamnus polydenius*. *Journal of Natural Products*, 68, pp.108-111.

Siewert B., Wiemann J., Kowitsch A. & Csuk R. (**2014**) The chemical and biological potential of C ring modified triterpenoids. *European Journal of Medicinal Chemistry*, 72, pp.84-101.

Sleno L. (**2012**) the use of mass defect in modern mass spectrometry. *Journal of Mass Spectrometry*, 47, pp.226-236.

Srivedavyasasri R. Hayes T. & Ross S.A. (**2017**) Phytochemical and biological evaluation of *Salvia apiana*. *Natural Product Research*, 31(17), pp.2058-2061.

Taniguchi S., Imayoshi Y., Kobayashi E., Takamatsu Y., Ito H., Hatano T., Sakagami H., Tokuda H., Nishino H., Sugita D., Shimura S. & Yoshida T. (**2002**) Production of bioactive triterpenes by *Eriobotrya japonica* calli. *Phytochemistry*, 59, pp.315-323.

Uddin M.N., Sharma G., Yang J.L., Choi H.S., Lim S.I., Kang K.W. & Oh W.K. (**2014**). Oleanane triterpenes as protein tyrosine phosphatase 1B (PTP1B) inhibitors from *Camellia japonica*. *Phytochemistry*, 103, pp.99-106.

Wang C. Wu P., Tian S., Xue J., Xu L., Li H. & Wei X. (**2016**) Bioactive Pentacyclic Triterpenoids from the Leaves of *Cleistocalyx operculatus*. *Journal of Natural. Products*, 79, pp.2912-2923.

Zimmet, P., Alberti, K. G. M. M. & Shaw, J. (**2001**). Global and societal implications of the diabetes epidemic. *Nature*, 414, pp.782-787.

국문초록

수용 (*Cleistocalyx operculatus* (Roxb.) Merr. Et L.M. Perry.는 도금양과(Myrtaceae)에 속하는 상록수로서 중국, 태국, 베트남, 호주 등 아시아 전역에 널리 분포되어 있다. 수용의 잎과 꽃봉오리는 여러 문화권에서 허브 차나 전통적인 약물로서 감기, 열, 항염, 위장질환 등 다양한 의학적 용도로 오래 전부터 사용되어 왔다. 꽃봉오리에 대한 연구는 활발히 진행 되어 왔으며 주로 chalcone, flavonoids, triterpenoids, acetophenone 관련 화합물들이 암세포 성장 저지효과, 콜린에스테라아제 억제, 항산화, 항고혈당, 항 인플루엔자, 항염 등 다양한 생리활성이 있다고 보고되었다. 그러나 지금까지 잎에 대한 연구는 상대적으로 미비한 실정이다.

최근에 분석 기술의 발전으로 HPLC-qTOF-MS와 같은 질량 분석기를 사용해서 식물 추출물과 같은 복잡한 혼합물의 분석을 단순화 시키는 방법이 잇따라 등장하고 있다. 현재까지 천연물 연구에서는 이미 많이 알려진 dereplication 기법을 통해 기존에 보고 된 화합물을 제외하고 신규 화합물의 효과적인 분리를 진행하고 있다. 본 연구는 이 기법에 상대적 질량 결손(RMD) 방법을 추가적으로 사용하였다. 단시간에 식물의 특정한 대사산물의 계열을 분자와 토막이온을 통해 추측하여 수용에서 특이적인 성분군인 pentacyclic-type triterpene 에 속하는 신규 화합물을 효과적으로 분리하여 생리활성을 규명하는 것을 주요 목적으로 하였다.

수용의 잎을 채집하여 50% 에탄올 추출물을 수득한 후 n-Hexane, n-BuOH 및 H_2O 층으로 분획하였다. 그 결과 triterpene 이 많이 함유되 있는 n-BuOH층에서 데이터베이스의 값과 비교하여 새로운 화합물이라고 여겨지는 RMD 값과 MASS 값을 가진 화합물을 가려내고, 산화가 많이 일어나고 변형된 pentacyclic-type triterpene 을 추정하여 분리를 진행했다. 그 결과, 17종의 triterpene (**1-15,19,20**)과 3종의 phenolic compounds (**16-18**)을 분리하고 구조동정 하였다. 분리한 화합물 중 3종은 pentacyclic-type triterpene (**1-3**)으로 천연에서 처음으로 분리보고 되는 물질이며 각각, cleistocalyxic acid L (**1**), cleistocalyxolides C (**2**), cleistocalyxic acid M (**3**)로 명명하였다. 분리된 기지화합물들의 구조는 Melaleucic acid 28-methyl ester (**4**), 19α-Hydroxyasiatic acid (**5**), Betulinic acid (**6**), Oleanolic acid (**7**), (2a, 3b, 12a)-Trihydroxy-olean-28-oic acid 28,13- lactone (**8**), Maslinic acid (**9**), Alphitolic acid (**10**), Erythrodiol (**11**), Ulmoidol (**12**), 2α,3β,19α-Trihydroxy-

24-norurs- 4(23),12-dien-28-oic acid (**13**), Arjunolic acid (**14**), Ilekudinol B (**15**), 2',4'-dihydroxy-6′ -methoxy-3',5'-dimethylchalcone (**16**), Demethoxymatteucinol (**17**), 7-hydroxy-5-methoxy-6,8-dimethylflavanone (**18**), 3-O-(E)-*p*-Coumaroyl maslinic acid (**19**), 3-O-(Z)-*p*-Coumaroyl maslinic acid (**20**)로 규명 되었다. 분리된 화합물은 RMD값과 Mass값의 차이로 인해 화합물의 계열이 쉽고 빠르게 도식화하여 극명하게 나뉘는 것을 확인하였다.

본 연구의 결과로부터 화합물의 화학적 특성을 규명하였을 뿐 아니라, 신규 화합물을 상대적 질량 결손 방법을 통하여 새로운 화합물의 존재 가능성을 확임함으로써 수용에서의 pentacyclic-type triterpene 화합물의 화학적 다양성을 제시하였다. 또한, 분리된 화합물의 PTP1B 저해 활성을 확인한 결과, 화합물 **6**과 **9** 에서 강한 활성 저해를 나타내었고, 화합물 **3**, **7**, **10**, **19**,와 **20** 에서 적당한 활성이 있음을 확인하였다. PTP1B 저해활성의 증진을 통해 수용의 잎이 PTP1B의 치료 물질로서의 활용가능성을 제시하였다.

주요어: Cleistocalyx operculatus (수용), 상대적 질량 결손 (RMD), cleistocalyx acid, cleistocalyxolide, triterpenoid, PTP1B, dimethylchalcone

학번: 2016-21854

Supplementary Information

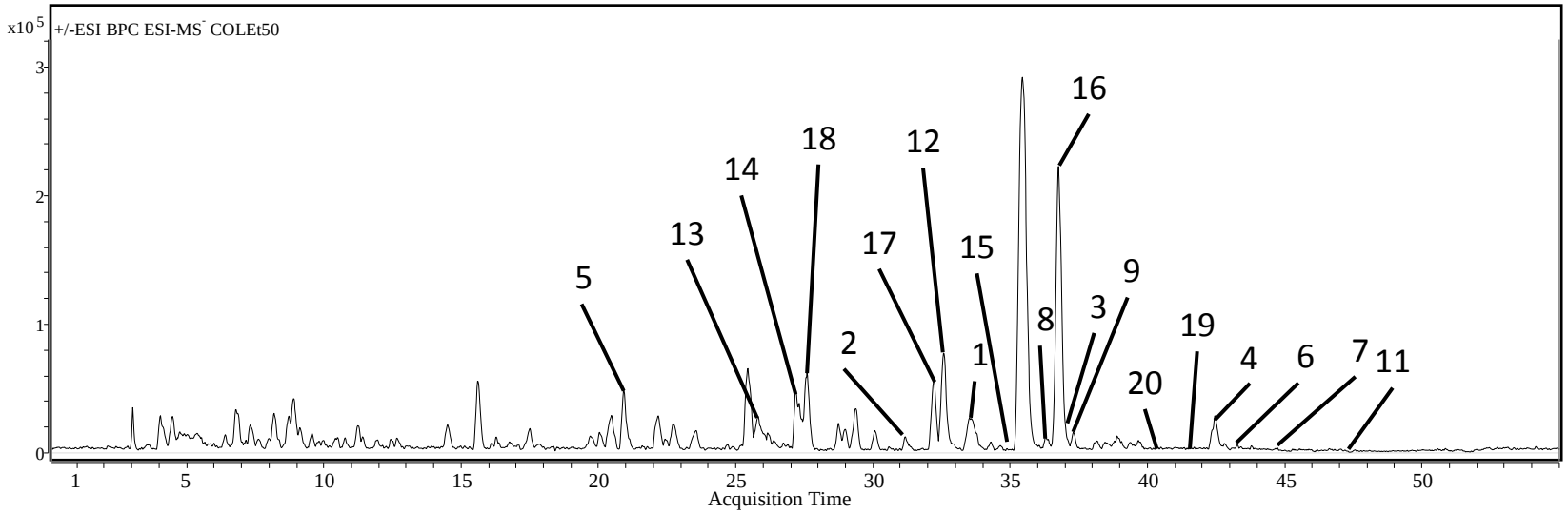

Figure S1. The LC/ESI-MS profile of isolated compounds from *n*-BuOH-soluble fraction of *C. operculatus* leaves. The system was set up with INNO C_{18} column (4.6 × 250 mm, 5 μm particle size) with ESI dual mode, positive & negative (CID. 150), and the solvent system was established ACN in H_2O containing 0.1% of formic acid (0-45 min: 30-100% ACN; 45-55 min: 100% ACN) with the flow rate of 0.6 mL/min.

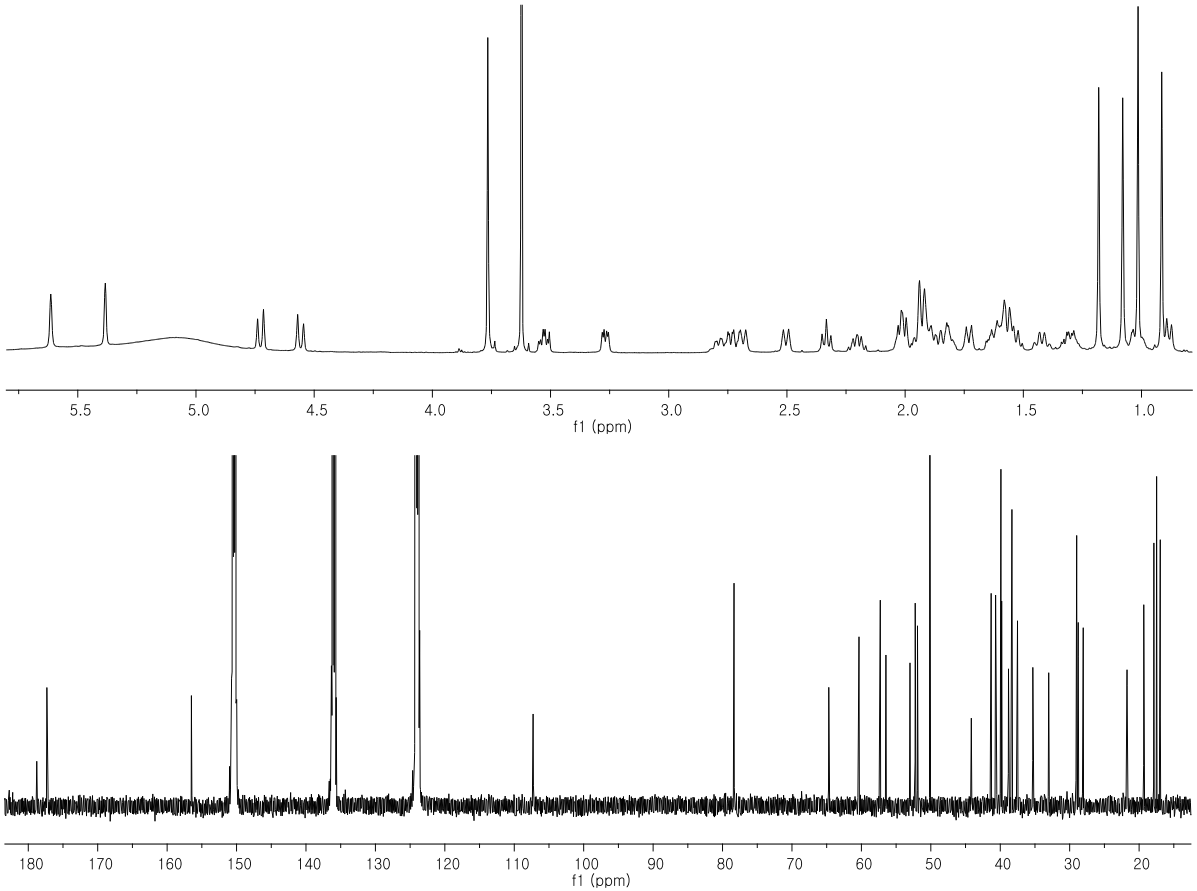

Figure S2. ^{1}H and ^{13}C NMR spectra of compound **1** in pyridine-d_5

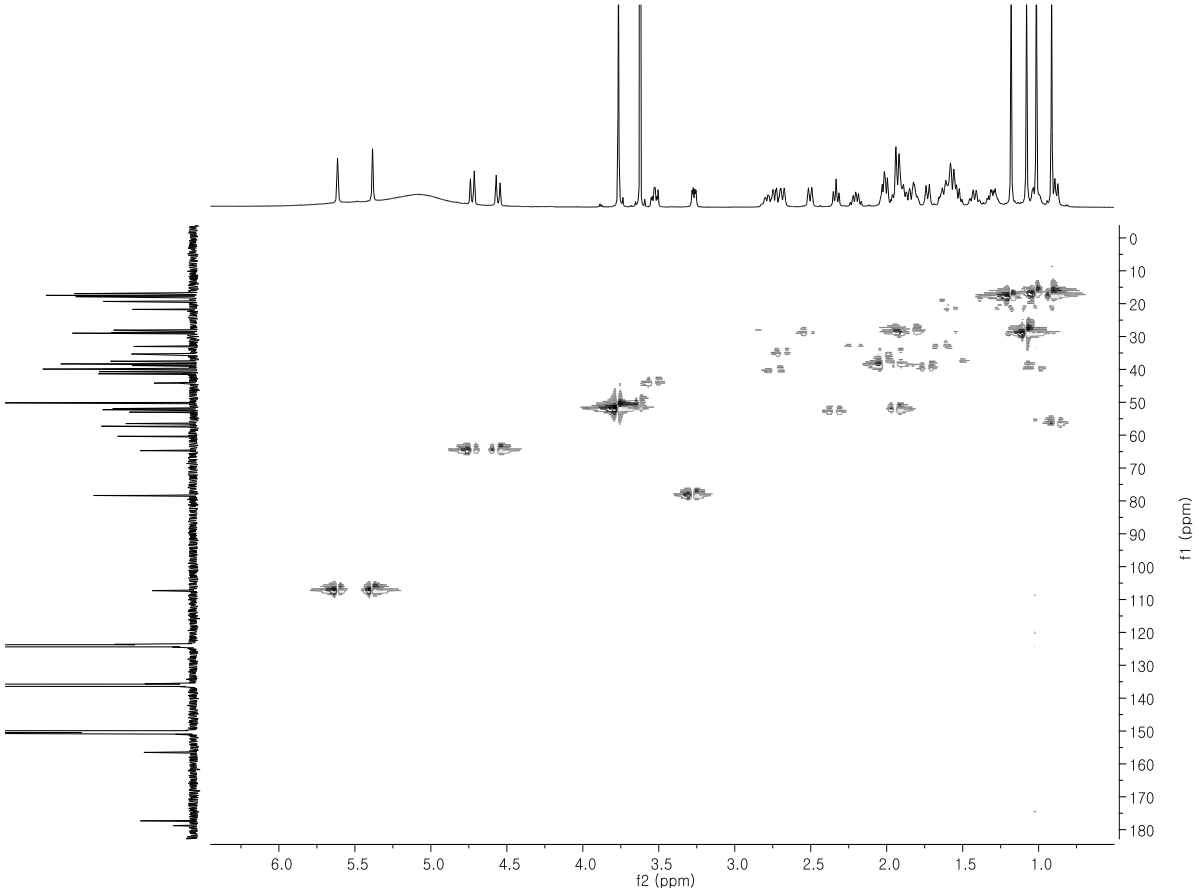

Figure S3. HSQC spectrum of compound **1** in pyridine-d_5

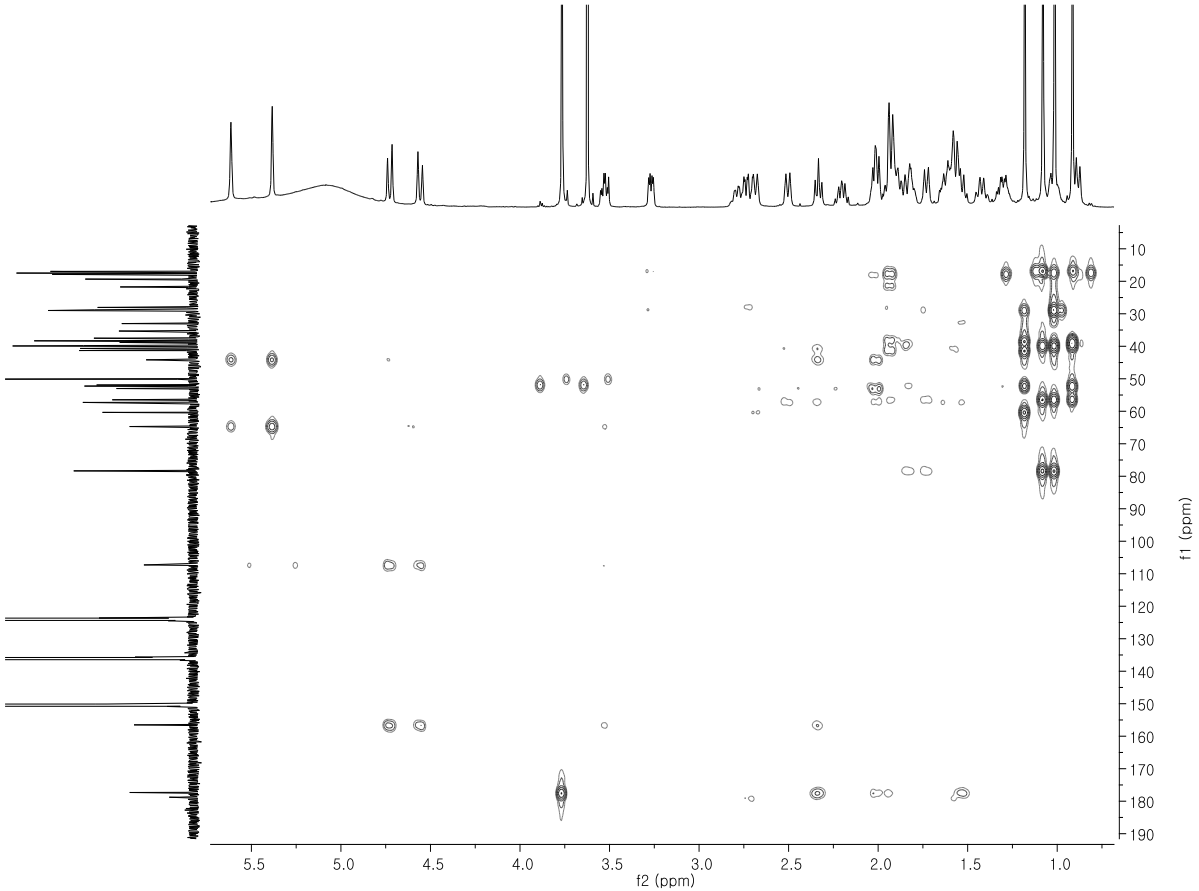

Figure S4. HMBC spectrum of compound **1** in pyridine-d_5

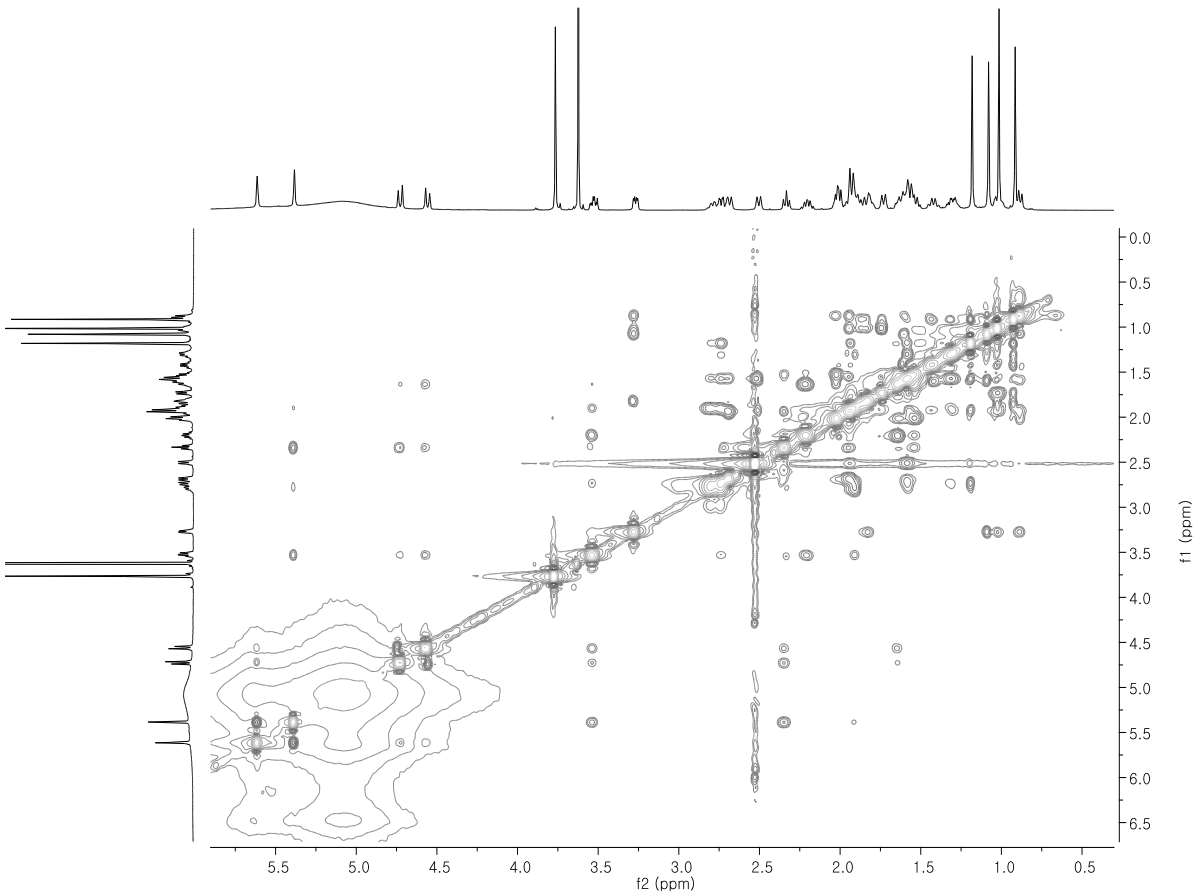

Figure S5. NOESY spectrum of compound **1** in pyridine-d_5

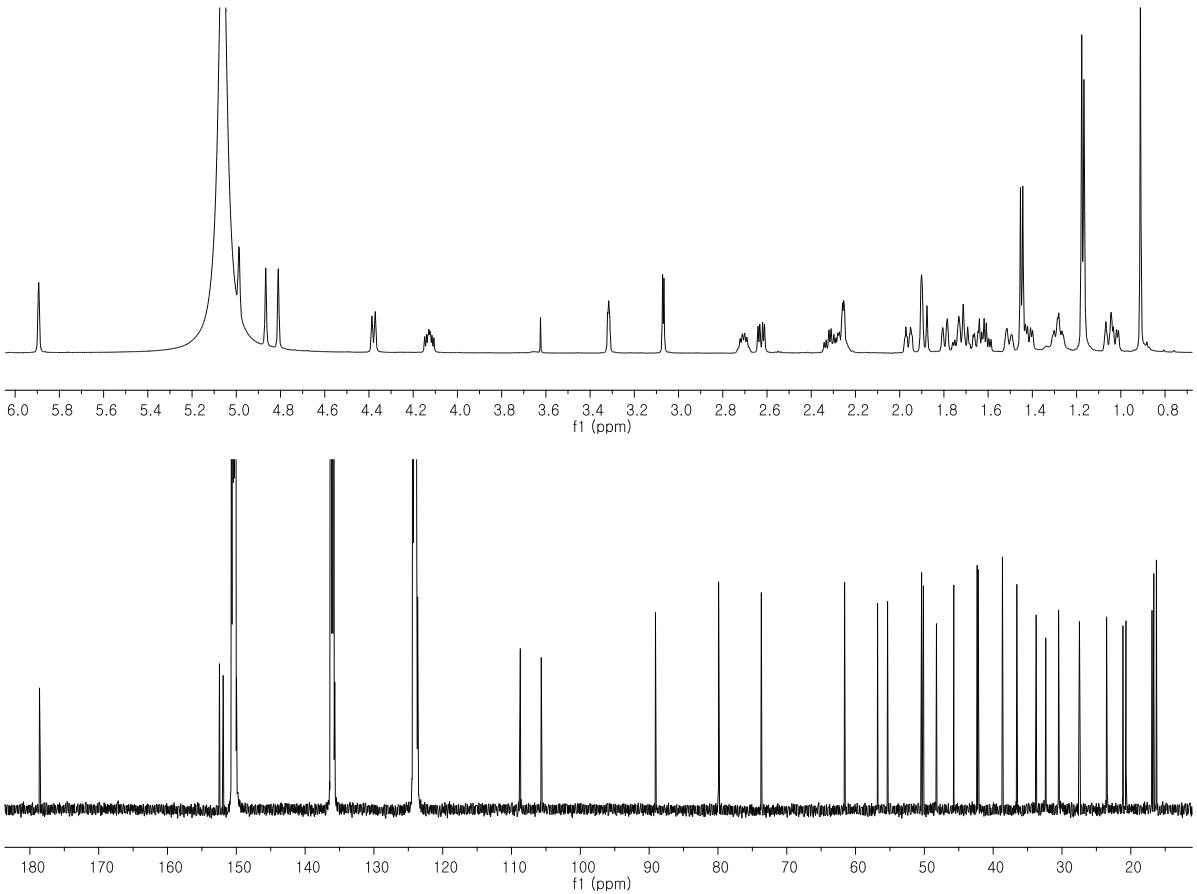

Figure S6. ^{1}H and ^{13}C NMR spectra of compound **2** in pyridine-d_5

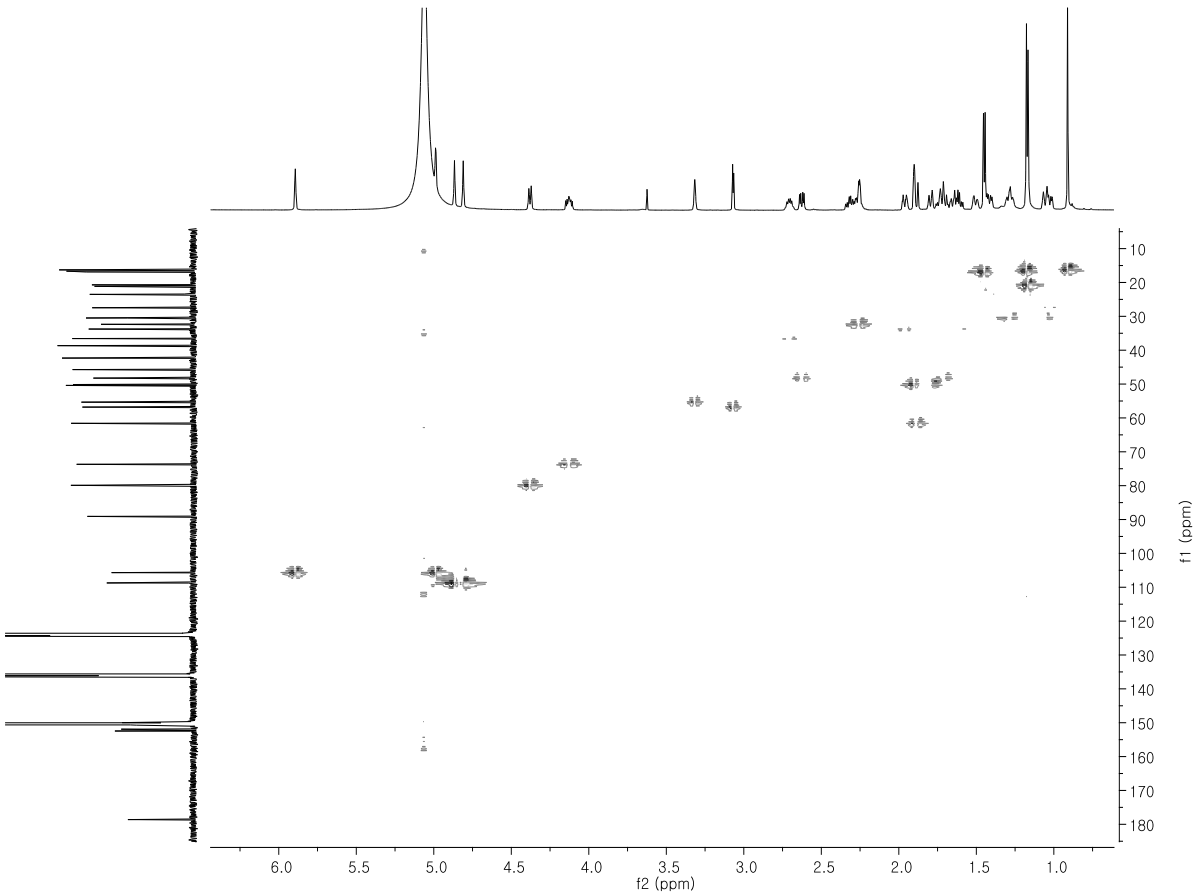

Figure S7. HSQC spectrum of compound **2** in pyridine-d_5

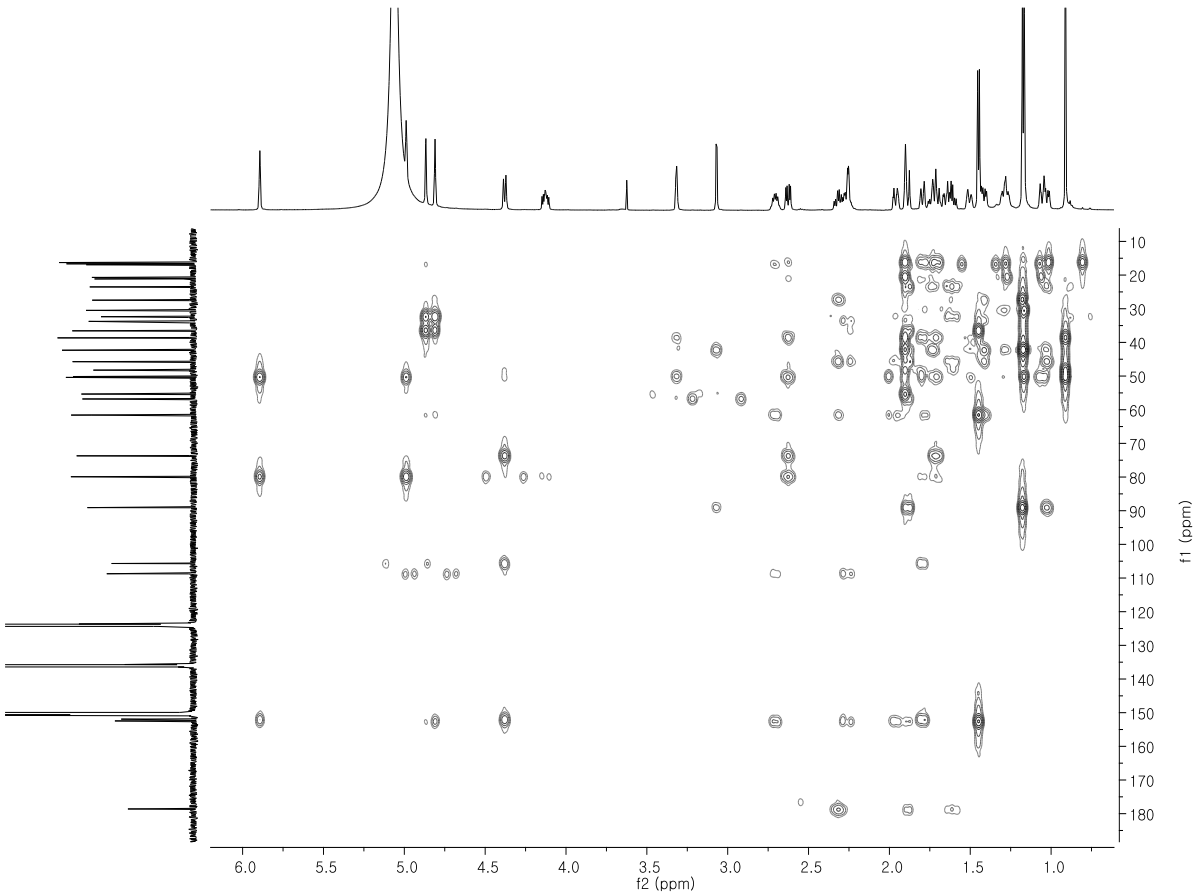

Figure S8. HMBC spectrum of compound **2** in pyridine-d_5

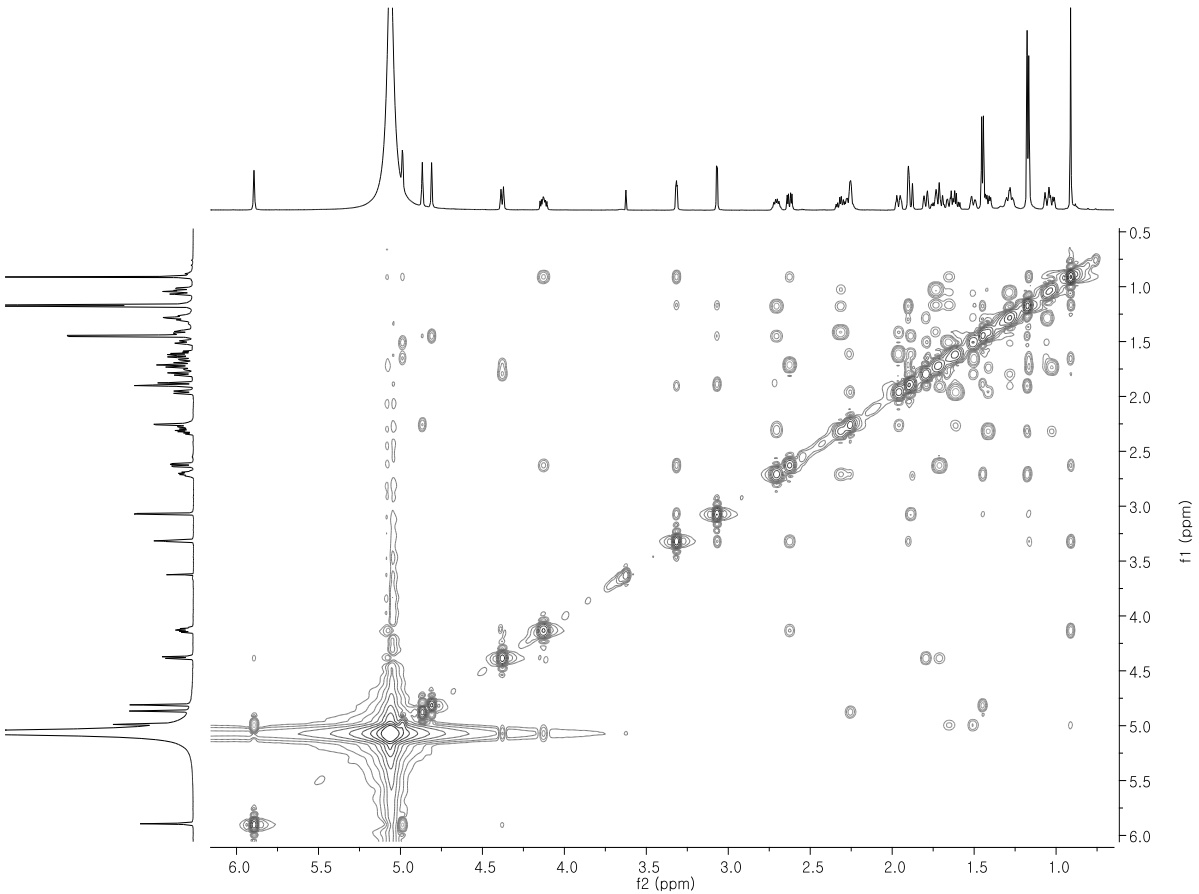

Figure S9. NOESY spectrum of compound **2** in pyridine-d_5

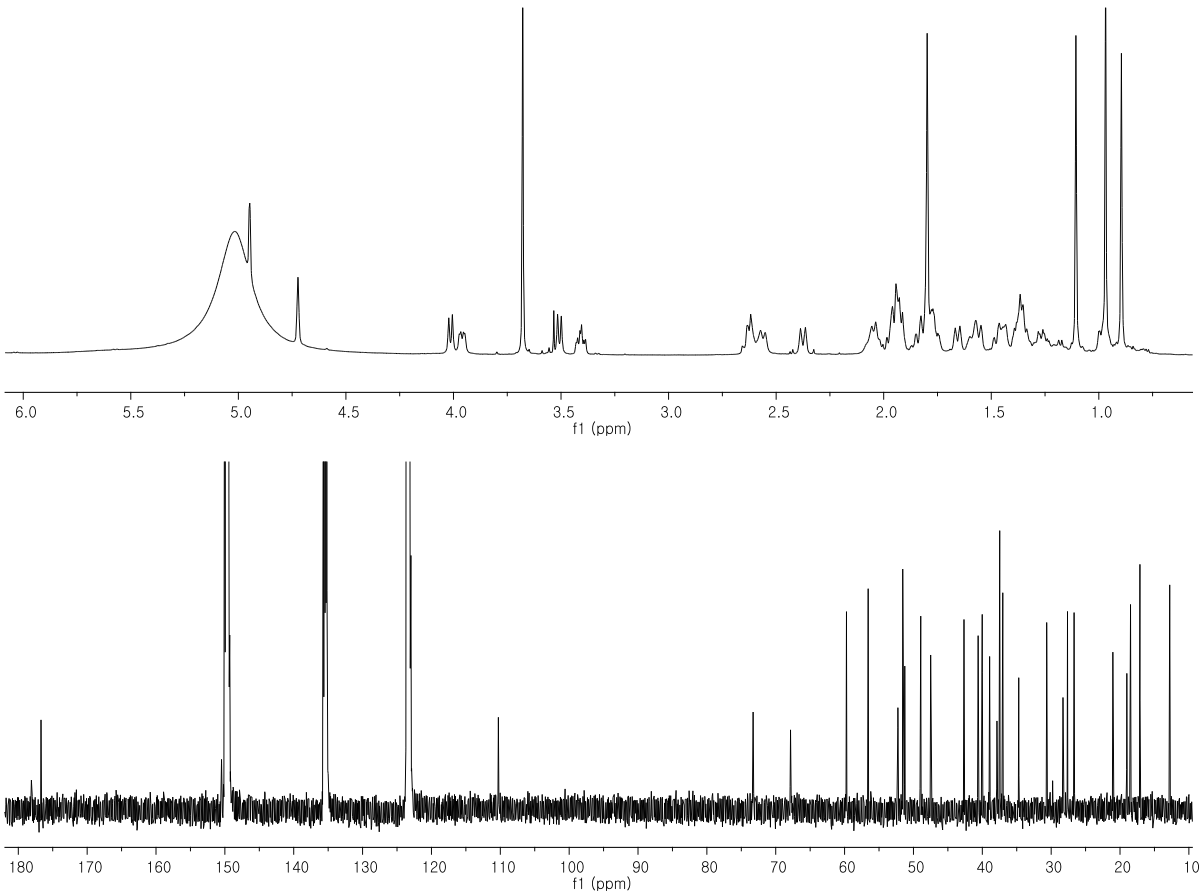

Figure S10. ^{1}H and ^{13}C NMR spectra of compound **3** in pyridine-d_5

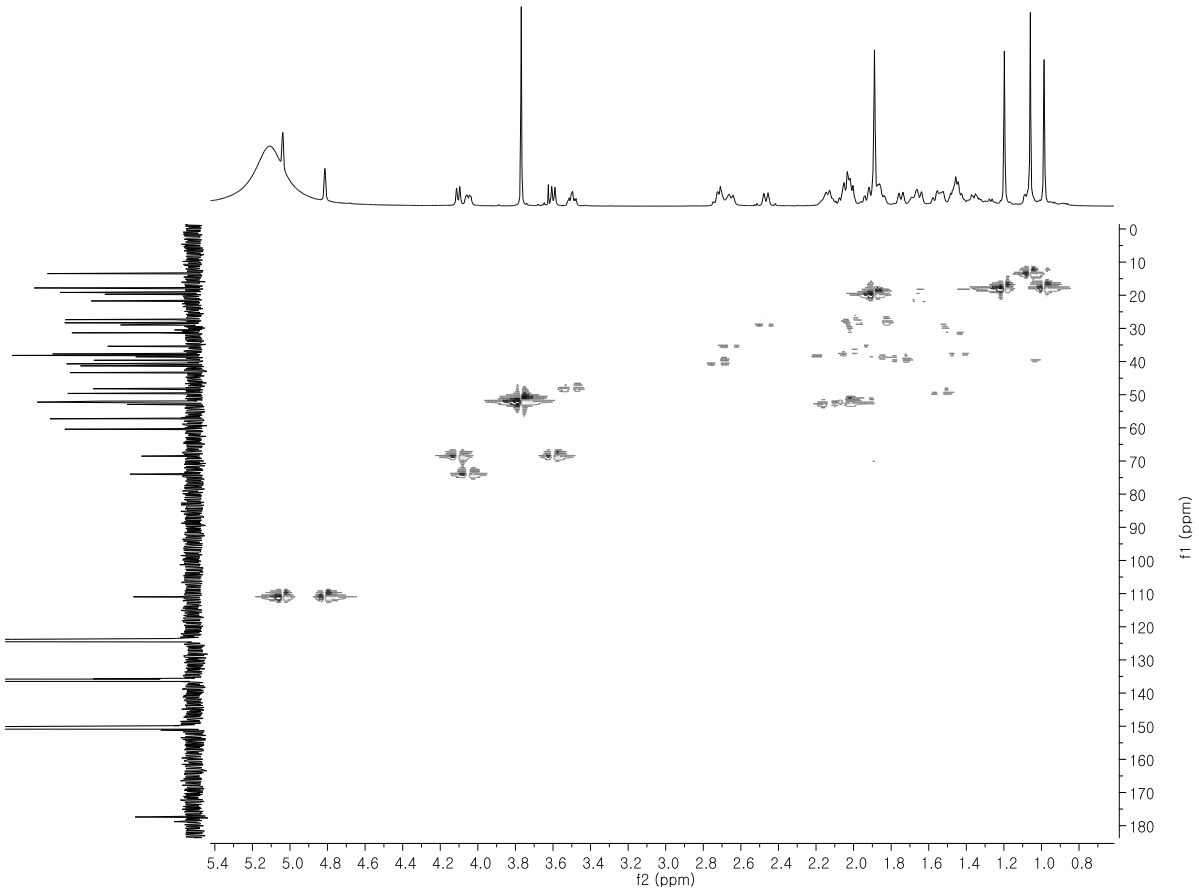

Figure S11. HSQC spectrum of compound **3** in pyridine-d_5

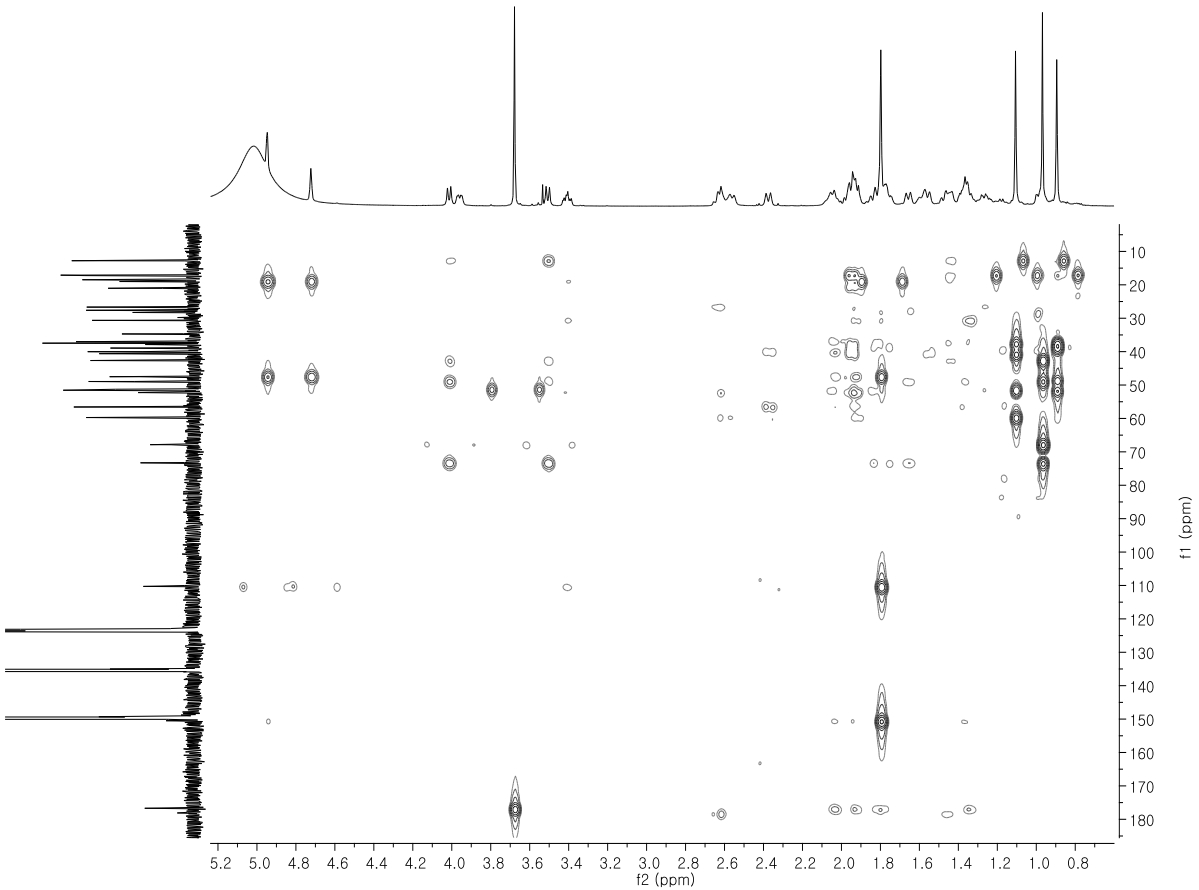

Figure S12. HMBC spectrum of compound **3** in pyridine-d_5

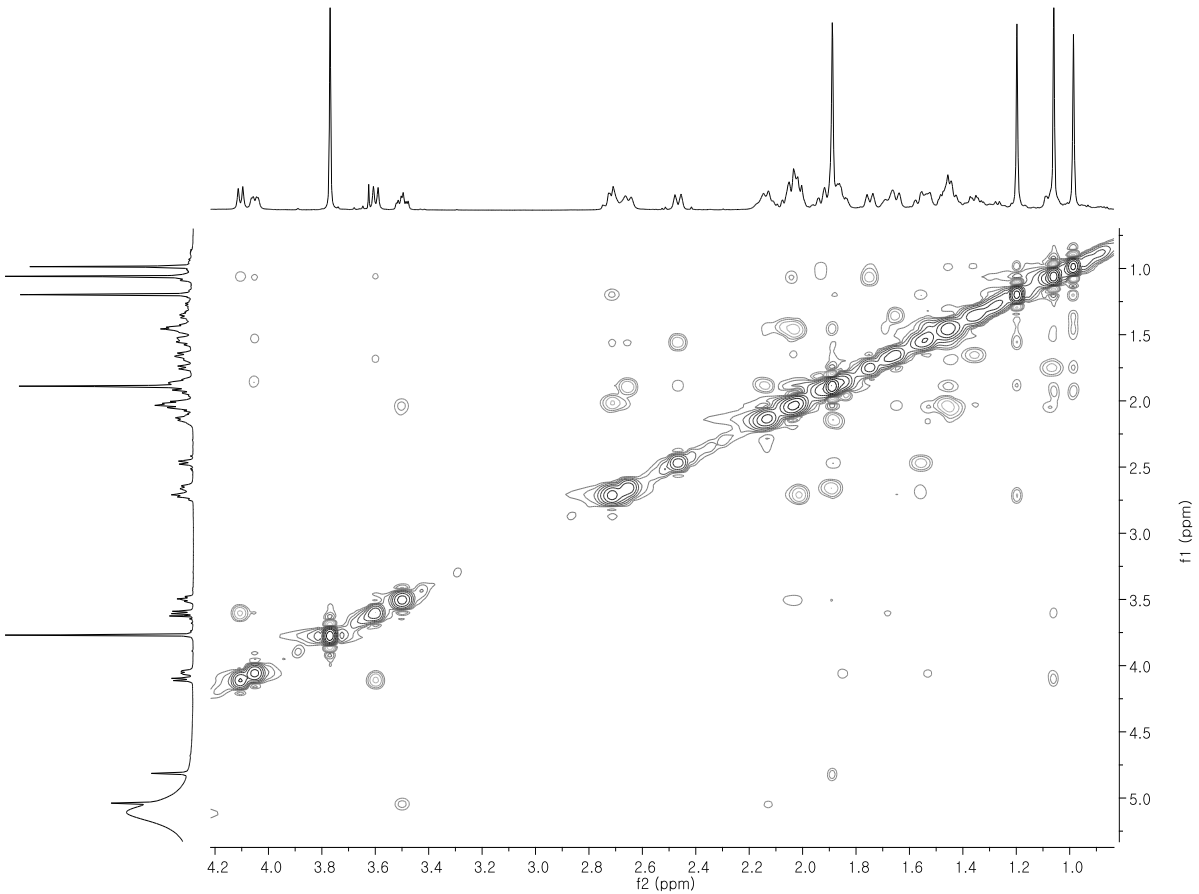

Figure S13. NOESY spectrum of compound **3** in pyridine-d_5